UNIVERSITY OF SOUTHAMPTON

FACULTY OF ENGINEERING, SCIENCE AND MATHEMATICS

SCHOOL OF OCEAN AND EARTH SCIENCE

ACCLIMATION AND PHENOTYPIC PLASTICITY OF ECHINODERM LARVAE IN A CHANGING OCEAN

by

Nadia Elisa Suárez Bosche

Thesis for the degree of Doctor of Philosophy

January 2011

A mis padres

Mario Cesar Suárez-Arriaga   &   Elke Amanda Bosche

Gracias a Ustedes con su apoyo, ejemplo y cariño este sueño fue posible

SCHOOL OF OCEAN AND EARTH SCIENCE

NATIONAL OCEANOGRAPHY CENTRE

This PhD dissertation by

Nadia Elisa Suárez Bosche

has been produced under the supervision of the following persons

Supervisors:

Dr. Debora Iglesias-Rodriguez

Prof. Paul Tyler

UNIVERSITY OF SOUTHAMPTON

ABSTRACT

FACULTY OF ENGINEERING, SCIENCE AND MATHEMATICS

SCHOOL OF OCEAN AND EARTH SCIENCE

Doctor of Philosophy

**ACCLIMATION AND PHENOTYPIC PLASTICITY OF ECHINODERM
LARVAE IN A CHANGING OCEAN**

Nadia Elisa Suárez Bosche

Echinoderms are keystone organisms that have representatives in virtually every marine ecosystem. They possess a number of features that makes them an excellent model system, namely 1) their susceptibility to changes in the chemistry of seawater and temperature 2) their ossified skeletons are major contributors to many carbonate formations 3) their variety of life history strategies that enable successful reproduction (e.g. asexual reproduction, fission, cloning and regeneration). In most parts of the ocean, CO_2 and temperature co-vary, making it difficult to extrapolate isolated effects of any one variable to natural scenarios. Laboratory and field work was conducted to assess the physiological and biogeochemical response of sea urchin *Psammechinus miliaris* larvae to changes in water carbonate chemistry. This study used two approaches: 1) the incubation of the larvae with naturally CO_2-enriched deep-seawater, and 2) the study of the effect of ocean acidification and ocean warming. It is reported that there was no effect of *in situ* naturally high CO_2 seawater, or laboratory induced CO_2 concentrations, on larval physiology or morphology. However, elevated CO_2 was found to cause a decrease in fertilization and calcification. An increase in temperature appeared to counteract significantly the negative effect that high CO_2 has on fertilization and biocalcification. Therefore, it is argued that the developmental stages of sea urchins may adapt to predicted ocean acidification and increasing temperature scenarios, which is advantageous to maintaining stability and survival of populations under environmental selection pressure. Furthermore, the regeneration capability of the Pacific seastar larvae *Pisaster ochraceus* and *Orthasterias koehleri* was investigated. The successful complete re-growth of the larvae can be considered a specific developmental strategy that facilitates the species' survival. This research suggests that echinoderm larvae are resilient to conditions in a changing ocean, due to their high acclimation capabilities and to their reproduction life history strategies. In this context, echinoderms may be considered an evolutionary success.

CONTENTS

CHAPTER 5: GROWING HALF OF THE BODY: DEVELOPMENT OF THE NERVOUS SYSTEM DURING REGENERATION IN SEASTAR LARVAE 87

LIST OF FIGURES

x

LIST OF TABLES

ABBREVIATIONS

ACC	Amorphous Calcium Carbonate
ALA	Antero-lateral Arms
A	Anus
BL	Body Length
$CaCO_3$	Calcium Carbonate
Cb	Ciliary Band
CO_3^{2-}	Carbonate Ion
1-MA	1-methyladenine
$2HCO_3^-$	Carbonic Acid
E	Oesophagus
FSW	Filtered Seawater
CO_2	Carbon Dioxide
CTD	Conductivity-temperature-depth
DIC	Dissolved Inorganic Carbon
HCO_3^-	Bicarbonate Ion
KCl	Potassium Chloride
Ksp	Solubility product at the *in situ* conditions of temperature, salinity, and pressure
M	Mouth
N	Neurites
PAP	Porcupine Abyssal Plain
PBS	Phosphate Buffered Saline
pCO_2	Partial Pressure of CO_2
PFA	Paraformaldehyde
PDA	Postero-dorsal Arm
PIC	Particulate Inorganic
PMCs	Primary Mesenchyme Cells
POA	Postoral Arm
POC	Particulate Organic Carbon
PROA	Preoral Arms

RT	Room Temperature
SD	Standard Desviation
SE	Standard Error
SMCs	Secondary Mesenchyme Cells
S	Stomach
SW	Seawater
Ω-Cal	Omega calcite
Ω-Arg	Omega Aragonite
TA	Total Alkalinity
TPC	Total Particulate Carbon

DECLARATION OF AUTHORSHIP

I, **Nadia Elisa Suárez Bosche**,

declare that the thesis entitled **"Acclimation and phenotypic plasticity of echinoderm larvae in a changing ocean"** and the work presented in the thesis are both my own, and have been generated by me as the result of my own original research.
I confirm that:

- this work was done wholly or mainly while in candidature for a research degree at this University;
- where any part of this thesis has previously been submitted for a degree or any other qualification at this University or any other institution, this has been clearly stated;
- where I have consulted the published work of others, this is always clearly attributed;
- where I have quoted from the work of others, the source is always given. With the exception of such quotations, this thesis is entirely my own work;
- I have acknowledged all main sources of help;
- where the thesis is based on work done by myself jointly with others, I have made clear exactly what was done by others and what I have contributed myself;
- part of this work have been published as:

Contributor

Lebrato M, Iglesias-Rodriguez D, Feely R, Greeley D, Jones D, Suarez-Bosche N, Lampitt R, Cartes J, Green D, Alker B (2010) Global contribution of echinoderms to the marine carbon cycle: a re-assessment of the oceanic $CaCO_3$ budget and the benthic compartments. *Ecological Monographs e-View*.

Signed: ………………………………………………………………………..

Date:……………………………………………………………………………

ACKNOWLEDGEMENTS

I would like to thank a number of people that made this work possible with their invaluable support and expertise. Particular thanks and gratitude go to my supervisor Dr. Debora Iglesias-Rodriguez for giving me the opportunity to start a PhD and for all her encouragement in starting novel experiments. Additionally, I would like to express my gratefulness to my second supervisor Prof. Paul Tyler who supported me in many critical stages of this research. I will always be in debt to him for giving me the great opportunity to be part of a deep-sea expedition; the experience of diving 1 km made this PhD ten times more worthwhile. To both of my supervisors I thank for sharing and for showing me your true excitement in science.

I would like to extend my immense gratitude to my colleagues at Friday Harbor Laboratories, WA, USA . Special thanks go to Dr. Svetlana Maslakova and Dr. George von Dassow; their knowledge and support have been the base of all this research. Moreover, to the people that helped me at Kristineberg Marine Research Station, Sweden. In particular, to Prof. Mike Thorndyke, Dr. Sam Dupont and Dr. Karen Wilson for their technical support and assistant during part of this research.

Many thanks to my NOCS colleagues that allowed me to succeed in this research (Neil Jenkinson, Mark Stinchcombe, Nigel Eastwood, Chris Hauton, Sue Hartmann, Jonathan Wilkinson, Richard Lampitt and John Allen). Special thanks go to Dr. John Gittins for always offering a friendly helping hand, for encouraging me to continue and for reading many of my manuscripts (and my father's); many many thanks. I am also greatly indebted to the National Council on Science and Technology of Mexico (CONACyT) for funding my PhD research.

Thanks to Martin Mella for making me laugh so many times, for your help and love and for sharing your happiness and kindness. To those friends that made my time in Southampton interesting and multicultural, thanks to those now old friends: Aaron Micallef, Joerg Frommlet, Heleen Vanneste, Mounir Lekouara, Phoebe Lomax, Alex Mustard, Stefano Bellati, Sergio Balzano, Teresa Madurel, Ana Hilario, Teresa Amaro,

Yolanda Kalantzi and Mercedes. Thanks to Mario Alberto Garcia for the long interesting conversations and for those exotic meals shared and those enjoyable dances, to Ceci Peralta for keeping in touch and helping me when necessary, also thanks to the new friends on the list Lizeth, Esteban y Nayi, and Dave Hamersley. Thanks to the members of the Southampton Mexican society for keeping the spirit up. And special thanks to the Thekchen centre for those warm words and advices when very much needed.

To Mario Lebrato, I am undoubtedly in debt with you for always being there and for your immense help and support, and for your true enthusiasm in science which kept me on board. For those motivating thoughts, conversations and discussions during this PhD and for being my friend.

To Eleonora Manca for sharing these four years with me, for your friendship, for showing me the New Forest and Sardinia and for taking me to many concerts. The next adventure is in Mexico! To Thanos Gritzalis-Papadopoulos, for being the best housemate that one could ask for, for sharing so many good moments and for being such a good person and friend.

Many thanks to Family Gardner (John, Alicia, Josh and Abby) because you were and always have been a keystone in this long process, for all your love and strong encouragement during the downhill part of this adventure, for making me feel part of the family, for sending me all your good energy and for showing me how to see life in different ways (*Nada es verdad nada es mentira, todo es segun el cristal con que se mira*). Thanks to Susan Hodson for building up a strong English base so that I could start a PhD and for your immense generosity. To my grandparents Annelise and Werner Bosche for making me laugh, for their extraordinary support and for passing on to the family your strength.

Thanks to my very good friends Ikerne and Eva, even though you are literally on the other side of the world (New Zealand and Canada) you were both a great support, thank you. Your friendship proves that distance is not an issue for good friends.

To my father and mother, Mario Cesar and Elke for always encouraging us to follow our dreams, and for motivating us to pursue an interesting and successful life. For your invaluable and infinite love, support and help at all levels throughout every period of my life. To my sister Karina and my brother Karsten for all your love, for your calls, visits, advices, smiles, hugs, and good times together.

To Tom Mortlock to you all my love and gratitude, for all your patience, kindness and for making sure that I was still eating, for all your love and limitless support in every aspect at the most critical part of this PhD. It wouldn't have been the same without you, your strength made me strong and made this possible. For sharing with me all your enthusiasm in life, for being so eager to discover things and show them to me, for your contagious passion and happiness of every day, for those seas explored and to be explored with a cocktail in the hand ;) and for having a plan A, B and C to continue the adventure together, in who-knows which exotic place(s).

Original sketch representing seastars "crawling" away from science. Drawn by Georgia Kalantzi.

CHAPTER 1

INTRODUCTION, AIMS AND OBJECTIVES

1   INTRODUCTION, AIMS AND OBJECTIVES

1.1   PROJECT SUMMARY

This study adopts a multidisciplinary approach which combines oceanographic research with methods more commonly used in the developmental biological sciences, including the study of the physiology, ecology and evolution of echinoderm life cycle (e.g. embryogenesis, larval development). Echinoderms occupy a unique place in embryological studies as they possess a number of features that makes them an excellent model organism. Firstly, they are extremely susceptible to changes in the chemistry of seawater and temperature, making them ideal subjects with which to examine environmental, ecological and evolutionary responses of marine biota to a changing ocean. Secondly, they have several strategies for successful reproduction (e.g. asexual reproduction, fission, cloning and regeneration).

This thesis discusses the physiological and evolutionary implications to the sea urchin *Psammechinus miliaris* (a model calcifier organism) of changes in ocean carbonate chemistry. By studying these sea urchin larvae, a more thorough comprehension may be inferred regarding the response of marine biota to rapid changes in seawater chemistry and temperature. Furthermore, this thesis has, for the first time, shed light on the morphogenesis and neurogenesis of seastar larvae *Pisaster ochraceus* and *Orthasterias koehleri* during regeneration.

1.2   GENERAL BACKGROUND AND THEORY

Revelle and Suess (1957) wrote a prophetic passage on our perturbations to the global carbon cycle which may be especially true for ocean acidification:
Thus human beings are now carrying out a large scale geophysical experiment of a kind that could not have happened in the past nor be reproduced in the future.

In 1958 Roger Revelle was one of the first scientists to recognise rising levels of atmospheric carbon dioxide and to monitor this trend in remote locations such as Antarctica. At the same time, Charles David Keeling started making measurements of atmospheric carbon dioxide (CO_2) from the top of Mauna Loa volcano in Hawaii. Their combined work presents the longest atmospheric CO_2 instrumental record in existence and shows a clear rise in CO_2 levels from the 1960s to the present day. When these studies began in the 1960s, atmospheric CO_2 levels were approximately 315 parts per million (ppm). Fossil fuel combustion has further pushed the global atmospheric carbon concentration from pre-industrial levels of approximately 280ppm to present values of around 380ppm. This exceeds by far the natural range over the last 850,000 years (180 to 300ppm) as determined from ice core records (IPCC, 2007). One could argue that throughout Earth's history there have been periods of abrupt change in temperature and CO_2. While this may be true, today's concern is the rapid rise in atmospheric CO_2 which is as much as 30 times faster than natural rates in the geological past (Kump *et al.*, 2009). Recently published data suggests total human CO_2 emissions may amount to approximately 10 billion tons of carbon annually (equivalent to one million tons per hour or, on a per capita basis, ~ 0.2 kg person^{-1} h^{-1}; where 1 billion tons equals 1 Pg or 1 x 10^{15} g) (Doney *et al.*, 2009a). If no action is taken to decrease carbon emissions by the global community, the concentrations of CO_2 in the atmosphere are predicted to reach double pre-industrial levels as early as 2035 (Orr *et al.*, 2005).

Global climate change will affect the physical, biological and biogeochemical characteristics of the oceans and coasts (IPCC, 2007). Over the past two centuries, it is estimated that the oceans have taken up approximately 40% of all anthropogenic atmospheric CO_2 (Sabine *et al.*, 2004). It is thought that this uptake has considerably slowed the rise in atmospheric CO_2 concentrations, but it also alters the ocean chemistry. In equilibrium with seawater, CO_2 forms carbonic acid and changes the balance of carbonate and bicarbonate ions making the ocean more acidic (Caldeira and Wickett, 2003; Caldeira and Wickett, 2005). Furthermore, the IPCC in their Forth Assessment Report (2007) note a 0.3^0C global average surface warming increase between 1990 and 2005 and project a further increase of between 0.6 and 4.0 ^{0}C by the end of the 21st century. The role of the ocean in mediating future atmospheric CO_2, temperature change, and the impact on marine life, is integral to understanding how best

to predict, respond and adapt to climate change. Notwithstanding, any detrimental impact on marine species because of oceanic carbon uptake will undoubtedly be felt by economies worldwide (Cooley *et al.*, 2009).

1.2.1   The carbonate system

The inorganic carbon system is one of the most important chemical equilibriums in the ocean and is largely responsible for controlling the pH of seawater. The carbonate system can be described by four parameters: dissolved inorganic carbon (DIC), alkalinity (TA), pH and $p\text{CO}_2$. Any two of these parameters, together with temperature and salinity, are necessary to calculate all other parameters of the carbonate system.

1.2.2   Dissolved inorganic carbon

Dissolved inorganic carbon exists in seawater in three major forms: bicarbonate ion (HCO_3^-), carbonate ion (CO_3^{2-}), and aqueous carbon dioxide ($CO_2(aq)$), which here also includes carbonic acid (H_2CO_3). At a pH of 8.2, 88% of the carbon is in the form of HCO_3^-, 11% in the form of CO_3^{2-}, and only 0.5% of the carbon is in the form of dissolved CO_2. These three species are in thermodynamic equilibrium in the seawater and with the atmospheric gaseous carbon dioxide, CO_2 (g) (Fig. 1.1):

$$CO_2\,(g)$$
$$\updownarrow$$
$$H_2O + CO_2\,(aq) \leftrightarrow H_2CO_3\,(aq) \leftrightarrow H^+\,(aq) + HCO_3^-\,(aq) \qquad\qquad (1)$$
$$\updownarrow$$
$$H^+\,(aq) + CO_3^{\,2-}\,(aq)$$
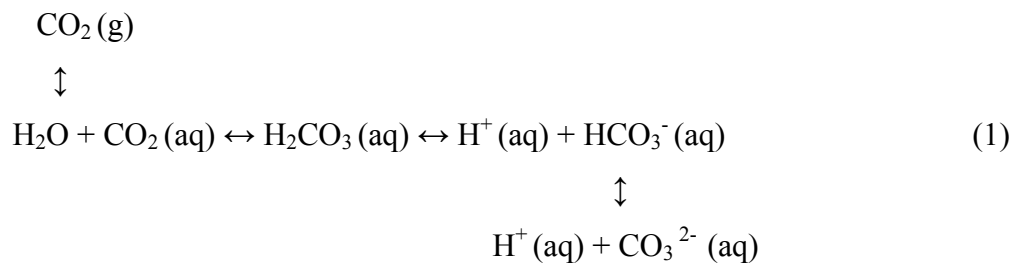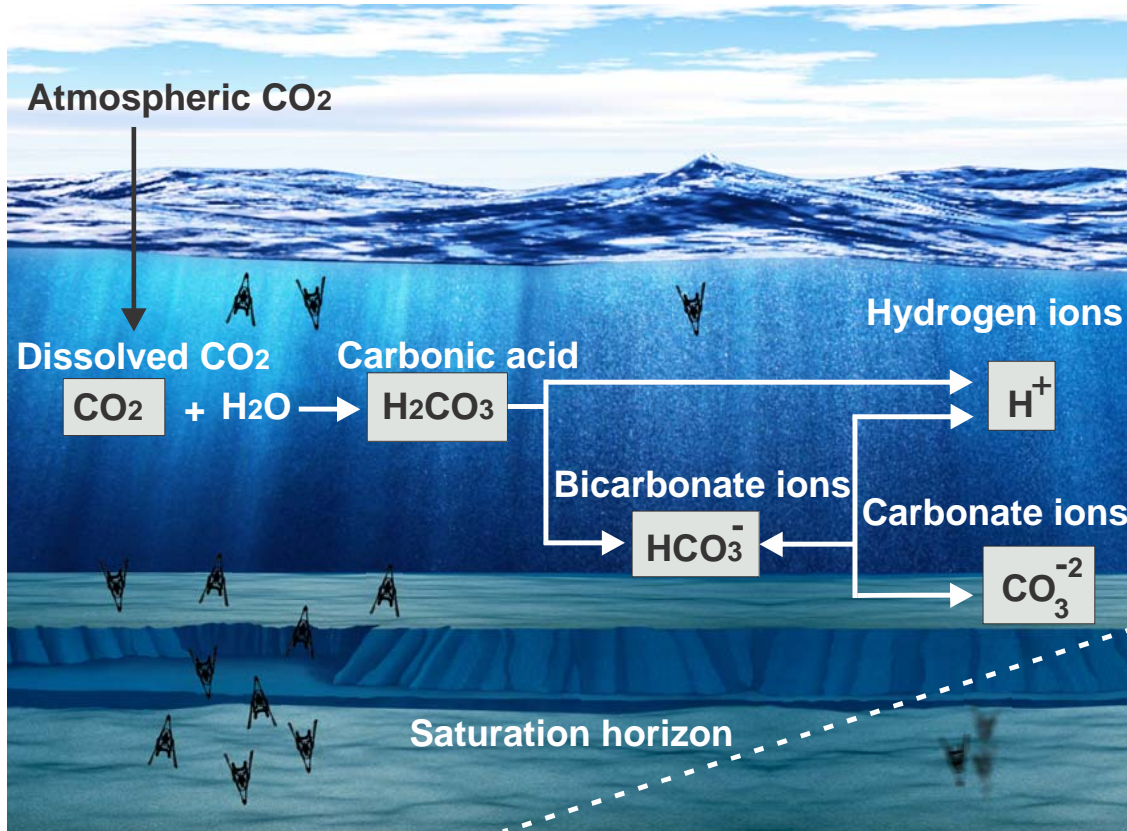
Figure 1.1. Carbon dioxide (CO_2) influx alters seawater carbonate chemistry. These chemical changes cause an upwards shift in the "saturation horizons" for calcite and aragonite. Below this horizon the shells of marine organisms made of these minerals dissolve. Diagram modified from Doney, 2006; *Scientific American,* 38-45.

1.2.3   Alkalinity

The total alkalinity of seawater has been defined by Dickson (1981) as:

"The number of moles of hydrogen ion equivalent to the excess of proton acceptors (bases formed from weak acids with a dissociation constant $K \leq 10^{-4.5}$ at 25°C and zero ionic strength) over proton donors (acids with $K \geq 10^{-4.5}$) in 1 kg of seawater"

The total alkalinity (TA) expression is represented by:

$$TA = [HCO_3^{-}] + 2[CO_3^{2-}] + [B(OH)_4^{-}] + [OH^{-}] + [HPO_4^{2-}] + 2[PO_4^{3-}]$$
$$+ [SiO(OH)_3^{-}] + [NH_3] + [HS^{-}] - [H^{+}]_F - [HSO_4^{-}] - [HF] - [H_3PO4] \qquad (2)$$

The total concentrations of these constituents in solution are represented in brackets and $[H^+]_F$ represents the free hydrogen ion concentration.

1.2.4   pH

By the term pH, the acidity of a liquid is described as the negative common logarithm of the concentration of hydrogen ions. All pH values in this study are on the total scale which includes the effect of sulfate ion which is expressed by:

$$pH_T = -\log([H^+]_F + [HSO_4^-]) = -\log[H^+]_T \qquad (3)$$

where $[H^+]_F$ is the 'free' hydrogen ion concentration, including hydrated forms.

Most organisms on Earth exist in an equilibrium regarding internal pH, thus any environmental change will affect their performance. Although the response of different marine organisms to changes in pH is expected to be inhomogeneous (Langer *et al.*, 2006), current evidence suggests that large and rapid changes in ocean pH will have adverse effects on a number of marine animals (Gattuso *et al.*, 1998; Kurihara and Shirayama, 2004; Havenhand *et al.*, 2008). Environmental pH changes will require that the organisms balance internal pH with the external changes. One concern is whether or to what extent animals are able to maintain this balance under projected ocean acidification scenarios, and the consequences on reproduction and organisms development remain an open question.

1.2.5 pCO_2

The partial pressure of CO_2 (pCO_2) is the pressure of CO_2 when considered separate from all other gases in its mixture or solution (the atmosphere or ocean) (Zeebe and Wolf-Gladrow, 2001). It is important that suitable corrections are applied in order to calculate pCO_2 at *in situ* conditions because pCO_2 varies strongly with temperature and pressure.

1.3   THE EFFECTS OF OCEAN ACIDIFICATION ON CALCIFYING ORGANISMS

Calcification is a widespread phenomenon among marine organisms, such as calcareous algae, foraminifera, corals, molluscs and echinoderms. Any increase in pCO_2 will have a dramatic effect on the carbonate saturation state of seawater. This, in turn, will affect the production rates of $CaCO_3$ minerals that are necessary for shell formation in marine organisms. Most benthic invertebrates secrete $CaCO_3$ in the form of aragonite, calcite, highmagnesium calcite (0.5 mole % $MgCO_3$), amorphous $CaCO_3$, or a mixture of these $CaCO_3$ phases. This relationship is shown in the following equation:

$$CO_3^{2-} + Ca^{2+} \rightarrow CaCO_3 \tag{4}$$

The projected decline in carbonate ion (CO_3^{2-}) concentrations due to seawater acidification (higher CO_2 waters) reduces the $CaCO_3$ saturation state (Ω) as shown below:

$$\Omega_{Cal/Arg} = \frac{[Ca^{2+}]_{sw} * [CO_3^{2-}]_{sw}}{K_{sp}} \tag{5}$$

$[Ca^{2+}]_{sw}$ and $[CO_3^{2-}]_{sw}$ are the calcium and carbonate concentrations in seawater and K_{sp} is the stoichiometric solubility product defined as:

$$K_{sp} = [Ca^{2+}]_{sat} \times [CO_3^{2-}]_{sat} \tag{6}$$

The saturation state of $CaCO_3$ (Ω-$CaCO_3$) can be critical for biogenic calcification. In regions where Ω-Arg or Ω-Cal is above or equal to 1.0, the formation of shells and skeletons is favoured. For values $\Omega < 1.0$, seawater is corrosive to $CaCO_3$ and dissolution will begin. The saturation state is generally highest in the tropics and lowest in the high latitudes, because the solubility of $CaCO_3$ increases with decreasing temperature and increasing pressure (Feely *et al.*, 2004). Climate change modelling has estimated that the South Pole will be undersaturated with respect to aragonite by the end

of the 21st century (Orr *et al.*, 2005). Calcification can be defined as the physiological process of calcium carbonate deposition (gross calcification) and/or as the trade-off between the biological production of $CaCO_3$ and the physical/chemical process of erosion and dissolution (resulting in net calcification).

$$Ca^{2+} + 2HCO_3^- \rightarrow CaCO_3 + CO_2 + H_2O \qquad (7)$$
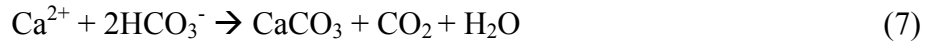
The production of mineral $CaCO_3$ from bicarbonate (HCO_3^-) creates a large carbon sink where echinoderms play a fundamental function in the process of remineralisation. A recent study (collaboration by the author, Lebrato *et. al.,* 2010; see Appendix 2) showed that echinoderms have a profound role in global carbon cycles. In fact, they are responsible for approximately 5% of the total ocean biological pump.

Recent work suggests that benthic invertebrate such as molluscs and echinoderms are sensitive to changes in seawater carbonate chemistry (Gazeau *et al.*, 2007; Dupont *et al.*, 2008; Clark *et al.*, 2009). Particularly, echinoderm larvae might be especially sensitive to ocean acidification as their skeletal parts consist of magnesium-bearing calcite, which is 30 times more soluble than calcite without magnesium (Politi *et al.*, 2004). The reason for this high solubility is that the embryos produce skeletons of amorphous $CaCO_3$, which is less stable than the crystalline phases of $CaCO_3$. The dissolution of the biomineral that sea urchins produce to build up their skeletons (high-magnesium calcite) is similar to or greater than that of aragonite (Walter and Morse, 1985).

1.3.1   The relevance of *Psammechinus miliaris*

Many benthic calcifying organisms are abundant in near-shore communities and have high economic and/or ecologic worth. For example, mussels and oysters have high commercial value for the fishing industry. Echinoderms are another example; one of the edible species of echinoids found on the coast of the United Kingdom is the sea urchin *Psammechinus miliaris* (Fig. 1.2). This species is considered to have a great potential as an aquaculture species (Kelly *et al.*, 1998). It is know that this sea urchin grows rapidly

(both somatic and gonadal) in response to extruded formulated feeds. Therefore, defining the effect of changes in pH and temperature predicted to occur before the year 2100 during larval stages is important in understanding the developmental and survival implications on the species.

Figure 1.2. Green sea urchin *Psammechinus miliaris*

1.4   ECHINODERMS

1.4.1   Why study echinoderms?

Echinoderms are morphologically and ecologically diverse marine animals, found at all ocean depths. The phylum Echinodermata contains about 7000 living species, making it the second largest group of deuterostomes, after the chordates. They are an ancient phylum with representatives present in the Lower Cambrian, and with several groups that went extinct in the Palaeozoic (Nielsen, 1998). Echinoderms have been extensively studied, because of their ecological importance in the marine environment, the interesting morphology of the adult organism and the advantage of experimentally manipulable embryos (Matranga, 2005). They are important both biologically and geologically; biologically because few other groups are as abundant in the biotic desert of the deep sea, as well as the shallower oceans, and geologically because their ossified skeletons are major contributors to many limestone formations and can provide valuable clues to the geological environment.

Furthermore, it has been proposed that the radiation of echinoderms was responsible for the Mesozoic revolution of marine life (Swalla, 2006). The phylum has a unique position in the evolutionary tree. They first appear in the Metazoa phylum with features of deuterostomes, in direct evolutionary line with chordates and vertebrates. Evolutionary echinoderms are less divergence from vertebrates than from other invertebrates (Matranga, 2005). The phylum contains five classes: Asteroidea (seastars o starfish), Echinoidea (sea urchins, sand dollars and sea biscuits), Holothuroidea (sea cucumbers), Ophiuroidea (brittle stars) and a sessile Crinoidea (sea lilies and feather stars) (Hyman, 1995). Echinoderms exhibit radial symmetry, have a biomineral endoskeleton and a water vascular system, which is a unique organ that is used for both locomotion and circulation (Gilbert and Raunio, 1997).

1.4.2   Reproductive system

Orton (1914) stated that *P. miliaris* tends to associate in pairs, most of which consist of opposite sexes, at spawning time. These species have a lifespan of more than 10 years, and the minimum size at sexual maturity is 8 mm (Orton, 1914). Regular echinoids, such as *P. miliaris*, have an annual reproductive cycle (Hyman, 1995) and the spawning season is in the early summer months. Natural spawning occurs over a period of one to several months and gametes may be shed several times during a season (Strathmann, 1987). However, most of the eggs are released at the first spawning (*pers. obs.*). The reproductive system consists of five gonads, suspended from the aboral side of the test via mesenterial strands (Hyman, 1995). Ripe echinoids spawn in response to treatment with certain salt solutions, most commonly potassium chloride (KCl).

1.4.3   Echinoid larvae

The first fossil records of echinoderms probably correspond to the skeletal fragments of echinopluteus larvae from the Upper Jurassic (Nielsen, 1998). Sea urchins freely spawn gametes into the water column, with females producing thousands to millions of eggs depending on the species and their reproduction is normally annual

(Young, 2002). The planktotrophic larva of echinoids, the echinopluteus, is a complex pelagic larva that typically possesses eight anteriorly directed arms that bear a ciliated band used for the capture of food (Shearer *et al.*, 1914; Strathmann, 1987).

1.4.4 Fertilization and larval development

Echinoid embryos are considered a living laboratory for studying development and morphogenesis. Fertilization is the first of a series of events in the several changes within development of echinoderm larvae. During fertilization an increase in the intracellular pH (by 0.3 units, from 7.3 to 7.6; Johnson *et al.*, 1976; Payan *et al.*, 1983) and free calcium ions gives rise to the elevation of the fertilization membrane (Fig. 1.3 B).

Psammechinus miliaris eggs are negatively buoyant and have a maximum diameter of 97-115 μm (Shearer *et al.*, 1914). Fertilization occurs immediately following activation by the sperm, elevating the vitelline layer into a fertilization membrane that prevents polyspermy (Fig. 1.3 B). Cleavage stages begin within 30 and 60 minutes after fertilization. There is a series of cell divisions, in which the three first divisions produces eight equivalent blastomeres, while the fourth cell division produces sixteen cells of different sizes. Eight cells called mesomeres at the animal pole, four macromeres and four micromeres at the vegetal pole (Fig. 1.3 F and G). It should be highlighted that most of the lineage founder cells for many tissues are established at the 64-cell stage, well before the appearance of any morphological difference of the later embryo (Matranga, 2005).

As cell divisions continue, the embryo develops and becomes a free-swimming blastula (Fig. 1.3 H and I). From this stage, a new rearrangement of the embryo begins. The first cells to move are the primary mesenchyme cells (PMCs). Short after the PMCs migrate towards two ventro-lateral sites the archenteron is formed, which is the future intestine (Fig. 1.3 L). This developmental stage is known as gastrulation.
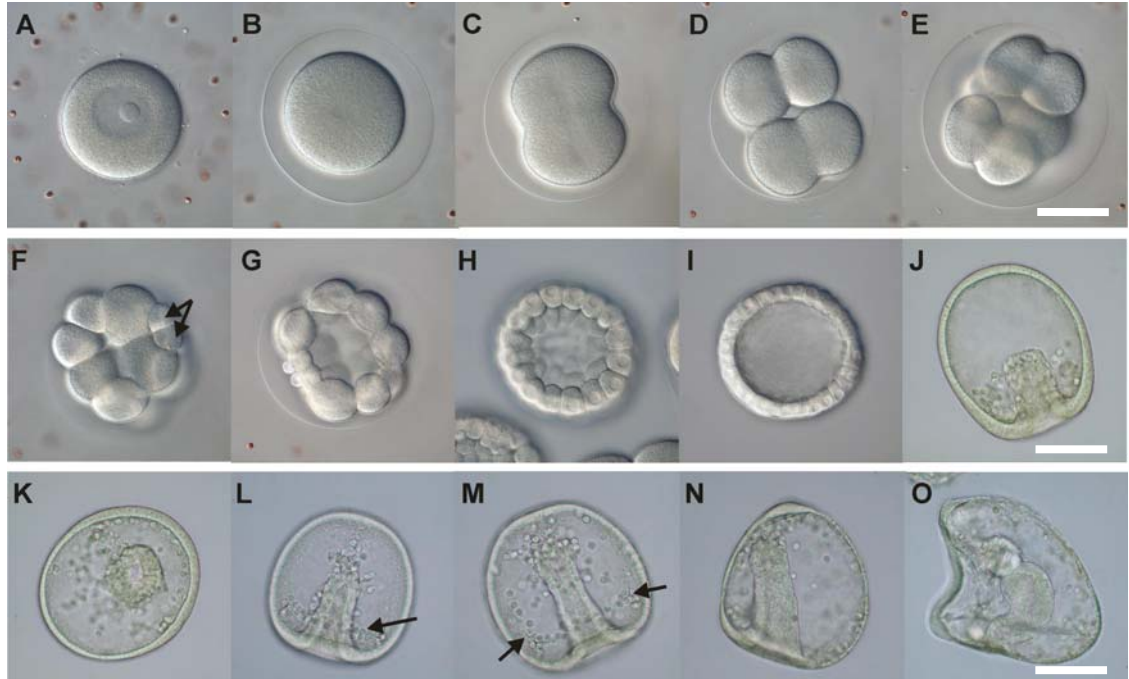
Figure 1.3 Development of an echinoid embryo (*Dendraster excentricus*). A) Egg undergoing fertilization; note the nucleus and the sperm around the follicle cells (red dots). B) After fertilization, the envelope had risen. C) First cell division (2 cells); D) Second cell division (4 cells); E) Third cell division (8 cells); F) Four cell division (16 cells); micromere formation is the first sign of cell differentiation in the embryo (shown by arrows); G) Early blastula; H) Blastula of an echinoid; I) Blastula stage. Scale bar corresponds to 80 µm. J) Gastrulation begins (invagination of the wall forms the archenteron); K) Early gastrula; L) Primary mesenchyme cells (arrow) during gastrulation); M) Triradiate spicules (arrows) deposited on the blastocoels to form the larval skeleton; N) The archenteron extends towards the ventro-lateral site and opens the larval mouth; O) The archenteron develops further to form the digestive system of the larva. Scale bar corresponds to 100 µm. Images courtesy of George von Dassow (Center for Cell Dynamics, Friday Harbor Laboratories, WA, USA).

The sea urchin skeleton is formed intracellularly by two types of mesenchyme cells: the primary (PMCs) and the secondary cells (SMCs) which are responsible for the calcification process (Fig. 1.4). First the endoskeleton is produced in the form of triradiate spicules deposited on the blastocoels, and then the spicules elongate and form in a complex species-specific matrix (Matranga, 2005). Echinoids deposit a biomineral matrix that results from the progressive crystallisation of a transient amorphous calcium carbonate phase (ACC) (Politi *et al.*, 2004) and magnesium carbonate. In contrast, asteroids (and holothurians) do not form larval spicules and do not have PMCs.

13

Figure 1.4 Larval skeleton formation. Left: development of the triradiate primary spicules (circled) with arrows indicating the primary mesenchyme cells; A, archenteron. Centre: the 4 armed pluteus larva has arms supported by rods that are extensions from the triradiate spicules . Right: the skeleton of a 6-armed echinopluteus observed using polarized light microscopy. Scale bar corresponds to 100 μm.

In the laboratory, the late gastrula transforms into the prim larva stage of pluteus after 48 hours post-fertilization. Subsequently, the larval mouth opens and a full intestine develops along a complex skeleton. Larval arms begin to form on both sides and grow longer. The post-oral pair of arms is the first to project anteriorly and is the best indicator of divergence of larval form (Strathmann *et al.*, 1992). The second pair of arms to develop is the anterolateral arms. The posterodorsal arms are the third pair arising, and lastly the fourth pair of arms the preoral arms presented in all echinoplutei larvae (Fig. 1.5; Emlet *et al.*, 2002). Once the larvae has opened the mouth and the digestive system has been completed the larvae must consume food (e.g. unicellular algae) to acquire energy and continue development to produce a juvenile sea urchin through metamorphosis.
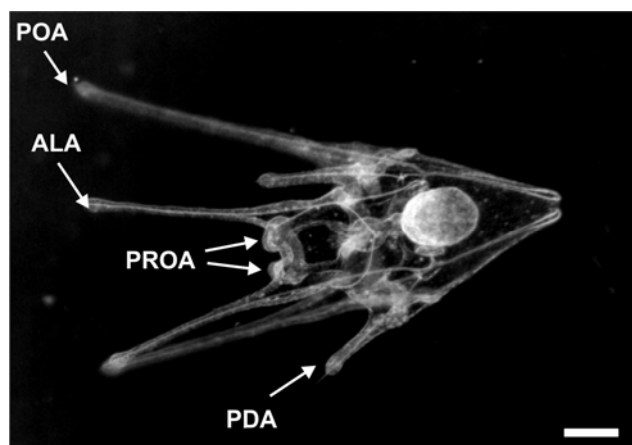
Figure 1.5 *Psammechinus miliaris* larval arms: postoral arm (POA), antero-lateral arm (ALA), postero-dorsal arm (PDA) and preoral arm (PROA). Scale bar corresponds to 100 μm.

In echinoids, adult structures (such as spines, tests and plates) are created in advance of metamophosis as of the forming juvenile rudiment and their larvae convert in a matter of minutes to a pentaradial symmetrical juvenile. In perhaps no other phylum is this metamorphic process so dramatic (Fig. 1.6); changes include body symmetry (from bilateral to pentaradial) and life style (from planktonic larva to benthic adult; Strathmann, 1987; Gilbert and Raunio, 1997).
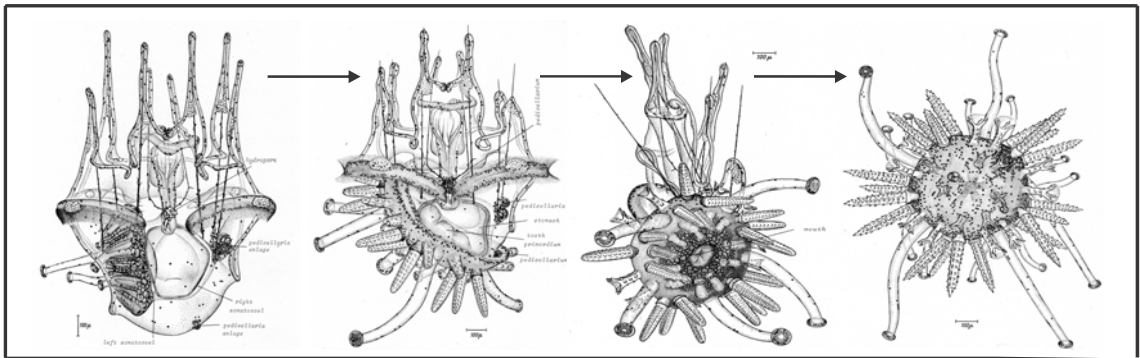
Figure 1.6 Schematic representation of *Psammechinus* sea urchin larvae undergoing metamorphosis to form a juvenile sea urchin. Drawings from G. Czihak. Scale bar represents 100 μm.

1.4.5   Asteroidea larvae

The Asteroide (commonly known as seastars) is one of the five classes of the phylum Echinodermata that have survived and contains approximately 1800 species to the present day. Seastars are organisms of sessile habits that tend to live in patches overloading areas and increasing the competition for food sources. Spawning of their eggs and sperm is usually limited to a few months of the year, particularly during the spring and summer periods. They have a pelagic larva that has the advantage of extending the species distribution (Clark, 1968). They are transported by the ocean currents where food (phytoplankton) is supplied in abundance. However, this brings also a disadvantage as they are an easy predation target. It has been reported that to overcome the high rates of mortality during the planktonic stage, seastars produce a large number of eggs. For example, the seastar *Asterias* is capable of spawning about two and a half million eggs (Clark, 1968).

The class Asteroidea has two characteristic larval types: the pelagic planktotrophic bipinnaria and the brachiolaria (McEdward *et al.*, 2002). The bipinnaria has a complex body form characterized by the bilateral arrangement of the pre- and post-oral ciliated swimming and feeding bands. The larvae have two ventral folds (oral and anal hoods), numerous lateral lobes and arms that are not supported by calcareous skeletal rods as echinoids larvae. They have a complete, functional gut (Fig. 1.7).
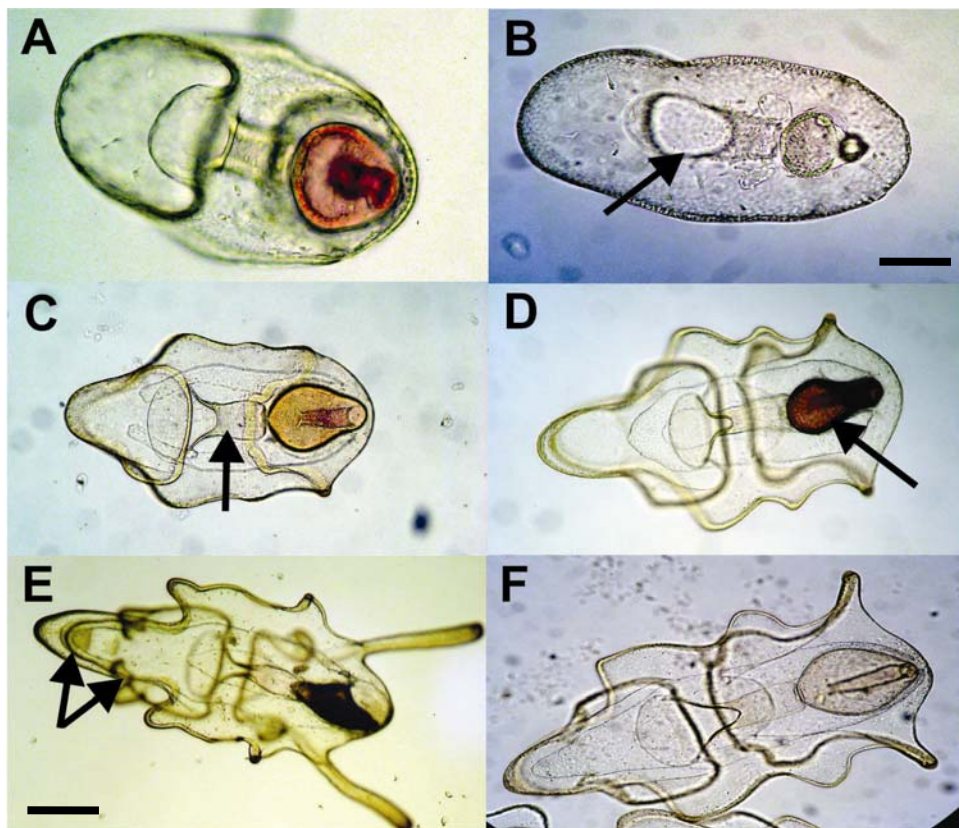
Figure 1.7 Development of asteroid larvae *Pisaster ochraceus* (A,C and E) and *Orthasterias koehleri* (B, D and F). Early bipinnaria of *Pisaster ochraceus* (A) and *Orthasterias koehleri* (B). The bipinnaria stage presents a pre- and post-oral lobe in which the mouth (B), oesophagus (C) and stomach (D) are diferentiated (the red colour of the stomach is characteristic of the pigments of the phytoplankton); The brachiolaria stage (E) presents brachiolar arms and attachment disk   (shown by arrows). Scale bar represents 100 μm (A,B,C and D) and 200 μm (E and F).

The brachiolaria is also a feeding larva and the main characteristic that makes it distinctive from the bipinnaria is the presence of specialised attachment structures on the pre-oral lobe: the brachiolar arms and attachment disk (Fig. 1.7 E). These arms are used by the larvae to test the substratum and provide adhesion during settlement (by secretion of cement from the adhesive disk). It is important to note that the presence of

the brachiolar settlement structures distinguishes morphologically the bipinnaria from the brachiolaria stage. They are not independently evolved types of larvae, but rather sequential developmental stages (McEdward *et al.*, 2002).

1.4.6   Regeneration in Asteroids

Developmental biology is a discipline that studies the mechanisms regulating embryogenesis and is becoming essential for the comprehension of many biological areas. The study of developmental processes mainly investigates the production and organisation of the different types of cells that constitute the adult organism (Matranga, 2005). However, development does not always mean embryogenesis; regenerations is in fact a distinct type of developmental process.

Regeneration is the reactivation of developmental processes during postembryonic life to restore damaged or missing tissues. It can involve limited processes of cell turnover and tissue repair, replacement of lost parts or organs, and even complete regrowth of whole individuals from small body fragments. Due to its close relation cloning processes, regeneration can be considered as the specific developmental strategy that complements asexual reproduction. Although regeneration resembles the process of embryogenesis in an accelerated form, the basics are not the same. During embryogenesis the structure is totally created *ex novo*, whereas in regeneration an existing structure is reformed after the loss structure (Carnevali, 2005). In fact, regeneration appears to depend upon the individual potential for histogenetic and morphogenetic plasticity expressed in terms of recruitment of stem cells and/or de-differentiated cells, cell proliferation and migration, supply of specific regulatory factors, and expression, or re-expression, of a specific developmental program (Carnevali, 2005).

In spite of the wide choice of potential models for studying regeneration, regrowth, an early evolutionary feature of all living organisms, regeneration has been explored only in a few organisms, yet our understanding of the critical mechanisms underlying this process is very poor (Carnevali, 2006). Historically, echinoderms were

the favourite models of the pioneers investigating the phenomenon of regeneration, finding its maximum expression in these organisms. Within the phylum of echinodermata, the seastars have been an excellent experimental system for investigating the regeneration process. Asteroids are well known for their striking regenerative potential. Embryos and seastar adults can rapidly and completely regenerate lost body part following self-induced or traumatic amputation. Furthermore, they provide a valuable experimental model for observation of morphogenesis, tissue renewal and for the neural regeneration process (Fig. 1.8).

Figure 1.8 The nervous system of the *O. koehleri* revealed by immunofluorescent staining. Scale bar represents 100 µm.

Echinoid and Asteroid larvae have a variety of life history strategies that enable marine species to reproduce successfully across a wide range of environmental conditions such as planktotrophy, lecitothrophy, brooding, asexual reproduction, cloning, hybridisation, regeneration among others. The relative success of each strategy is believed to be a consequence of a range of environmental selective pressures. To better understand the consequences of climate change in marine invertebrates, it is necessary to acquire knowledge of the evolutionary rules that will shape ocean ecosystem structure because of species sensitivity.

1.5   KEY AIMS AND OBJECTIVES

The aims of the present study were to examine environmental controls on echinoderm larval development and to assess echinoderm larval plasticity, tolerance and ability to persist in a changing ocean. Echinoderms posses the distinctive ability to resist physical damage, a strategy to reduce threat from predation (e.g. acclimation, phenotypic plasticity, regeneration, cloning, asexual reproduction). This thesis explores the biological plasticity of echinoderm larvae, by studying the acclimation and tolerance of echinoderms to climate change variability and also the ability to regenerate missing body parts. It is these processes that secure species survival. In order to achieve these aims, two major hypotheses and objectives have been followed:

Hypothesis 1:

That changes in the carbonate chemistry and ocean warming have a detrimental effect on echinoderm larval development. Changes in the degree of the saturation state decrease larval calcification and that has an effect on larval physiology and survival.

1) Studying the effect of changes in seawater carbonate chemistry and ocean warming in a model calcifier organism, the sea urchin *Psammechinus miliaris.* Specifically:

1. Investigating the fertilization success and mortality rates in near-future levels of ocean acidification and ocean warming

2. Investigating the larval growth and development under different seawater carbonate chemistry and ocean warming

3. Investigating the changes to larval calcification rates under CO_2-induced ocean acidification and ocean warming scenarios

To achieve these objectives a CO_2 system that mimics predicted climate change scenarios was developed at the National Oceanography Centre (see Chapter 2, Fig. 2.1 for schematic representation of the system). New protocols were developed to quantify biocalcification of the larval skeleton under a variety of predicted climate change scenarios. The effect of environmental stressors (e. g. CO_2 and temperature) on the *P.*

miliaris larvae were analysed for the complete larval cycle (from fertilization to metamorphosis).

Hypothesis 2:

That the capacity of seastar larvae to regenerate would allow the regrowth of missing body parts after bisection of the seastar. During regeneration, organogenesis and the nervous system are completed.

2) Studying the nervous system during regeneration of the seastar larvae *Pisaster ochraceus* and *Orthasterias koehleri*

1. Investigating morphogenesis during re-growth of both seastars larvae species
2. Investigating the neurogenesis during the regeneration process

This objective was achieved by using state-of-the art facilities at the marine Friday Harbor Laboratories, University of Washington, Washington, USA. The instrumentation, marine biota, expertise and logistic support were fundamental for the success of this project. New protocols to optimise the immunostaining of antibodies for the development of neurogenesis during re-growth of seastar larvae were developed. Larval regeneration was examined until reformation was completed.

1.6 STRUCTURE OF THE THESIS

This thesis contributes to the limited knowledge of the effect of changes in the water carbonate chemistry on marine invertebrates, specifically in the physiology and ecology of sea urchin larvae. Moreover, the strategies for successful reproduction (e.g. regeneration) were investigated in two seastar species. This thesis follows the format of separate scientific articles as chapters and is divided as follows:

- **Chapter 1** contextualises and highlights the relevance of this study by giving an introductory background to the field, literature and fundamental marine biological concepts.

- **Chapter 2** describes and discusses the implications of ocean acidification on the development and biocalcification of the sea urchin larvae *Psammechinus miliairis.*

- **Chapter 3** presents novel findings on the effect of changes in water carbon chemistry on larval development, using naturally occurring CO_2-enriched deep seawater that does not rely on chemical manipulations.

- **Chapter 4** studies the interactive effects of temperature and CO_2 on the development and biocalcification of *Psammechinus miliaris.*

- **Chapter 5** investigates the development of the nervous system during regeneration in the seastar larvae *Pisaster ochraceus* and *Orthasterias koehleri.*

- **Chapter 6** brings together all the major finding of this thesis, discussing and contextualising major implications with regard to the wider scientific community. Limitations and uncertainties are also highlighted.

- **Chapter 7** presents the final conclusions of this research, before outlining recommendations for further work.

CHAPTER 2

THE PHYSIOLOGICAL TOLERANCE OF THE SEA URCHIN SPECIES *PSAMMECHINUS MILIARIS* TO HYPERCAPNIC CONDITIONS
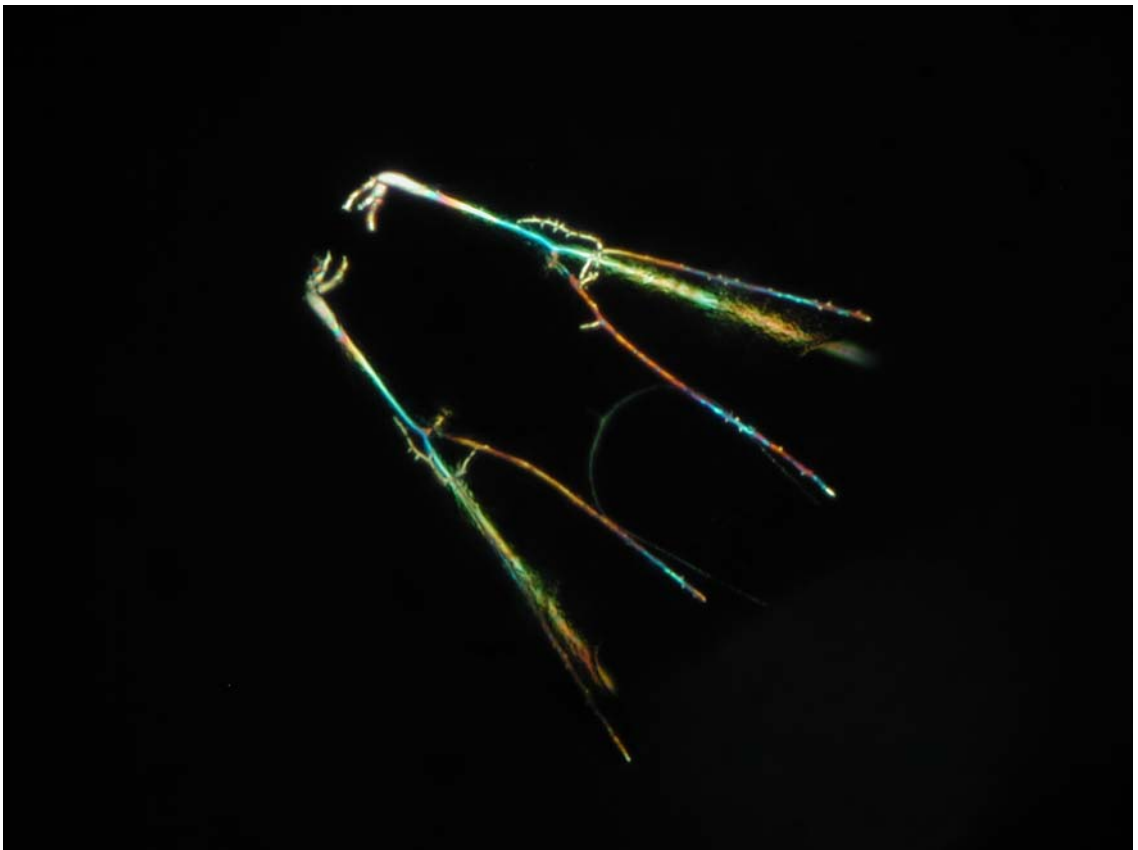
2 THE PHYSIOLOGICAL TOLERANCE OF THE SEA URCHIN SPECIES *PSAMMECHINUS MILIARIS* TO HYPERCAPNIC CONDITIONS

2.1 INTRODUCTION

Carbon dioxide is in quantity the most significant greenhouse gas after water vapour in the Earth's atmosphere (Zeebe and Wolf-Gladrow, 2001). Since the beginning of industrialisation in the mid-19th century, combustion of fossil fuels has released more than 250 billion tons of carbon in the form of CO_2 into the atmosphere (Royal Society, 2005). Around 50% of this fossil fuel CO_2 is absorbed by the oceans and is stored in the upper 200 m of the water column (Feely *et al.*, 2004; Sabine *et al.*, 2004). Oceanic uptake of anthropogenic CO_2 emissions causes an increase in partial pressure of CO_2 (pCO_2) with a concomitant decrease in the sea surface pH (known as "ocean acidification" (Caldeira and Wickett, 2005) and a decrease in the degree of supersaturation of calcium carbonate ($CaCO_3$). The decrease in $CaCO_3$ in seawater has implications for the saturation state of calcite (Ω- Cal) and aragonite (Ω-Arg) (the two polymorphs of calcium carbonate) with potential repercussions for calcifiying marine organisms. The $CaCO_3$ saturation state (Ω), is the product of the concentrations of calcium (Ca^{2+}) and carbonate ions ($CO_3{}^{2-}$):

$$\Omega = \frac{[Ca^{2+}]_{sw} * [CO_3{}^{2-}]_{sw}}{K_{sp}} \qquad (1)$$

where $[Ca^{2+}]_{sw}$ and $[CO_3{}^{2-}]_{sw}$ are the concentrations of calcium and carbonate ions, respectively, in seawater, and K_{sp} is the solubility product at the *in situ* conditions of temperature, salinity, and pressure (Zeebe and Wolf-Gladrow, 2001). The value of $\Omega > 1$ corresponds to supersaturation, whereas $\Omega < 1$ corresponds to undersaturation (e.g. Feely *et al.*, 2004).

The chemical reaction for calcification involves the consumption of two bicarbonate ions and the production of CO_2 for each $CaCO_3$ molecule precipitated:

$$Ca^{2+} + 2HCO^-_3 \rightarrow CaCO_3 + CO_2 + H_2O \qquad\qquad (2)$$
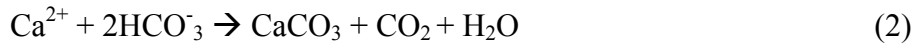
The vast majority of marine calcium carbonate is produced by organisms which secrete calcitic or aragonitic shells and skeletons. It is known that elevated pCO_2 in seawater (also known as hypercapnia) can impact marine organisms both via alteration of the metabolic acid-base balance and by decreased $CaCO_3$ saturation, which affects calcification rates and physiology (Dupont *et al.*, 2008; Pörtner, 2008; Widdicombe and Spicer, 2008; Melzner *et al.*, 2009). Hypercapnic conditions, due to an increase in seawater pCO_2 levels, are projected to reach 700 ppm in the year 2100 (Orr *et al.*, 2005), almost twice as much as the present value of 385 ppm. However, these levels are proposed for seawaters from the open ocean, while most of the marine ecosystems inhabit coastal areas where pCO_2 conditions vary from 350 ppm to approximately 700-900 ppm on a seasonal base (Menendez *et al.*, 2001; Wootton *et al.*, 2008). There is a limited understanding of the effect of ocean acidification and the accompanying changes in seawater chemistry on marine calcifiers, which are largely responsible for carbon sequestration [coccolithophores: (Balch *et al.*, 2007); foraminifera: (Schiebel, 2002); echinoderms: (Lebrato *et al.*, 2010)].

Both laboratory and field studies have shown that ocean acidification can negatively impact calcification in corals, molluscs, phytoplankton and echinoderms (Engel *et al.*, 2005; Kleypas *et al.*, 2006; Gazeau *et al.*, 2007; Miles *et al.*, 2007; Hall-Spencer *et al.*, 2008) although other studies have demonstrated an increase in calcification (Iglesias-Rodriguez *et al.*, 2008; Wood *et al.*, 2008; Shi *et al.*, 2009; Dupont *et al.*, 2010a). Echinoderms are calcifiying benthic organisms that are believed to be threatened by ocean acidification. In particular, echinoids produce a planktonic larva during which they synthesize an endoskeleton composed of high-magnesium calcite, one of the most soluble forms of calcium carbonate (Weber, 1969). Because calcification is central to their development and survival, in both larval and adult stages, these organisms have recently become a focus of attention with regards to the effect of ocean acidification. In this study, the echinoid larva of the coastal species

Psammechinus miliaris was used as a model organism to test its responses to different pCO_2 concentrations and to the saturation state of Ω-Cal.

2.2   MATERIALS AND METHODS

2.2.1   Study organism and exposure to stressors

Psammechinus miliaris were collected at low tide at Corbyn Head, Torquay, England (50° 6N; 3° 32 W) in April 2009. The sea urchins were kept in aquaria in a constant temperature room at 14 ± 1 ^{o}C. This temperature was similar to the ambient temperature experienced by *P. miliaris* in their natural environment, as determined from a local reference station (http://www.sea-temperature.com/water/torquay/338). Within 24 hours of collection the sea urchins were induced to spawn by injection of 1-2 ml of 0.5 M KCl into the inter-coelomic cavity. Two experiments were performed; the first experiment was to test the fertilization success and the second was to test the larval plasticity/tolerance to hypercapnic conditions. Two females and four males were used for each experiment. The eggs were spawned into 200 ml beakers of filtered seawater (0.22 μm) and the sperm was collected dry using pipettes. Before use, the quality of the gametes source was verified, the eggs were checked for shape and integrity and the sperm for motility. The eggs were fertilized by adding dilute sperm, and only batches of eggs with a fertilization rate $\geq$ 95% were accepted for use. To avoid the potential of pseudo-replication by mixing the eggs and sperm from multiple individuals into a single container, independently the sperm of each male was tested for fertilization succes. In this way the potential for all offspring being from a single male was ruled out. For the fertilization experiment, 16 beakers were used (four replicas, for four different pH levels). Approximately 800 eggs (~4 eggs ml^{-1}) were placed in the beakers (200 ml) containing the experimental seawater for 20 minutes prior to the introduction of the sperm. The number of sperm required to achieve a sperm to egg ratio of 1000:1, was calculated through haemocytometer counts. The sperm was activated in experimental seawater in the beakers containing the eggs. At 2 hours fertilization succes was determined by considering the number of eggs that exhibit an envelope or cleavage.

For the second experiment the flasks with experimental seawater were allowed to equilibrate for 48 hours with the desired pH before the cultures began. To investigate the tolerance of the larvae to hypercapnic conditions the cleaving embryos (two-four cell stage) were placed in 5 l flasks filled with experimental filtered seawater (FSW), taken from the sampling site. For this experiment 12 flasks (three replicas, for four different pH levels) each containing a density of 4 larvae ml^{-1} were used. Larvae were fed *Isochrysis galbana* and *Rhodomonas* sp. (see Appendix 4 for phytoplankton growth and medium preparation) at a concentration of 6,000 and 3,000 cells ml^{-1} respectively. Feeding was achieved by pipetting concentrated algae (the algae were gently centrifuged and seawater was discharged) to minimise any disruption of the seawater carbon chemistry achieved by bubbling CO_2 in the experimental flasks. All spawning, fertilization and larval cultures were carried out at 14.6 ^{o}C in a temperature-controlled room.

On days 3, 7, 14 and 21 culture subsamples of 60 larvae were collected to monitor and to record major ontogenetic stages. The larvae were fixed in 4% paraformaldehyde (EM GRADE, Science Services) in FSW for later analysis. Larvae were placed on a slide and photographed with a digital camera mounted on a compound microscope (MEIJI TECHNO CO., LTD) using polarised light to visualise the skeleton. Three morphometric parameters were measured for each larva: postoral arm length (POA), body length (BL) and stomach area (St). Image J software (available at http://rsb.info.nih.gov/ij; developed by Wayne Rasband, National Institutes of Health, Bethesda, MD) was used to measure the above parameters.

2.2.2   Scanning electron microscopy of larval skeletons

Larvae were collected to examine skeletal state. A mild solution of hyperchlorite diluted with a solution of distilled water saturated with sodium tetraborate (which acts as a buffer) was added to the samples to remove larval tissue. Skeletal sample rods were washed three times with distilled water, mounted on SEM stubs, gold coated and examined using a Leo 1450VP scanning electron microscope for evidence of abnormalities.

2.2.3   Carbonate chemistry system and experimental design

A range of seawater $p\text{CO}_2$ predicted to occur by the year 2100 [an increase from 385 ppm to 1200 ppm; (Caldeira and Wickett, 2003; Caldeira and Wickett, 2005; Riebesell U. *et al.*, 2010)] was selected, and regulated by manipulation of CO_2 levels. The treatments were: pH 8.1 (control seawater, 416.96 ppm), pH 7.9 (665.76 ppm), pH 7.7 (926.41 ppm) and an extreme condition pH 7.4 (1895.63 ppm), achieved by bubbling with different air/CO_2 mixtures (Fig. 2.1 and Table 2.1). The flasks were continuously bubbled with air mantaining dissolved oxygen (DO) >90%.
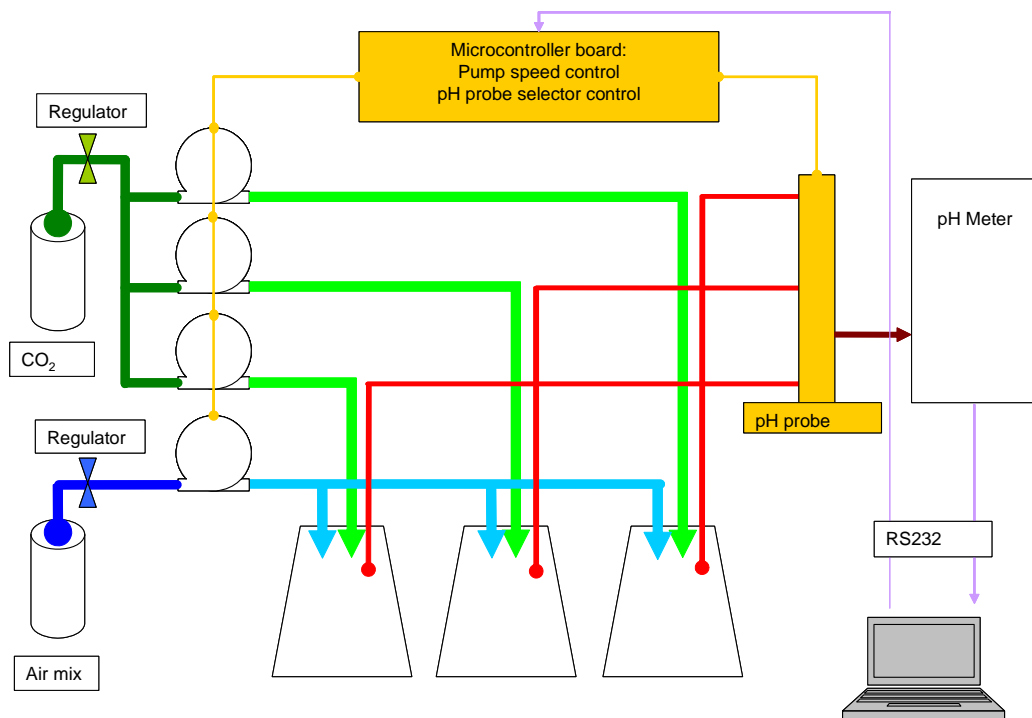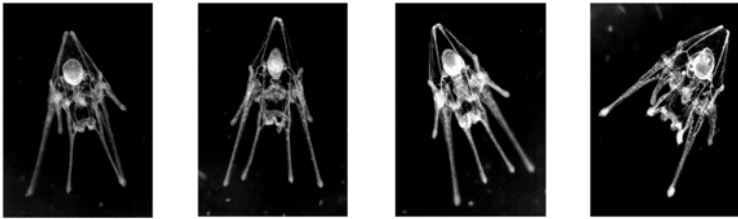
Figure 2.1 Schematic diagram of the system used for the multifactorial CO_2 bubbling experiment. The system simulated four different conditions; normal air containing present atmospheric levels (~385 ppm) as a control, two predicted ocean acidification scenarios for the year 2100 (of 750 ppm and 1200 ppm), and one extreme scenario (~1900 ppm).

Water sample aliquots in triplicate for dissolved inorganic carbon (DIC) and total alkalinity (TA) were collected before starting the experiment (initial condition) and at the end of the experiment to assess the changes in carbonate chemistry of the seawater during growth of the sea urchin larvae. The samples were stored in sealed borosilicate

29

glass bottles and an aliquot of $HgCl_2$ (0.4 mM) was added to prevent microbial growth (see Appendix 3). TA and DIC were measured using the Versatile INstrument for the Determination of Titration Alkalinity (VINDTA). From TA and DIC, aragonite and calcite saturation (Ω-Arg and Ω-Cal), pCO_2, seawater pH_{total}, CO_2, HCO_3^- and CO_3^{2-} concentrations were calculated with the *in situ* temperature, salinity, and nutrient concentration. The CO2 System Calculation Program (Lewis and Wallace 1998) (using the constants of Millero; KSO4 Dickson; pH: total scale; cited in Lewis and Wallace, 1998) was used and values corrected for density in Matlab R2009a (The MathWorks, Inc. 2009). Water carbonate chemistry for the duration of the experiment (21 days) is provided in Appendix 6.

Table 2.1 Physicochemical parameters of the acidified seawater used during sea urchin *Psammechinus miliaris* exposure. SD indicates the standard deviation of triplicate measurements.

Data set derived from the experiments			
Water carbon chemistry			
TA (μmol kg^{-1})	2394.48 ± 25.24	2404.38 ± 14.41	2403.13 ± 8.12	2451.27 ± 11.38
DIC (μmol kg^{-1})	2165.32 ± 8.02	2254.65 ± 12.55	2305.12 ± 16.86	2359.14 ± 122.79
pH_{total}	8.05 ± 0.03	7.87 ± 0.05	7.74 ± 0.02	7.46 ± 0.05
pCO_2 (μatm)	416.96 ± 37.60	665.76 ± 93.59	926.41 ± 61.91	1895.63 ± 199.92
CO_2 (μmol kg^{-1})	15.66 ± 1.44	25.01 ± 3.51	34.80 ± 2.32	71.22 ± 7.51
HCO_3^- (μmol kg^{-1})	1983.80 ± 10.44	2111.16 ± 23.34	2180.38 ± 18.89	2301.01 ± 35.52
CO_3^{2-} (μmol kg^{-1})	165.86 ± 13.41	118.48 ± 14.89	89.94 ± 4.39	49.20 ± 6.69
Ω-Cal	3.93 ± 0.31	2.80 ± 0.35	2.13 ± 0.10	1.16 ± 0.15
Ω-Arg	2.52 ± 0.20	1.80 ± 0.22	1.37 ± 0.06	0.75 ± 0.10

2.2.4   Particulate carbon analyses

From each experimental condition the total particulate carbon (TPC) and particulate organic carbon (POC) were analysed using 50 larvae in triplicate for every pCO$_2$ condition. Once the larvae were collected, they were washed 3 times in phosphate buffered saline (PBS) buffer to rinse off seawater. The larvae were pipetted into pre-combusted silver capsules (Elemental Microanalysis, UK) and stored at -20°C for further analysis. Knowing the exact number of collected larvae reduces uncertainties in the measurement of carbon per larvae, since the precise bulk carbon averaged per 50 larvae is known. To measure POC, inorganic carbon was removed by acidification using a concentrated HCl solution under vacuum for 96 hours. POC and TPC capsules were dried at 60°C for 48 hours, and analysed on a Thermo Finnegan flash EA1112 elemental analyser using acetanilide as the calibration standard (see Appendix 5 for full details of methodology). Particulate inorganic carbon (PIC) was calculated by subtracting the POC from the TPC values (Riebesell *et al.* 2000).

2.2.5   Statistical analyses

All dependent variables (fertilization success, POA, BL and St) were analysed by one-way ANOVA with pH as a fixed factor. The parametric Tukey Test for multiple comparisons was used for *post hoc* analyses. The One-Sample Kolmogorov-Smirnov test (POA, P >0.150; BL, P >0.150; and St, P >0.150) was used to ensure that the distribution was homogeneous and normally distributed. Analyses were performed using Minitab 15 (Minitab 15® Statistical Sotware for Windows®, 2007, Coventry, UK) and Statistica 9 (StatSoft, Inc. Oklahoma, USA) software.

2.3   RESULTS

2.3.1   Experimental seawater carbonate chemistry

During the experimental conditions the water carbonate chemisty varied from the initial conditions with higher CO_2 concentrations. Dissolved inorganic carbon (DIC) and bicarbonate ions (HCO_3^-) increased while carbonate ions (CO_3^{2-}) and Ω-Cal decreased from day 0 to day 21 for all treatments (see Appendix 6 for full carbonate chemistry). These changes reflect the DIC and TA concentrations variability that are mainly affected by photosyntesis, larval respiration (CO_2 release), material descomposition and calcium carbonate formation or dissolution. Calcium carbonate formation decreases both DIC and TA when $CaCO_3$ precipitates.

2.3.2   Effects on fertilization

The fertilization rate of the sea urchin *P. miliaris* decreased by approximately 30% with increasing pCO_2 concentrations (207 to 2036 ppm, pH 8.2 to 7.4). There was a significant reduction in fertilization success from 95% (pH = 8.2) to 65% (pH = 7.4) ($F_{3, 60}$ = 49.98 P < 0.01) (Fig. 2.2 A). The data showed a 20% decrease of fertilization success for pH conditions (pH 8.2 to 7.7, see Table 2.2) which, according to Caldeira (2005), lies within predicted ocean acidification scenarios for the year 2100. At the highest CO_2 condition, survival was greater than 70% at pH 7.4 (pCO_2 = 1895). However, the CO_2 stressor factor showed there was a rise in larvae mortality as pCO_2 increased (Fig. 2.2 B). Statistical analysis (Tukey Post-hoc test) indicated that the survival was dependent on seawater pH ($F_{3, 8}$ = 17.52 P < 0.001).
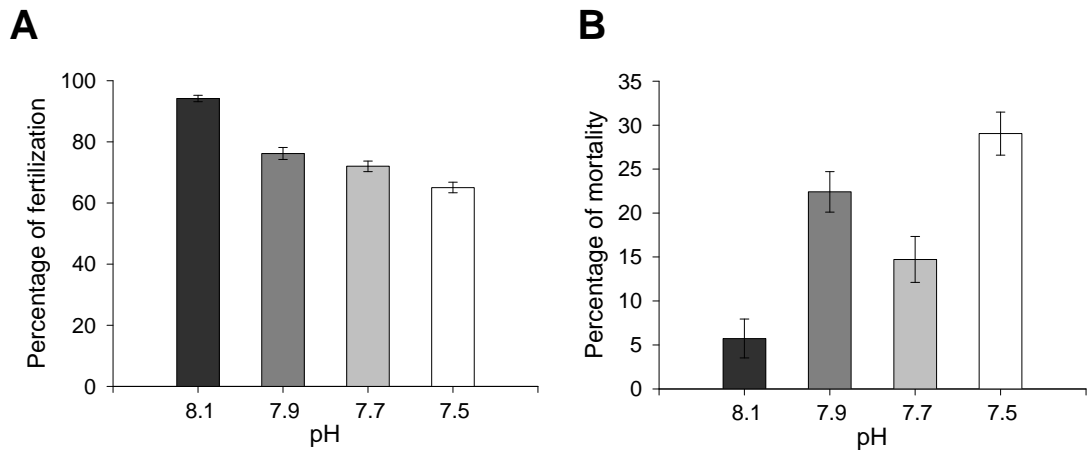
Figure 2.2 Effect of pH_{Total} on the percentage of fertilization (A) and mortality (B) of *P. miliaris*. The mortality was calculated for the last sampling day (total duration of 21days).

2.3.3 Effects on larval growth under hypercapnic conditions

The chronology of development of *P. miliaris* pluteus larvae followed the pattern described by Shearer 1914. Throughout the experiment duration, both larval morphological parameters (POA and BL length) showed no notable change during developmental stages. The exception to this was on day 3 where larvae growth showed a significant reduction in POA ($F3, 37 = 13.09$ $P < 0.01$) and BL ($F3, 37 = 9.96$ $P < 0.01$) lengths at the lowest pH condition (7.4) (Fig. 2.3 A,B). A high proportion of the larvae culture at high pCO_2 (1895 ppm) had shorter antero-lateral arms (ALA) and preoral arms (PROA) than the control (Fig. 2.6).

The data showed that there was no significant effect on larval size (POA and BL) with respect to increasing levels of pCO_2. Accordingly, the particulate organic carbon (POC) results revealed comparable values for all treatments with respect to the larval size tissue (Fig. 2.4 and Table 2.2). The larvae showed no delay in developmental stage all sampled specimens presented 2, 4, 6 and 8 arms according to the time of development, independent of the treatment.

Table 2.2 Summary of one-way ANOVA comparing the effect of different levels of $p\mathrm{CO_2}$ with fertilization success, morphology and particulate carbon on the sea urchin larvae *P. miliaris*. SE indicates the standard error of triplicate measurements.

	Treatment	Treatment	Treatment	Treatment	Statistics
	Mean ± SE / N	Mean ± SE / N	Mean ± SE / N	Mean ± SE / N	One-way ANOVA
A) Percentage of					
Fertilization (%)	94.16±1.04 / 16	76.18±1.96 / 16	72.00±1.73 / 16	65.05±1.73 / 15	$F_{3, 60}$ = 49.98 P < 0.01
Mortality (%)	5.73±2.22 / 3	22.41±2.3 / 3	14.72±2.61 / 3	29.04±2.45 / 3	$F_{3, 8}$ = 17.52 P < 0.001
B) Morphology [a]					
Postoral arm (mm) $_i$	0.531±0.012 / 11	0.559±0.009 / 9	0.574±0.007 / 11	0.476±0.016 / 10	$F_{3, 37}$ = 13.09 P < 0.01
Postoral arm (mm) $_f$	0.928±0.014 / 11	0.910±0.011 / 12	0.871±0.024 / 13	0.900±0.031 / 12	$F_{3, 44}$ = 1.14 P = 0.342
Body length (mm) $_i$	0.398±0.008 / 11	0.403±0.003 / 9	0.405±0.005 / 11	0.357±0.009 / 10	$F_{3, 37}$ = 9.96 P < 0.01
Body length (mm) $_f$	0.536±0.008 / 11	0.535±0.007 / 12	0.544±0.009 / 13	0.521±0.006 / 12	$F_{3, 44}$ = 1.51 P = 0.225
Stomach area (mm^2) $_i$	0.006±0.000 / 11	0.006±0.000 / 9	0.005±0.000 / 11	0.004±0.000 / 10	$F_{3, 37}$ = 6.16 P < 0.01
Stomach area (mm^2) $_f$	0.011±0.000 / 11	0.010±0.000 / 12	0.012±0.000 / 13	0.009±0.000 / 12	$F_{3, 44}$ = 5.51 P < 0.01
C) Particulate carbon [b]					
TPC (µg C)	0.227±0.012 / 3	0.225±0.013 / 3	0.192±0.004 / 3	0.218±0.010 / 3	$F_{3, 8}$ = 2.27 P = 0.157
POC (µg C)	0.178±0.008 / 3	0.202±0.011 / 3	0.189±0.011 / 3	0.211±0.008 / 3	$F_{3, 8}$ = 2.06 P = 0.184
PIC (µg C)	0.045±0.007 / 3	0.022±0.003 / 3	0.010±0.000 / 3	0.007±0.003 / 3	$F_{3, 8}$ = 15.77 P < 0.01
PIC:POC	0.255±0.039 / 3	0.168±0.056 / 3	0.056±0.004 / 3	0.034±0.017 / 3	$F_{3, 8}$ = 8.36 P < 0.01
D) Carbonate ratios [c]					
CO_3^{2-} : HCO_3^- $_i$	0.145±0.001 / 3	0.117±0.007 / 3	0.074±0.005 / 3	0.019±0.003 / 2	$F_{3, 7}$ = 93.66 P < 0.001
CO_3^{2-} : HCO_3^- $_f$	0.083±0.004 / 3	0.056±0.004 / 3	0.041±0.001 / 3	0.021±0.001 / 2	$F_{3, 7}$ = 51.86 P < 0.001

[a] 9 to 13 larvae were analysed for each parameter

[b] Measurements taken during the 21st day of development 8-armed pluteus larvae (50 larvae in triplicates were analysed). The particulate carbon values are per larva.

[c] Measurements taken at day 0 (initial condition = i) and at day 21 (final condition = f).

Note: The initial condition for the morphological measurement is at day 3 (i) of development 4-armed pluteus larvae.
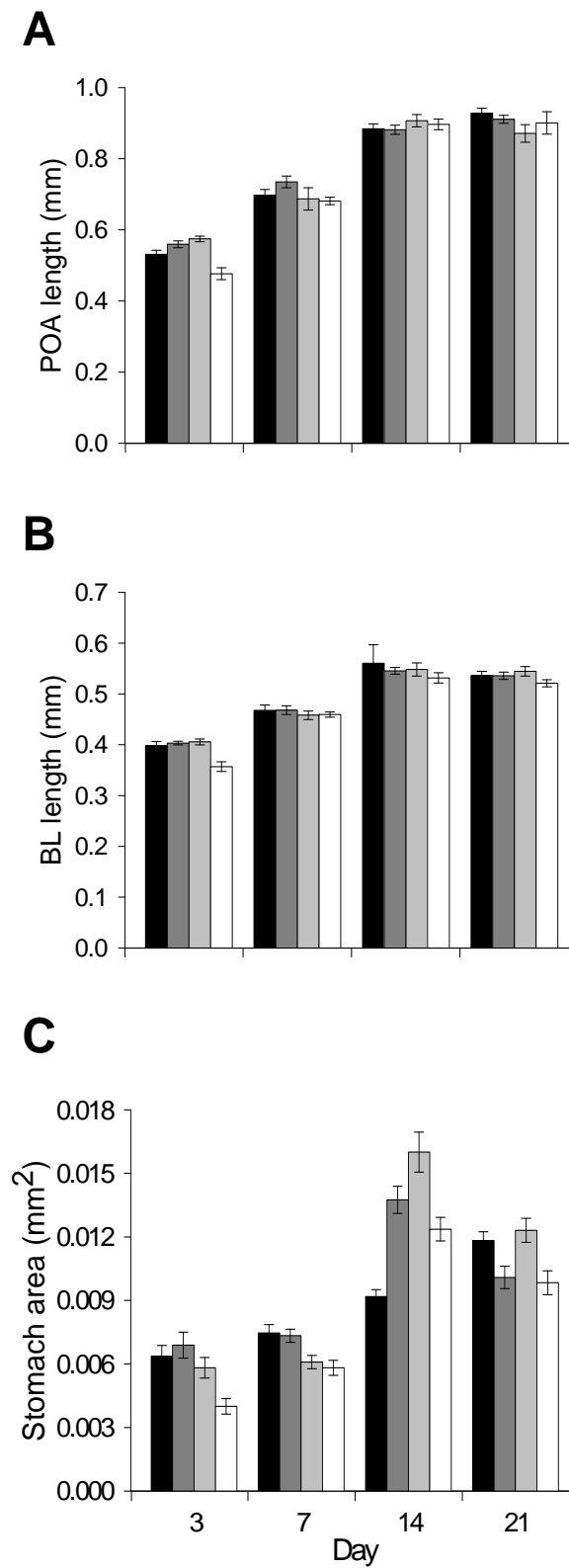
Figure 2.3 Morphological changes in the larval parameters (A) postoral arm length (POA), (B) body length (BL) and (C) stomach area during the experimental period. pH is represented as black bars, 8.1; dark grey bars, 7.9; light grey bars, 7.7; white bars, 7.5. Values are means ± SE.

2.3.4   The effect on feeding structures of the larvae under hypercapnic conditions

Additionally, the effect of pCO_2 levels on the larval stomach size was investigated. The results showed a direct relationship between CO_2 and larval gut area in every treatment throughout the duration of the experiment (Fig. 2.3 C). The stomach area for pH 7.7 (pCO_2 = 926 ppm) was significantly larger on day 14 at the 6-armed pluteus ($F_{3, 38}$ = 20 $P < 0.01$) and day 21 at the 8-armed pluteus ($F_{3, 44}$ = 5.51 $P < 0.01$) than those seen in other treatments. In general the stomach area decreased when exposed to the lowest pH condition in all sampling days (with the exception of the control on day 14). Larvae from all cultures were consistently observed with full stomachs, regardless of pH level.

2.3.5   Larval skeleton

Seawater CO_2 and the associated carbonate chemistry did not cause a visible corrosion on the larval skeletons. However, there was an apparent difference in skeleton structures as a result of changes in CO_2 concentrations. The skeletal rods from the larvae grown in control pCO_2 showed bigger skeletal structures compared to the lower pH treatment as revealed by the scanning electron microscopy examinations (Fig. 2.6). Additionally, evidence is presented of the plasticity of skeletal growth. The larvae showed a detrimental reduction in particulate inorganic carbon (PIC) and the ratio of carbonate and bicarbonate ions (CO_3^{2-} : HCO_3^-) as an index of calcification. Calcified organisms (such as sea urchin larvae) can regulate an increase in HCO_3^- concentration through the dissolution of calcite (Clark *et al.*, 2009). The present results indicate a decrease (~80%) in production of PIC for pH 7.7 (PIC = 0.010 μg C) and pH 7.4 (PIC = 0.007 μg C) compared to the control (PIC = 0.045 μg C) (Fig. 2.4).
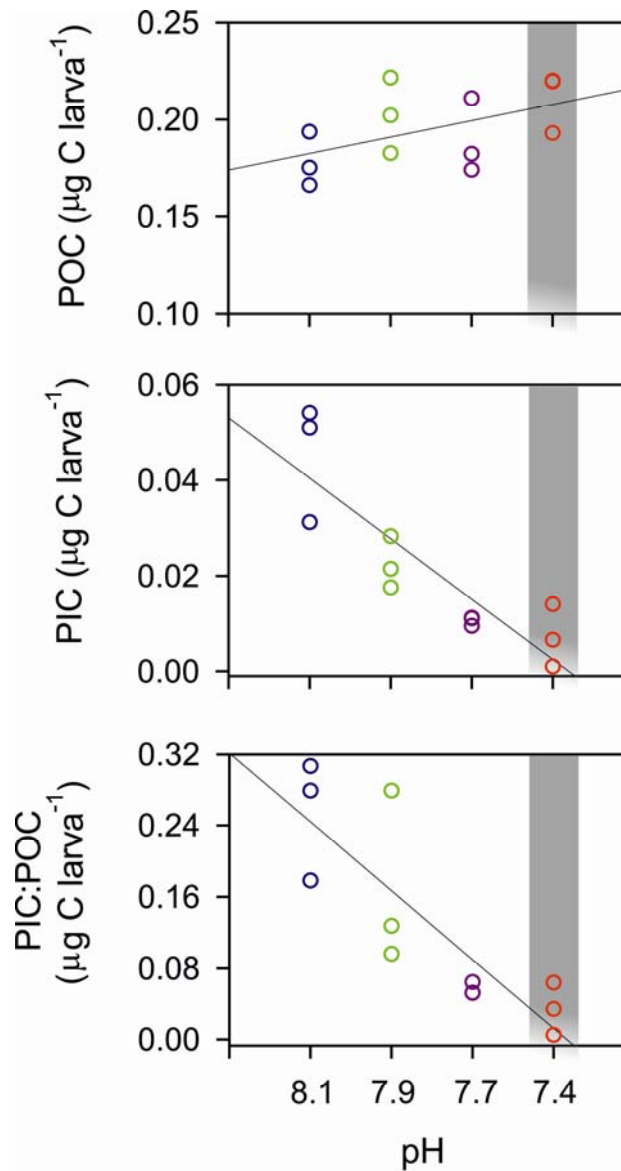
Figure 2.4 Mean values for particulate organic carbon (POC), particulate inorganic carbon (PIC) and PIC:POC ratio per larva. Grey rectangles highlight the undersaturated conditions with respect to Ω-Arg

This reduction in PIC production is in agreement with a decrease in the uptake of CO_3^{2-} : HCO_3^- from 0.145 to 0.019 for the first day of the experiment (gastrula stage), whereas on day 21 (8-armed pluteus larvae) the uptake was reduced from 0.083 (pH = 8.1) to 0.021 (pH = 7.4) (Fig. 2.5). These results suggest that the calcification index of the sea urchin larvae *P. miliaris* presents an adaptive plasticity (significantly shorter skeletal arm rods) to different pH conditions.
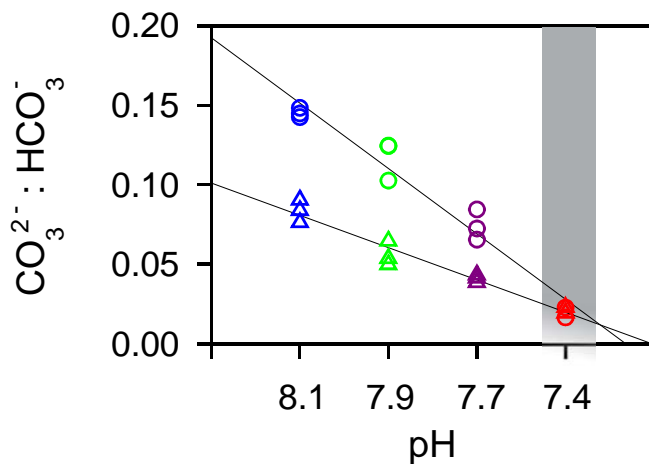
Figure 2.5 Mean values bicarbonate (HCO$_3^-$) and carbonate ion (CO$_3^{2-}$) ratio in *P. miliaris* larvae. Circles represent conditions for the first day of the experiment (gastrula stage), and triangles day 21 (8-armed pluteus larvae). Grey rectangles highlight the undersaturated conditions with respect to Ω-Arg.

2.4   DISCUSSION

2.4.1   Fertilization success under ocean acidification conditions

The elevated CO$_2$ conditions (hypercapnia) decreases the fertilization success on the sea urchin *P. miliaris*. One reason for the decrease in fertilization is likely to be the diffusion capability of CO$_2$ across the cell membrane. It is known that in marine organisms, blood gases are close to equilibrium with the ambient water (Pörtner and Reipschläger, 1996). Therefore, any increase in seawater *p*CO$_2$ will lead to an increase in intracellular CO$_2$ until a new level sufficient to restore CO$_2$ extrusion is reached. Studies by Johnson *et al.* (1976) and Payan *et al.* (1983) suggest that during fertilization the intracellular pH of the sea urchin embryo increases by 0.3 units; from 7.3 to 7.6, and the level is maintained by a proton exchange (Na$^+$/H$^+$) and by excreting H$^+$ (Payan *et al.*, 1983). Egg fertilization is a rapid process, occurring within seconds (Strathmann, 1987) therefore the compensation with increasing seawater *p*CO$_2$ in the extracellular environment is probably limited. Recent studies found that the sperm motility and swimming speed in the sea urchin *Heliocidaris erythrogramma* decreased when

exposed to seawater pCO_2 1000 ppm (pH = 7.7) compared to the controls (Havenhand *et al.*, 2008). Fertilization is a fragile process and sea urchins might encounter an evolutionary disadvantage if the eggs need to balance the internal pH with the surrounding seawater by an exchange of extracellular Na^+ for intracellular H^+ (Johnson *et al.*, 1976).

2.4.2   Larval growth, development and calcification

The effect of high levels of pCO_2 on larval growth was investigated once the eggs were fertilized. For practical purposes, the embryos were placed in the experimental flasks once they had developed to the second and third cell division. In this way, the unhealthy or failed embryos were excluded during the exposure to elevated CO_2 in the first few hours of fertilization. The decrease of fertilization may be due to the intracellular increase in pH that is required. However, Johnson *et al.* (1981) concluded that in the sea urchin embryos of the species *Lytechinus pictus* and *Strongylocentrotus purpuratus* the fluctuations of pH during cell division are not significant. This would suggest that pH is not the major regulator of protein synthesis during embryological development (after the first and second cell divisions).

Even though there was a small decrease in larval size at lower pH levels, the data presented here shows that the experimental exposure to reduced pH and the associated changes in seawater carbonate chemistry did not exhibit a detrimental effect on larval size even in the presence of near and/or undersaturated conditions (where Ω-Cal = 1.16 and Ω-Arg = 0.75). This suggests that the early life history of *P. miliaris* is likely to tolerate a broad range of pH, characteristic of their habitat due to photosynthetic activity (e.g. pH 8.3- 7.5) (as proposed by Menendez *et al.,* 2001; Wootton *et al.,* 2008).

Additionally, the effect on the size of the larval stomach was studied. In marine invertebrates with planktotrophic larval stages, once the digestive tract differentiates, the larvae can feed but do not require food to continue development because maternal nutrients are still available (Sewell *et al.*, 2004; Byrne *et al.*, 2008). An effect on the gut size, suggested that elevated pCO_2 might threaten the larval feeding process. Any

further increase in the stomach area after maternal sources are exhausted (8 days are reported as the longest period post-fertilization, see Byrne *et al.* 2008) may be caused by the larval need of food. The physiological role of the echinopluteus larval gut may be an important nutrient storage organ (Bertram and Strathmann, 1998; Byrne *et al.*, 2008). The results of the present study suggest there is a developmental plasticity in stomach size during exposure to different pH conditions. Well fed and "healthy" larvae are able to develop at a faster pace than under-fed larvae since less energy is spent on the growth of larval arms, leaving more to develop the rudiment. This more rapid development rate reduces the time needed to metamorphise, thereby increasing survival rate (in accordance with studies by Bertram and Strathmann, 1998; Byrne *et al.*, 2008).

Another noteworthy finding is the acclimation of the echinoplutei larvae to high levels of pCO$_2$ with time. Higher CO$_2$ levels exerted a negative effect on larval growth for the first developmental stage (gastrula and 4-armed pluteus). However, this negative effect was overcome by the larvae after the 4-armed stage (after day 7).

2.4.3   Calcification of echinoplutei larvae

Increasing concentrations of CO$_2$ in the ocean increase the solubility of calcium carbonate biominerals (Fabry *et al.*, 2008). It is these minerals that are used to build the larvae skeleton by echinoplutei. It may be expected that CO$_2$-enriched waters would result in a slow-down in the overall calcification process.

The high magnesium calcite skeleton of echinopluteus and brittlestars larvae (Politi *et al.*, 2004; Politi *et al.*, 2006) is integral to larvae survival. The skeleton helps to maintain larval body shape for orientation, buoyancy and migration (Strathmann, 2000; Kurihara, 2008), for feeding (Bertram and Strathmann, 1998; Strathmann, 2007), as a defence against predators (Emlet, 1982) and as a pH regulation (Johnson and Epel, 1981). Any slow-down in the rate of calcification is likely to have a knock-on effect on larval mobility, feeding, and settling leading to a potential increase in the mortality rate (Staver and Strathmann, 2002). Results from this investigation lead to the conclusion that there is a causal relationship between abnormal skeletogenesis and gut size of the

sea urchin larvae *P. miliaris* and its ability to develop. Any prolonging of the planktonic development stage will further expose larvae to predators, subsequently increasing their mortality rate.

Results also suggest that the degree to which larvae acclimate to ocean acidification will depend on their ability to calcify. Data suggest that a higher-acidity ocean and hypercapnia have a detrimental effect on the skeletogenesis of echinopluteus larvae, and hence their ability to calcify. This assertion is in line with several other studies which highlight the negative effect of ocean acidification on the skeletogenesis of other marine species [sea urchins: (Kurihara, 2008; Byrne *et al.*, 2009; Clark *et al.*, 2009; Sheppard Brennand *et al.*, 2010); brittlestar: (Dupont *et al.*, 2008; Wood *et al.*, 2008); and other marine species: oyster: (Gazeau *et al.*, 2007; Watson *et al.*, 2009); corals: (Kleypas *et al.*, 2006)].
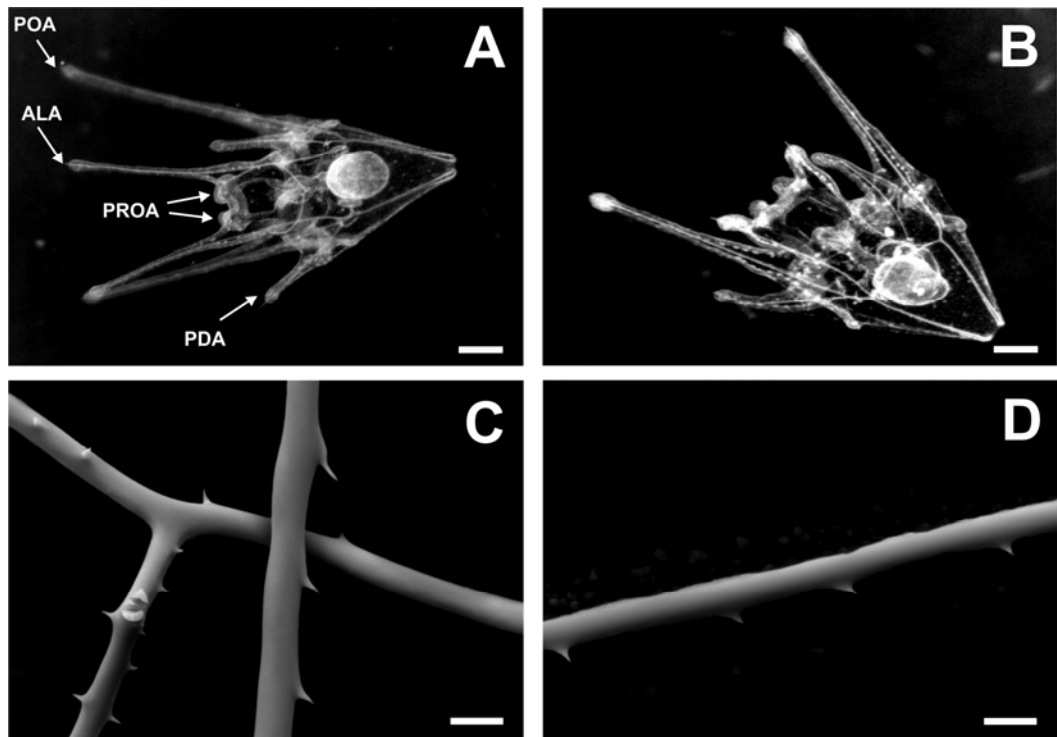
Figure 2.6 *Psammechinus miliaris* morphological parameters: postoral arm (POA), antero-lateral arm (ALA), preoral arm (PROA) and postero-dorsal arm (PDA) of a 21 days larvae grown under control pH =8.1 (A) and lowered pH =7.4 (B). Note the absence of ALA for the low experimental pH condition. Scale bar corresponds to 100 μm. Scanning electron micrographs of larval skeletal rods from larvae grown in control pH=8.1 seawater (C) and lowered pH=7.4 seawater (D). Scale bar corresponds to 10 μm.

The detrimental effect that ocean acidification has on the skeletogenesis of the larvae may have implications on the carbon budget given that echinoderms are major contributors to global $CaCO_3$ with more than 5% of the total ocean biological pump (0.1 Pg C yr^{-1} to the global carbon export, see Lebrato *et al.*, 2010). This is important because the effect of a reduction in PIC may scale up to echinoderm adults, which could potentially reduce the production of $CaCO_3$.

2.4.4   Conclusions

Results from this study suggest that these highly versatile larvae may have the potential to acclimate, throughout their developmental life, to the future projected environmental conditions even in the presence of nearly-undersaturated waters. Intertidal species are adapted to environments with high CO_2 gradients [similar to Antarctic species (Clark *et al.*, 2009)] and have developed a high capacity to changes in seawater carbonate chemistry. The limits to acclimation are set by trade-offs at a calcification level.

The larvae showed phenotypic plasticity during skeleton growth under high CO_2 concentrations. Larvae growing under high CO_2 concentrations were not able to grow as long skeletons as larvae of the same age from the control treatment. The difference in larval skeleton growth must result from a metabolic trade-off through minimising energy to calcify their skeletons in order to continue development and achieve metamorphosis during climate variability.

Whether or not decreased skeletal growth would compensate for high levels of CO_2 cannot be determined from this experiment alone. The phenotypic plasticity of skeleton growth under high CO_2 conditions enables the larvae to develop at the same stage compared to the control. However, it is not know whether the implications for a smaller skeleton production might have consequences at a post-larval stage (e.g. a delay in metamorphosis or smaller and weaker juveniles). If there were no implications at a later developmental stage then the phenotypic plasticity of skeleton growth might be adaptively and functionally significant to compensate for environmental stress.

CHAPTER 3

THE ACCLIMATION OF ECHINODERM LARVAE TO CO$_2$-ENRICHED DEEP OCEAN WATERS

3   THE ACCLIMATION OF ECHINODERM LARVAE TO CO_2-ENRICHED DEEP OCEAN WATERS

3.1   INTRODUCTION

In the marine environment, organisms with alternating pelagic and benthic life stages populate distinct parts of the water column during their life history, therefore encountering variable carbonate chemistry conditions. In particular, many echinoderms have a meroplanktonic life stage, entering pelagic waters until they settle at the seabed (where they undergo metamorphosis), and develop to adult stages. They have a wide distribution, from shallow waters in the continental shelf to the deep-sea in all oceans and at all latitudes.

Echinoids are one of the five classes of echinoderms, playing a key role in maintaining the balance and energy flow in marine ecosystems (e.g. grazing, burrowing, calcifying) (McClintock 1994, Turon et al. 1995). Additionally, they channel elements and export carbon, in some cases more than 1000 g $CaCO_3$ m^{-2} yr^{-1}, contributing to the global echinoderms carbonate export (> 0.1 Pg C yr^{-1}) (Lebrato et al. 2010). These organisms inhabit waters that are increasing in CO_2 concentration at a rate that is already measurable (Sabine et al. 2004), as a consequence of anthropogenic carbon emissions. The accelerated dissolution of CO_2 in seawater or "ocean acidification" (Caldeira & Wickett 2005) results in an increased concentration of hydrogen ions (H^+), bicarbonate ions (HCO_3^-), and a decrease of carbonate ions (CO_3^{2-}). This is important because CO_3^{2-} largely controls the saturation state of calcium carbonate (Ω-Cal = [CO_3^{2-}][Ca^{2+}]/K_{sp}) (< 1= undersaturation; > 1= supersaturated) where K_{sp} is the solubility constant for the $CaCO_3$ biomineral (Mucci 1983).

The chemical changes induced by increasing CO_2 are known to affect the physiology of pelagic and benthic organisms including corals (Langdon et al. 2000), coccolithophores (Riebesell et al. 2000, Zondervan et al. 2001, Iglesias-Rodriguez et al. 2008), molluscs (Gazeau et al. 2007, Gazeau et al. 2010) and echinoderms (including echinoid larvae) (Dupont et al. 2008, Clark et al. 2009). Recent concern about the

ongoing decrease in Ω -Cal caused by ocean acidification has raised questions about the future of echinoderm populations, and their contribution to the marine carbon cycle.

Echinoderms may be susceptible to changes in the water carbonate chemistry, including changes in CO_2 and Ω-Cal, which they encounter during their life history from larvae (pelagic) to adult stages (benthic). These changes have been mainly assessed in laboratory enclosures where controlled environmental conditions allow the exploration of individual responses (e.g. morphological, developmental, and biochemical) to high CO_2 conditions. However, laboratory incubations heavily depend on artificial manipulations of the medium chemistry (Riebesell et al. 2010), thus they are necessarily an abstraction from the ocean.

Natural carbonate chemistry gradients provide the opportunity to incubate organisms without interfering with the medium chemistry. These gradients are experienced in the oceans as a consequence of different processes. Firstly, water column stratification/ventilation. In the water column, CO_2 increases with increasing depth as a result of *in situ* pressure, but it is also induced by the water masses respiration of sinking and decomposing biogenic material. Therefore, CO_2 concentrations increase (Ω-Cal decreases) at shallower depths from the Atlantic to the Pacific Ocean (Feely et al. 2004). The calcite compensation depth (CCD), below which the rate of production of $CaCO_3$ is exceeded by its rate of dissolution, is critical to organisms such as echinoderms that form $CaCO_3$ skeleton during their life cycle (Feely et al. 2004, Fabry et al. 2008), controlling the magnitude of exported biomineral to the ocean's interior. The CCD has moved closer to the surface and nearer to the coast owing to anthropogenic emissions and the increasing oceanic uptake of CO_2 (Feely et al. 2004, Feely et al. 2008). Recent research on echinoderms suggests that deep-sea populations (in the Southern Ocean) are already at the boundaries of the CCD undersaturated waters at 3000 m, and organisms below those depths have weakly calcified skeletons (Sewell & Hofmann 2010). Secondly, gradients are experienced in the oceans as a result of natural upwelling events whereby deep CO_2-rich and low Ω-Cal waters surface in seasonal processes associated with major coastal currents such as the Canary Current (off northwest Africa), the Benguela Current (off Namibia), the Humboldt Current (off Peru and Chile), the Somali Current (off Somalia) and the California Current (off

California and Oregon) (Mann & Lazier 1991). Oxygen minimum zones (OMZs) are associated with some upwelling events (e.g. Humboldt Current and the Arabian sea) and provide a field opportunity to test natural carbonate chemistry gradients (Paulmier et al. 2011). In shelf seas, seasonal upwelling (from shallow depths) of low oxygen and high CO_2 water masses (e.g. Baltic Sea) could also be used as a natural testing site (Thomsen et al. 2010). Thirdly, geophysical features (e.g. volcanic CO_2 vents); natural venting sites occur at the seabed as a consequence of volcanic activity, which emits CO_2 (> 90%), among other gases. These sites have been used to test natural gradients of CO_2 on benthic communities (Hall-Spencer *et al.* 2008, Cigliano *et al.* 2010) and also on pelagic calcifyers (Passaro *et al.* 2011).

At present, little is known about the effect of naturally high CO_2 and low Ω-Cal waters on the ecological success and physiological performance of marine biota. Therefore, for the first time the natural vertical gradient of the water column in ~5000 m of water in the North Atlantic Ocean was used to investigate the effects on development and biogeochemical features of the larvae of the sea urchin species *Psammechinus miliaris*. The waters used have distinct carbonate chemistries that allow for testing short term responses and the biological plasticity of sea urchins to physico-chemical changes in a natural medium.

Given that deep-sea environments are naturally associated with high CO_2 concentrations and low Ω-Cal conditions (Feely *et al.*, 2004), this study provides a natural laboratory which does not rely on manual carbon chemistry manipulation, to test the effect of 'acidified' waters. Additionally, this study sheds light on the extent of evolutionary adaptation of larvae to environmental change and the potential colonisation of deep-sea environments by tolerating broad carbonate chemistry conditions.

3.2   MATERIALS AND METHODS

3.2.1   Study site

The experiment was carried out during May 2009 aboard RRS *James Cook* in the region of the Porcupine Abyssal Plain (PAP) (49 °N, 16 °W; ~ 4840 m water depth). A conductivity-temperature-depth (CTD) rosette at 49 01.559 °N, 015 10.226 °W was used to retrieve water from different depths (250, 2000, 4000, 4600 and 4710 m) representing water masses with different carbonate chemistries (Table 3.1).

3.2.2   Experimental conditions

The echinoid species *Psammechinus miliaris* were hand-collected in the intertidal at Torbay, UK (50° N 3°33′ W) and maintained in aerated seawater aboard RRS *James Cook* until the experiment was conducted. The specimens collected were in healthy condition, and stress was minimized by using the same intertidal seawater, temperature and salinity that the organisms had in their natural environment until the experiments were conducted. All onboard experiments were conducted at 9 $\pm1^{o}$C in a temperature controlled room.

3.2.3   Fertilization and larval culture

The sea urchins were induced to spawn by injection of 1 ml of 0.5 M KCl just before the CTD water was recovered on deck. In the fertilization experiment, the gametes from 4 males and 2 females were collected and the quality of each gamete source was analyzed with a microscope. The sperm motility and the eggs appearance/shape were checked. The eggs were placed in filter-sterilized seawater (0.22 μm filters, Millipore® Steriup™, Sigma-Aldrich) and the sperm were collected dry. The total numbers of eggs used in the experiment were counted from a 20 ml suspension

determined through counts of 100 µl aliquots. In the experiment, the eggs were split into 20 beakers containing 200 ml of experimental water at a density of ~3-4 eggs per ml in each treatment with water from different depths. Fertilization was performed by inoculating 1 µl of the combined sperm from all males. Sperm was activated directly in the vessels containing eggs that had been pre-acclimated to each experimental condition (water from different depths) for ~20 minutes. Sperm was counted using a haemocytometer and a final concentration of 10^3 sperm per ml was calculated, which typically yields high fertilization success and development. After 3 hours, fertilization success was determined as the eggs that had a fertilization envelope or showed cleavage at the 2 to 4 cell stage. Fertilization counts were taken from 4 replicates in each treatment (~60 eggs were taken from the eggs in suspension). To monitor the embryonic and larval morphology, an independent source of gametes was fertilized and placed in triplicate 2.5 litre vessels at densities of 3-4 eggs per ml, for each experimental condition (15 sealed containers to minimize atmospheric CO_2 exchange). The gastrula stage (~24 hours after fertilization) and four-armed pluteus larvae stage (5 days after fertilization) were sampled to assess developmental changes among treatments. Oxygen (mean = 352.1 µM ± 5.4) and temperature (mean = 8.9 ^{o}C ± 0.15) were recorded daily with an Oxygen Optode/Temperature sensor (AANDERAA 3830) in each of the experimental vessels.

3.2.4   Larval development and morphology

Morphological analyses were performed on larval postoral arm length (POA) and body length (BL) in specimens incubated in waters from each depth that were fixed in 4% paraformaldehyde (EM GRADE, Science Services), and cleaned 3 times through filtered sea water. The larvae were mounted on a microscope slide and photographed for analysis. The larval characters were measured using the software Image J (available at http://rsb.info.nih.gov/ij; developed by Wayne Rasband, National Institutes of Health, Bethesda, MD).

3.2.5   Particulate carbon analyses and calcification

Total particulate carbon (TPC) and particulate organic carbon (POC) were analyzed in triplicate using 50 larvae from each experiment. Larvae were isolated and washed 3 times in phosphate buffered saline (PBS) buffer to rinse off seawater. The larvae were pipetted into pre-combusted silver capsules (Elemental Microanalysis, UK) and stored at -20 ^{o}C for further analysis. For POC analysis, inorganic carbon was removed by acidification using a concentrated HCl solution under vacuum for 96 hours. The capsules for both POC and TPC were dried at 60 ^{o}C for 48 hours, and analyzed on a Thermo Finnegan flash EA1112 elemental analyzer using acetanilide as the calibration standard. Particulate inorganic carbon (PIC) was calculated by subtracting the POC from the TPC values (Riebesell et al. 2000). This method reduces uncertainties in the measurement of carbon per larvae, since an exact number of larvae was used to ascertain precisely the bulk carbon averaged per 50 larvae, which was not previously available in larval experiments conducted in the laboratory.

3.2.6   Natural seawater carbonate chemistry

Water sample aliquots for *in situ* dissolved inorganic carbon (DIC) and total alkalinity (TA) were collected directly from the CTD Niskin bottles 15 minutes before starting the experiment (immediately upon recovery of the CTD, to avoid aeration). The second sample point was 24 hours and 120 hours after the start of the experiment to assess the changes in carbonate chemistry of the seawater during the development of the sea urchin larvae. The samples were taken at each experimental depth (in triplicate) and stored in sealed borosilicate glass bottles. An aliquot of $HgCl_2$ (0.4 mM) was added to the samples to prevent microbial growth. The Versatile INstrument for the Determination of Titration Alkalinity (VINDTA) was used to measure TA and DIC. The carbonate system [aragonite and calcite saturation (Ω-Arg and Ω-Cal), seawater pH$_{total}$, partial pressure of CO_2 (pCO$_2$), CO_2, HCO_3^-, CO_3^{2-} concentration] was calculated from measurements of TA, DIC, temperature, salinity, and nutrients using CO2 System Calculation Program (Lewis & Wallace 1998) [using the constants of

Dickson and Millero (Dickson & Millero 1987); KSO_4 Dickson; pH: total scale; cited in Lewis and Wallace, 1998] and corrected for density in Matlab R2009a (The MathWorks, Inc. 2009). The temperature and pressure effects on the water carbonate chemistry were taken into account in the measurements of DIC and TA at the start and end of the experiment (see Table in Appendix 8).

3.2.7   Calculation and representation of Ω-Cal from the WOCE A16 transect line

Oceanographic data in the Atlantic Ocean from 60°N to 60°S used in Figure 3.1 were accessed on the Global Ocean Data Analysis Project (GLODAP) (Key *et al.*, 2004) from the World Ocean Circulation Experiment (WOCE) from cruise line A16N (04/06/2003 to 11/08/2003) and A16S (11/01/2005 to 24/02/2005). The Ω-Cal calculations were made with the software CO2SYS (Lewis and Wallace 1998, Pierrot et al. 2006). In the calculations the dissociation constants were used from Mehrbach *et al.* (1973) refitted by Dickson and Millero (1987), $KHSO_4$ from Dickson (1990), and the input parameters were total carbon (TC), total alkalinity (TA), temperature, salinity, pressure, silicate, and phosphate *in situ*. To construct the transect line profile the data were gridded using the minimum curvature method (e.g. Smith and Wessel, 1990) with 62 field lines (spacing of 3°) in the x-axis (latitude) and 129 field lines (spacing of 50 m) in the y-axis (depth) from 60°N to 60°S and from 0 to 6000 m. The seabed is included (grey) and it is plotted from latitude and pressure data inside a polygon (Fig. 3.1). All data were plotted using the software Surfer v8 [TM] (Golden Software 2002, Colorado, USA).
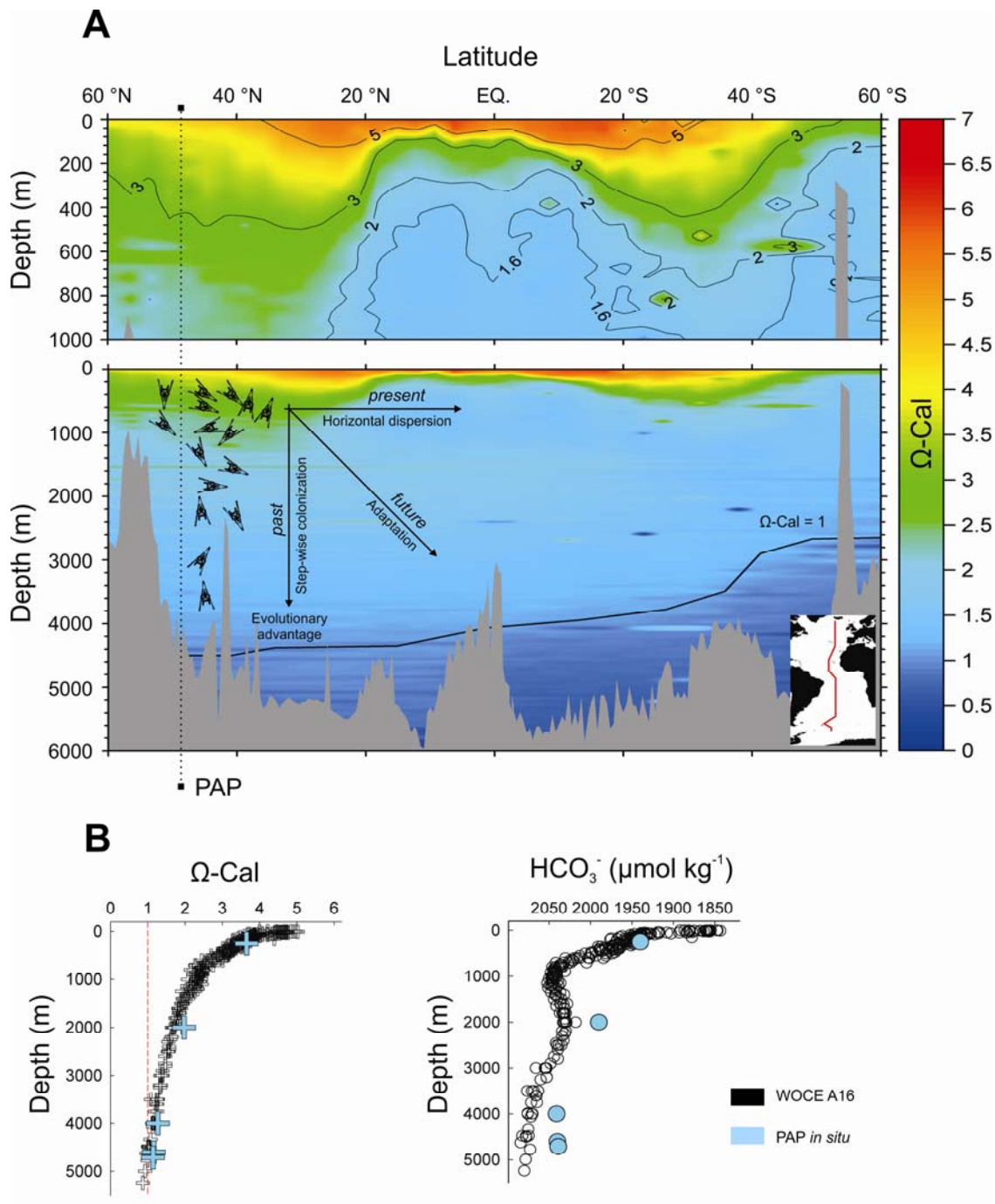
Figure 3.1 (A) The vertical distribution of Ω-Cal along the WOCE A16 (from the GLODAP atlas) transect line in the Atlantic Ocean (map on the right corner) from 0 to 1000 m (top plot) and from 0 to 6000 m (bottom plot). The black line in the bottom plot indicates where Ω-Cal values equal 1 (drawn from an interpolation of the nearest Ω-Cal = 1). PAP denotes the location of the Porcupine Abyssal Plain and the conditions of the current study. Arrows indicate past (vertical gradient and colonization in the water column), present (the possibility of horizontal dispersion/migration), and future (a possible adaptation to environmental change) events involving echinoderm larvae. (B) Ω-Cal and HCO_3^- profiles from 40 °N to 50 °N [using the WOCE A16 transect line data from the GLODAP atlas (Key *et al.*, 2004)] and *in situ* data at the Porcupine Abyssal Plain (PAP; 49 °N, 16 °W).

3.2.8   Scanning electron microscopy of larval skeleton

Larval tissue was removed in a mild solution of hyperchlorite diluted with a solution of distilled water saturated with sodium tetraborate (which acts as a buffer) and filtered to remove any particle in suspension. Samples (skeletal rods) were washed three times with distilled water, mounted in SEM stubs and gold coated. Images were obtained with a Leo 1450VP scanning electron microscope.

3.2.9   Natural seawater elemental composition

The concentrations of calcium (Ca^{2+}) and magnesium (Mg^{2+}) in water samples from all depths were measured to rule out seawater effects on calcification (Table 3.1) following (Ries 2010). Elemental seawater composition was determined in triplicate by inductively coupled plasma optical emission (ICP-OES) using a Perkin Elmer optima 4300DV. The material for the samples was acid cleaned with nitric acid to avoid contamination. Samples were diluted in 0.3M HCl and calibrated against multi-element standard solutions that bracketed the concentration ranges in the sample solutions. Standards were prepared gravimetrically using certified and traceable VWR Aristar single-element standard solutions, Romil UpA nitric acid and Milli-Q water. A standard seawater solution (IAPSO) and Certified Reference Materials (CRM) were analysed for cross-reference.

3.2.10   Statistical analyses

Data analyses were performed in Minitab 15 (Minitab 15® Statistical Software for Windows®, 2007, Coventry, UK) and Statistica 9 (StatSoft, Inc. Oklahoma, USA) software. The experimental data were analyzed with one-way ANOVA (water source as a fixed factor) with four replicates for the fertilization experiment (20 in total) and triplicates for the larval growth (15 containers in total) for every experimental condition to increase accuracy. The morphology data were normally distributed and a One-Sample Kolmogorov-Smirnov test (P >0.150) was used to ensure that the distribution was

homogeneous. Fertilization success, morphometric data and particulate carbon (POC and PIC) were analyzed with a one-way ANOVA. The parametric Tukey test for multiple comparisons was used for *post hoc* analyses.

3.3   RESULTS

3.3.1   Natural seawater carbonate chemistry analyses

At the PAP site (North Atlantic Ocean), as in most ocean basins (Takahashi et al. 1979), there is a gradient of increasing bicarbonate ions (HCO_3^-) and dissolved inorganic carbon (DIC), and a decrease in carbonate ions (CO_3^{2-}) and Ω-Cal with depth, while total alkalinity (TA) remains constant (Fig. 3.1B, Table 3.1). The measured samples (corrected for pressure and *in situ* temperature effect at depth) agreed well with the WOCE A16 transect line data in the region 40 °N-50 °N (Fig. 3.1B).

Under the experimental conditions on board at ~9°C and with surface pressure (1 atm), the water carbonate chemistry gradients were maintained for the water from 250 to 4710 m but with different CO_2 concentrations (see Table 3.1). DIC and HCO_3^- increased from 2116 and 1940 µmol kg^{-1} at 250 m to 2175 and 2024 µmol kg^{-1} at 4710 m. The CO_3^{2-} and Ω-Cal varied from 161 µmol kg^{-1} and 3.84 (at 250 m) to 132 µmol kg^{-1} and 3.15 at 4710 m respectively. These changes reflect the increase in atmospheric CO_2 and the ocean's interior respiration that changes the chemistry in the deep-sea, resulting in a transition of the carbonate system from a predominately calcite-saturated water column above 4000 m to undersaturated conditions below this depth in the Atlantic Ocean.

Table 3.1 Carbonate chemistry, oceanographic experimental conditions and seawater elemental composition.

	Depth (water sample)				
	250 m	2000 m	4000 m	4600 m	4710 m
A) Oceanographic parameters [a]					
Temperature (°C)	11.67	3.44	2.53	2.54	2.55
Salinity	35.60 ± 0.0	34.91± 0.0	34.91± 0.0	34.91± 0.0	34.92 ± 0.0
Oxygen (µM)	357.04 ± 2.8	357.64 ± 1.2	349.25 ± 3.5	347.16 ± 5.6	349.55 ± 3.66
B) Water carbon chemistry [b]					
TA (μmol kg^{-1})	2344.55 ± 4.56	2307.63 ± 3.64	2351.76 ± 4.77	2356.22 ± 1.01	2356.34 ± 4.56
DIC (μmol kg^{-1})	2116.13 ± 3.06	2130.66 ± 5.09	2175.37 ± 3.77	2176.41 ± 3.83	2175.83 ± 0.94
pCO$_2$ (μatm)	314.49 ± 6.35	404.55 ± 1.47	407.27 ± 7.12	414.58 ± 6.29	412.91 ± 9.50
CO_2 (μmol kg^{-1})	14.16 ± 0.52	18.29 ± 0.07	19.31 ± 0.71	18.74 ± 0.51	18.67 ± 0.43
HCO_3^- (μmol kg^{-1})	1940.03 ± 6.51	1982.96 ± 1.36	2028.54 ± 6.71	2025.83 ± 6.06	2024.90 ± 2.46
CO_3^{2-} (μmol kg^{-1})	161.95 ± 4.87	129.70 ± 1.25	128.42 ± 4.40	131.83 ± 2.76	132.27 ± 2.76
Ω_{Cal}	3.84 ± 0.06	3.08 ± 0.01	3.09 ± 0.06	3.14 ± 0.03	3.15 ± 0.03
Ω_{Arg}	2.44 ± 0.07	1.96 ± 0.00	1.94 ± 0.04	2.00 ± 0.04	2.00 ± 0.04
pH_{total}	8.14 ± 0.01	8.04 ± 0.00	8.03 ± 0.02	8.04 ± 0.01	8.04 ± 0.01
C) Seawater elemental composition					
Ca^{2+} (μg g^{-1})	10.59 ± 0.41	10.22 ± 0.10	10.34 ± 0.02	10.46 ± 0.14	10.36 ± 0.07
Mg^{2+} (μg g^{-1})	33.95 ± 1.28	32.74 ± 0.36	33.03 ± 0.01	33.42 ± 0.43	33.04 ± 0.29
Mg:Ca (molar)	5.29 ± 0.00	5.27 ± 0.01	5.25 ± 0.00	5.25 ± 0.01	5.25 ± 0.00

[a] Water sampled obtained with a CTD and Niskin bottles

[b] Water carbon chemistry calculated from TA and DIC values and nutrients. The CO_2 concentrations correspond to the different depths for the Porcupine Abyssal Plain (PAP) site. SD indicates the standard deviation of triplicate measurements.

3.3.2   Fertilization and larval development

The average number of fertilized eggs (monitored after 2 hours post-fertilization) was significantly different across treatments ($F_{4, 59}$ = 14.34 $P < 0.001$), from 250 m to 4710 m (Fig. 3.2 A). Results showed a decrease in fertilization success of 68% in the deepest seawater samples (4000 m, 4600 m and 4710 m) compared to 85% in the shallowest water (250 m).

Development and tissue morphology of *P. miliaris* larvae were not affected by deep water incubations (elevated HCO_3^- conditions and low CO_3^{2-} and Ω-Cal between 4000 and 4710 m). The null effect of the deep water on larval development [POA; $F_{4, 45}$ = 1.75, P = 0.157 and BL; $F_{4, 45}$ = 1.15, P = 0.347] was comparable across treatments over the 5 days of the incubations (Fig. 3.2 B and Table in Appendix 7). The data were especially variable in the incubations with water from below 4000 m.
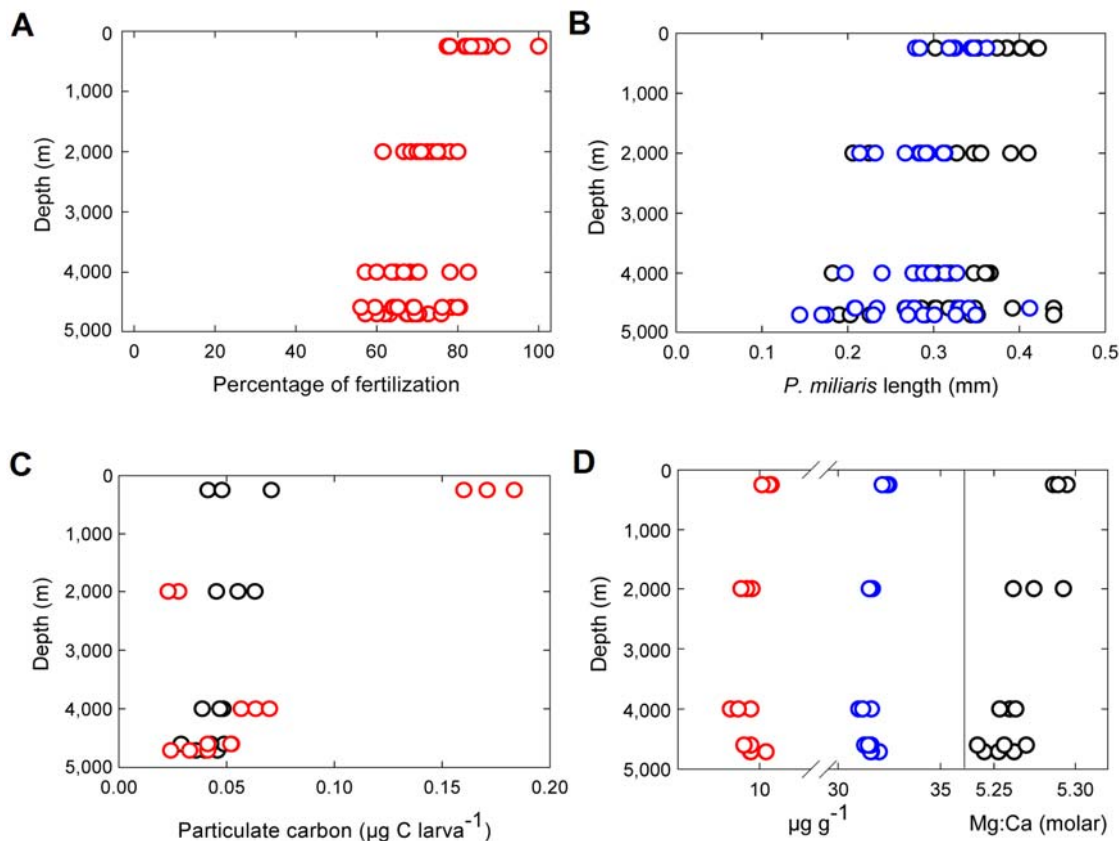
Figure 3.2 Development and growth conditions of *P. miliaris* larvae. (A) Effects on fertilization success, (B) larval morphology [Postoral arm (black) and Body length (blue)], (C) particulate carbon [PIC (red) and POC (black) in triplicates per larva at day 5 of development], and (D) major elements (Ca^{2+} in red and Mg^{2+} in blue) of seawater (Mg:Ca = 5.27 ± 0.01 from 250 to 4710 m).

3.3.3 Particulate carbon and calcification

The incubations allowed investigation of the effect of changes in carbon chemistry on calcification in early stages of *P. miliaris* larvae. Particulate inorganic carbon (PIC) was used as an indicator of calcium carbonate content per larvae. There was a doubling in larval PIC ($F_{4, 13} = 201.26$ $P < 0.01$) in the incubation with water from 250 m in agreement with observations of larger skeletons (Fig. 3.2 C) and the same trend was observed for PIC:POC (Fig. 3.3 A). A decline in calcification was observed in all incubations except from 250 m (the control) with respect to depth.
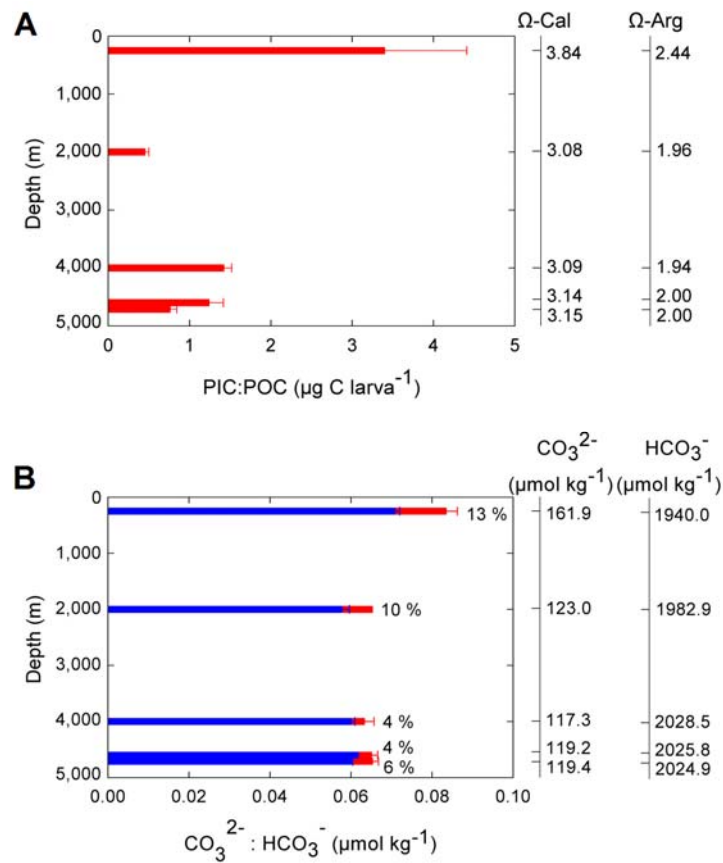
Figure 3.3 Carbon production and chemistry of *P. miliaris* larvae. (A) Organic, and inorganic carbon (values are per larva). (B) Carbonate:bicarbonate ratio. Note that red bars correspond to the beginning of the experiment (day 0) and blue bars to the end (day 5) showing a maximum uptake of 13% of CO_3^{2-} during larval development. Error bars denote SD (n = 3). Also indicated are corresponding values of Ω-Cal, Ω-Arg, [HCO_3^-] and [CO_3^{2-}] against depth.

Scanning electron microscopy examinations revealed a decrease in size of the larval skeletons with decreasing Ω-Cal, although there was no evidence of corrosion. The effect of CO_3^{2-} availability (reduced in deeper waters) on the growth of the larval skeleton revealed an uptake of 13% of CO_3^{2-}:HCO_3^- at the surface 250 m (Ω-Cal= 3.84) compared to a 4-6% in incubations with water below 4000 m (Ω-Cal = 3.15) (Fig. 3.3 B). The reduction in calcification (decrease in PIC and uptake of CO_3^{2-}) was confirmed by observations of smaller spicules as seen by the smaller skeleton rods (Fig. 3.4). Particulate organic carbon (POC) content per larvae was not significantly different across treatments ($F_{4, 13} = 1.04$ $P > 0.05$; Fig. 3.2 C. See Table in Appendix 7 for raw data).
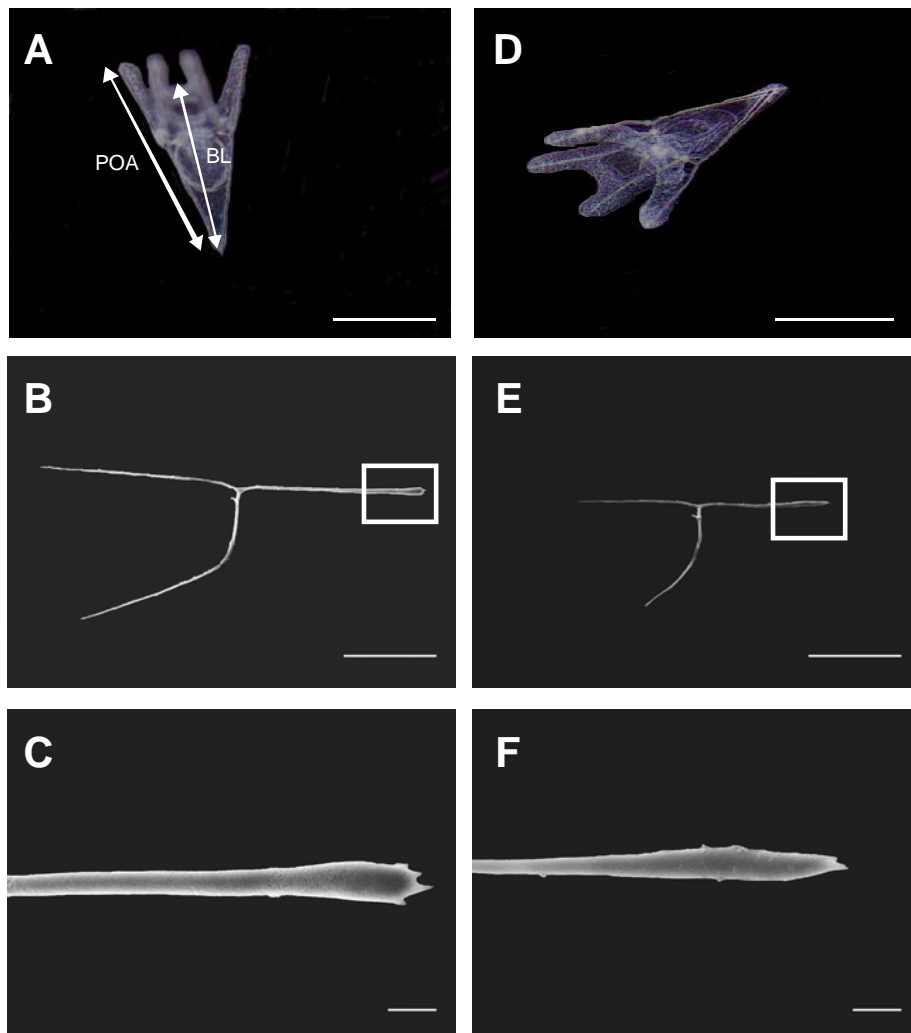
Figure 3.4 Morphometrics and skeletal rods of *P. miliaris* larvae. The whole skeleton of an incubated 5 day pluteus larvae using the shallowest water 250 m (A, B, C) and the deepest 4710 m (D, E, F), scale bar represents 100 μm. Both images have superimposed white rectangles that indicate magnified areas from the tip of the rod (C and F respectively), scale bar refers to 10 μm.

3.4   DISCUSSION

3.4.1   Physiological response of *P. miliaris* to CO_2-enriched deep seawaters

The phenotypic plasticity of *P. miliaris* in the water carbon chemistry gradients presented here shows that shallow water echinoids (e.g. *P. miliaris* occupies intertidal and subtidal areas in the northeast Atlantic) have the potential to adapt to a distinct gradient of carbon chemistry conditions during early development. This tolerance has been reported for early larval development in Antarctic echinoderms (Clark *et al.*, 2009). This is a direct consequence of echinoids evolving in a habitat where pH changes can exceed up to 0.1 units on a daily basis (Menendez *et al.*, 2001), and 0.4 units in months (Wootton *et al.*, 2008). The results indicate a 20% decrease in fertilization success at Ω-Cal values near 3. This is in agreement with some laboratory studies showing that low pH seawater affects sperm motility and speed (Havenhand *et al.*, 2008) and the low intracellular pH of the oocyte may prevent a successful fertilization ((Grainger *et al.* 1979). However, recent studies indicate that acidification does not affect fertilization success in the sea urchin species *Heliocidaris erythrogramma* (Byrne *et al.*, 2010a). This suggests that the susceptibility of fertilization to ocean acidification may be species-specific. The tolerance of the larvae seems to be higher as they already encounter large variations in carbonate chemistry conditions during the larval stage (e.g. the sporadic exposure to deep CO_2 rich water associated with coastal upwelling events, and the diverse chemistry of the ocean currents on which they are transported).

3.4.2   Particulate carbon and calcification

Particulate organic carbon (POC) in the larval body remained almost constant over all depths tested. This is consistent with the lack of change in larval size. However, the decline in larval PIC observed in all treatments compared to the 250 m incubation suggests that under deep seawater conditions the larvae divert energy towards growing soft tissue rather than producing long skeletal rods (inorganic carbon, PIC). The growth of long arms (tissue) explains the increased efficiency of food collection by the larvae

because of the extension of the ciliated bands along the arms (Strathmann, 2007). A decrease in calcification would result in weaker skeletons that could potentially increase larval mortality (Staver and Strathmann, 2002) given that the skeletal rods play an important role in larval feeding, motility and settling. However, the larvae may compensate this PIC loss by allocating energy to other vital functions such as production of soft tissue. The decrease in calcification may also be a consequence of dissolution of high Mg calcite phases (> 4% MgCO$_3$), which appears to occur in the skeleton of sea urchins (Weber, 1969; Politi *et al.*, 2004; Politi *et al.*, 2006; Hermans *et al.* 2010). This is caused by the greater susceptibility to dissolution of calcite with Mg, compared to that of calcite alone (Morse *et al.*, 2006). However it is not clear whether and to what extent MgCO$_3$ is incorporated in early larval stages, and therefore if dissolution is an important process affecting skeleton formation during the first 5 days of development.

3.4.3   The effect of seawater composition on larval development

Seawater collected from different depths typically has different chemical characteristics, and therefore the possibility of water properties other than carbonate chemistry affecting larval physiology cannot be ignore. The elemental composition of seawater, particularly the Mg:Ca, is known to drive calcification and the net inorganic carbon content of many organisms (Stanley *et al.*, 2005; Ries, 2009; Ries 2010). Under all the experimental conditions tested, [Ca^{2+}] and [Mg^{2+}] remained near constant with a slight decrease with depth, staying on an averaged 5.27 molar ratio (Mg:Ca), which is on the upper limit of the Ries (2010) dataset for a variety of calcifying species. Therefore an effect of seawater Mg:Ca ratios on development and carbon acquisition can be eliminated.

3.4.4   Evolutionary adaptation to the deep-sea

The tolerance of *P. miliaris* larvae to the deep-seawater chemistry supports the notion that larval and juvenile stages of organisms are more resilient to environmental

changes than adults given the varied hydrographic conditions and chemistry they experience when transported in the water column (Howell *et al.*, 2002). This contrasts with laboratory incubations, where often larvae/juveniles are seen as the most susceptible to ocean acidification (Kurihara & Shirayama 2004, Dupont *et al.* 2008). Field studies indicate that larvae and juveniles [in species with planktotrophic and lecithotrophic reproduction mode (Sumida *et al.* 2000)] normally inhabit much deeper depths than the adults (> 1000 m deeper in some cases) (Gage & Tyler 1981, Howell *et al.* 2002). This is irrevocable evidence that they encounter (at least in the Atlantic Ocean) carbon chemistries similar to the present study, and that they tolerate them. However, juveniles settling out of adult ranges tend not to survive (Gage & Tyler 1981), leading to the hypothesis that pressure and temperature shape the bathymetric distribution. It is suggested that there may also be an ontogenic tolerance change to distinct carbon chemistries determining the niches for settlement and development.

From an evolutionary perspective, the ability of larvae to cope with broad changes in water chemistry conditions may have determined the ability of shallow water echinoderms to colonise progressively deeper environments early in their evolutionary history (Young *et al.*, 1997; Villalobos *et al.*, 2006; Mestre *et al.*, 2009) (Fig. 3.1 A). Previous studies on deep-sea colonisation of the genus *Echinus* spp. (Tyler and Young, 1998) indicate that the species may have originated in shallow waters in the North Atlantic, while the genus *Sterechinus* spp. is restricted to Antarctica (Tyler *et al.*, 2000). This suggests that those species might have undergone bathymetric migration and speciation from a shallow-water ancestor, helped by favourable hydrographic conditions (with the formation of deep-water masses both in the North Atlantic and in Antarctica) and tolerating extreme carbon chemistry variations. This experiment demonstrates that the different carbon chemistry conditions that echinoderms may naturally encounter in the water masses of the North Atlantic ocean are not a major limiting factor in the colonisation of deep-sea habitats. It is known that larval tolerance increases with age, the swimming stage larvae being the most likely invaders of the deep-sea and also the most tolerant to deep-sea conditions (Young *et al.*, 1997). The data suggest that larvae of this species could colonise and adapt to new carbon chemistry conditions in the future and that they could have done the same with a step-wise invasion in the past. Data for temperature and pressure effects on the later stages of larval development in *P.*

miliaris suggest that they are more tolerant than at the early embryo stages (Aquino-Souza *et al.*, 2008). The present results are in accordance with previous studies on deep-sea invasion of this species (Aquino-Souza *et al.*, 2008), suggesting that the depth distribution of *P. miliaris* cannot be explained by either physiological or chemical frontiers during planktonic stages. Deep-sea echinoids may have evolved the ability to cope with profound seawater chemical changes from a distant tolerant ancestor inhabiting a shallower ocean and these data suggest that they may well survive environmental change in the future.

CHAPTER 4

TEMPERATURE COUNTERACTS OCEAN ACIDIFICATION EFFECT ON FERTILIZATION AND BIOCALCIFICATION OF SEA URCHIN LARVAE UNDER CLIMATE CHANGE SCENARIOS

4   TEMPERATURE COUNTERACTS OCEAN ACIDIFICATION EFFECT ON FERTILIZATION AND BIOCALCIFICATION OF SEA URCHIN LARVAE UNDER CLIMATE CHANGE SCENARIOS

4.1   INTRODUCTION

The vast carbon input of anthropogenic fossil fuel combustion has exceed by far the natural range of global atmospheric carbon concentration over the last 650,000 years (180 to 300ppm) as determined from ice core records (IPCC, 2007). The IPCC, in their Forth Assessment Report (2007) noted a $0.3^{o}C$ global average surface warming increase between 1990 and 2005 and projected a further increase of between 0.6 and $4.0^{o}C$ by the end of the 21st century. The role of the ocean in buffering any future atmospheric temperature change, and the impact on marine life, is integral to understanding how best to predict, respond and adapt to climate change scenarios.

The ocean acts as a major temperature regulator, absorbing approximately 80 per cent of the additional heat generated by global warming (IPCC, 2007). Sea-surface temperatures (SST) are therefore predicted to continue increasing as anthropogenic carbon dioxide (CO_2) concentrations rise. During the past 25 years, water temperatures in the north-east Atlantic and around the UK have risen by $0.6^{o}C$ per decade (Hughes *et al.*, 2010). The largest increase has occurred in the eastern English Channel and the southern North Sea at a rate of 0.6 to $0.8^{o}C$ per decade (Hughes *et al.*, 2010). Models predict further SST increments for the next 100 years, by about 3.0 to $3.9^{o}C$ in the shallower southern North Sea and English Channel (Sheppard, 2004).

The global ocean is estimated to have absorbed around half of the CO_2 released into the atmosphere since the mid-19th century (Caldeira and Wickett, 2003; Feely *et al.*, 2004; Sabine *et al.*, 2004; Caldeira and Wickett, 2005; Orr *et al.*, 2005). As the oceans absorb atmospheric CO_2, the seawater pH falls in a phenomenon known as ocean

acidification (Caldeira and Wickett, 2003). Under these conditions, the concentrations of CO_2 and bicarbonate ions (HCO_3^-) increase and pH and carbonate ions (CO_3^{2-}) decrease. This decline in CO_3^{2-} lowers the saturation state for carbonate minerals such as calcite and aragonite ($CaCO_3$), which are thought to affect the production rates of $CaCO_3$ minerals that are necessary for biogenic calcification in marine organisms. This relationship is shown in Equation 1:

$$CO_3^{2-} + Ca^{2+} \rightarrow CaCO_3 \tag{1}$$

The projected decline in CO_3^{2-} concentration owing to seawater acidification (increasing dissolved pCO_2) reduces $CaCO_3$ saturation state (Ω) with respect to mineral phases:

$$\Omega_{Cal/Arg} = \frac{[Ca^{2+}]_{sw} * [CO_3^{2-}]_{sw}}{K_{sp}} \tag{2}$$

The reduction of Ω in seawater represents a major challenge to calcifiers owing to the strong linear relationship between the calcification rate and the saturation state of calcium carbonate (Langdon *et al.*, 2000; Feely *et al.*, 2004; Gazeau *et al.*, 2007; Gutowska *et al.*, 2008). Recent research has focussed on the physiological plasticity to high levels of pCO_2 and the biocalcification of marine calcifiers (Engel *et al.*, 2005; Gazeau *et al.*, 2007; Hall-Spencer *et al.*, 2008; Bulling *et al.*, 2010; Dupont *et al.*, 2010b). However, few studies have examined the *combined* effect of CO_2 and temperature changes in marine organisms (Byrne *et al.*, 2009; Sheppard Brennand *et al.*, 2010).

Carbon dioxide concentrations can strongly vary in marine ecosystems on a daily and/or seasonal basis (Pörtner, 2008; Wootton *et al.*, 2008) while temperature is the most important environmental factor controlling the biogeography, physiological performance, behaviour, and functional structure of marine populations (Pörtner, 2008; Doney *et al.*, 2009a; Doney *et al.*, 2009b). In most parts of the ocean, CO_2 and temperature co-vary, making it both difficult and irrelevant to isolate CO_2 as a limiting factor.

Echinoderms are an appropriate model marine calcifying organism to test the effect of CO_2 in combination with changing temperature as they play a fundamental function in the process of remineralisation (Lebrato *et al.*, 2010), and are valuable members of the food chain for the fishing industry (Kelly *et al.*, 1998; Cooley *et al.*, 2009). Importantly for this study, the echinoid *Psammechinus miliaris* is common around British coastal waters (Mortensen, 1927) and is considered an edible species with great potential as an aquaculture species (Kelly *et al.*, 1998; Kelly *et al.*, 2000). Additionally, echinoids possess a planktotrophic larvae that have been shown to form skeletons from amorphous calcite crystal, which is 30 times more soluble than normal calcite (Weber, 1969; Politi *et al.*, 2004). It is therefore likely that echinoid larvae will be particularly susceptible to climate change stressor factors (e.g. CO_2 and temperature).

As the seawater temperature decreases, CO_2 absorption increases because of its higher solubility. Conversely, ocean warming enhances CO_2 release. Little is known about the tolerance of marine calcifiers to covariance in temperature and pCO_2. Investigations have largely focussed on responses to a single parameter (e.g. pCO_2) (Kurihara, 2008; Dupont *et al.*, 2010b). Most studies indicate that hypercapnia (low pH, high CO_2) reduces calcification rates of marine biota (Gattuso *et al.*, 1998; Leclercq *et al.*, 2002; Dupont *et al.*, 2008; Clark *et al.*, 2009), but some find little change or variable responses to ocean acidification (Iglesias-Rodriguez *et al.*, 2008; Dupont *et al.*, 2010a). A question therefore arises as to whether the simultaneous variance in temperature and CO_2 will bias the physiological response of organisms in a different way than by just modifying one parameter in isolation.

The present study addresses the physiological and morphological tolerance of echinoid larvae to ocean acidification in the context of rising temperatures, aiming to mimic the conditions the organisms will encounter in near-future climate change scenarios. Additionally, the carbon production of the larvae was assessed under environmentally changing conditions (e.g. seawater carbonate chemistry, temperature).

4.2 MATERIALS AND METHODS

4.2.1 Experimental conditions and rearing

Psammechinus miliaris were collected near Rhosneigr, Anglesey, Wales, UK (53° 13'41" N; 4° 31'16" W) in July 2009, and were maintained in flow-through aquaria at $14 \pm 1 \ ^oC$. To test the effect of ocean warming and ocean acidification the experiments consisted of two major parts: a) to test the effect of those stressor factors on the fertlization proccess and b) to test the effect on growth and development of sea urchin larvae under climate changes scenarios. For the fertilization success experiment, adult sea urchins were induced to spawn by an inter-coelomic injection of 0.5 mol l^{-1} KCl using standard techniques (Strathmann, 1987). The eggs of three females were spawned into beakers containing filtered seawater (FSW 0.20 μm), and the sperm of three males was collected dry and kept at 4^oC. The eggs shape/quality and the sperm motility were microscopically checked before starting the experiments. The total number of eggs were measured from a 20 ml suspension calculated through counts of 100 μl aliquots for each experiment. The fertilization experiment was performed separately in replicate beakers (60 ml) containing experimental water and kept at the experimental temperature (15, 18 and 20^oC) at densities of approximately 3-4 eggs ml^{-1}. Prior to fertilization the eggs were placed in the experimental rearing beakers for 20 minutes and the amount of sperm required to achieve a sperm to egg ratio of 1000:1 was added (the sperm calculation was achieved by haemocytometer counts). The sperm was briefly activated in the experimental seawater in the beakers containing the eggs. After two hours the eggs that presented a fertilization membrane and cleavage were counted to determine the fertlization success. For the experiment, two different pH levels (8.2 and 7.7) were used at three different temperature conditions (15°C, 18°C and 20°C). Four replicates were used for each temperature/pH combination and this set of experiments was run twice to increase accuracy of results.

The embryos were reared in separate microcosms adjusted for three experimental temperatures 15^oC (control) 18^oC and 20^oC and two pH levels 8.2 (control) and 7.7. In all combinations, 5 l flasks (in triplicates) per treatment were used. All microcosms

were equilibrated for 36 hours until the desired pCO$_2$ and corresponding temperature scenarios were achieved. Larvae were fed on the marine microalgae *Isochrysis galbana* and *Rhodomonas* sp. at a concentration of 6,000 and 3,000 cells ml^{-1} respectively (see Appendix 4 for phytoplankton growth and medium preparation). *Psammechinus miliaris* larvae were grown in experimental seawater pH that was bubbled with the desirable air/CO$_2$ mixture to mimic predicted future atmospheric conditions (pH ~7.7, see Table 4.1). The controls were bubbled with air only by using an aquarium pump to achieve pH 8.2. Constant dissolved oxygen (DO) levels were maintained by the simultaneous bubbling of air in all experimental flasks. In a recent study, it was showed that reduced oxygen increased pCO$_2$ in solution (Melzner *et al.*, 2009).

The 5 l flasks were placed in 60 l tanks in a temperature-controlled room at 15°C as the control temperature. Water was warmed and maintained constant at the required temperatures [control + 3°C (18°C) and control + 5°C (20°C)] using aquarium heaters (see Table 4.1). Aquarium propellers were used to mix the water, maintaining a homogenous temperature around the experimental flasks. The control temperature scenario was set at 15°C as this is the mean annual temperature of British coastal waters in which adult echinoids inhabit. The second and third temperature scenarios are predicted to occur before the end of the 21st century, according to the IPCC (2007). The pH level of 8.2 is set as the control, whereas pH 7.7 represents the 2100 'business-as-usual' scenario (IPCC, 2007).

4.2.2   Morphological analysis

Approximately 60 larvae were collected at random at different developmental stages (2, 4, 6 and 8 armed pluteus larvae) from each experimental flask to monitor the major ontogenetic changes. They were fixed in 4% paraformaldehyde (EM GRADE, Science Services) in FSW and specimen growth was measured from each experimental microcosm. A digital camera mounted on a compound microscope was used to photograph the larvae for a posterior image analysis using Image J software (NIH, USA). For each larva the length of the postoral arm (POA), body length (BL) and

stomach area (St) were measured. Larvae were reared to the rudiment stage (38 days) to assess the different effect of pH and temperature at a later developmental stage.

4.2.3   Carbonate chemistry analysis

Samples for total alkalinity (TA) and dissolved inorganic carbon (DIC) measurements were collected in 250 ml borosilicate bottles, fixed with 1ml of 0.40 mM $HgCl_2$ solution and measured with the Versatile INstrument for the Determination of Titration Alkalinity (VINDTA) (see Appendix 3 for full details of methodology). Values for CO_2, HCO_3^-, CO_3^{2-}, and the saturation state of aragonite (Ω-Arg) and calcite (Ω-Cal) were determined from TA, DIC, salinity and nutrients data using the CO2SYS (CO_2 system calculation program) (Lewis and Wallace, 1998). Detailed experimental water parameters (pH 8.2 and 7.7) in combination with temperature (15, 18 and 20 ^{o}C) are shown in Table 4.1.

Table 4.1 *Psammechinus miliaris* culture conditions of the larval growth in control pH (8.2) seawater, and in seawater with low pH (7.7) predicted by the year 2100. Temperature, carbonate chemistry, nutrients, and experimental duration (i = day 0, and f = day 38) are reported. Values correspond to mean ± S.D., $n = 3$.

	Environmental data					
	Temperature 15 ^{o}C		**Temperature 18 ^{o}C**		**Temperature 20 ^{o}C**	
		Predicted		Predicted		Predicted
	Control	pCO$_2$	Control	pCO$_2$	Control	pCO$_2$
A) Experimental conditions						
Temperature (^{o}C)	15.4 ± 0.31	15.6 ± 0.42	17.8 ± 0.77	17.6 ± 0.27	20.1 ± 0.62	20.8 ± 0.75
Salinity	36 ± 0.0	36 ± 0.0	36 ± 0.0	36 ± 0.0	36 ± 0.0	36 ± 0.0
Nitrate (μmol l^{-1})	0.27± 0.03	0.20 ± 0.06	1.06 ± 0.48	0.15 ± 0.06	0.19 ± 0.07	0.44 ± 0.01
Phosphate (μmol l^{-1})	0.10 ± 0.01	0.05 ± 0.01	0.08 ± 0.04	0.07 ± 0.03	0.05 ± 0.01	0.06 ± 0.02
Silicate (μmol l^{-1})	4.16 ± 0.49	3.11 ± 0.79	4.39 ± 0.33	3.23 ± 1.16	4.85 ± 0.60	4.27 ± 0.63
B) Water carbon chemistry						
TA (μmol kg^{-1}) $_{(i)}$	2341.66 ± 39.39	2321.66 ± 2.37	2327.82 ± 4.39	2323.69 ± 6.18	2309.66 ± 12.05	2309.79 ± 13.55
TA (μmol kg^{-1}) $_{(f)}$	2288.85 ± 41.34	2278.44 ± 6.75	2263.72 ± 11.44	2283.27 ± 7.13	2263.30 ± 2.39	2277.87 ± 12.73
DIC (μmol kg^{-1}) $_{(i)}$	1953.62 ± 60.27	2233.49 ± 23.09	1938.18 ± 23.50	2204.47 ± 1.32	1912.79 ± 56.16	2214.82 ± 7.71
DIC (μmol kg^{-1}) $_{(f)}$	2133.66 ± 39.07	2236.03 ± 19.62	2132.49 ± 22.25	2240.75 ± 15.37	2083.83 ± 8.58	2242.44 ± 16.62

$pH_{total\ (i)}$	8.31 ± 0.04	7.71 ± 0.07	8.28 ± 0.04	7.76 ± 0.02	8.26 ± 0.07	7.66 ± 0.02
$pH_{total\ (f)}$	7.89 ± 0.01	7.57 ± 0.07	7.80 ± 0.08	7.55 ± 0.03	7.88 ± 0.02	7.49 ± 0.01
$pCO_2\ (\mu atm)_{(i)}$	193.39 ± 26.91	984.21 ± 173.34	208.64 ± 21.34	861.46 ± 37.30	220.83 ± 45.26	1099.46 ± 36.64
$pCO_2\ (\mu atm)_{(f)}$	608.83 ± 17.41	1367.23 ± 231.6	765.84 ± 159.81	1458.25 ± 102.9	620.63 ± 33.61	1660.14 ± 59.41
$CO_2\ (\mu mol\ kg^{-1})_{(i)}$	7.09 ± 0.99	36.09 ± 6.36	7.13 ± 0.73	29.44 ± 1.27	7.07 ± 1.45	35.22 ± 1.17
$CO_2\ (\mu mol\ kg^{-1})_{(f)}$	22.33 ± 0.64	50.14 ± 8.49	26.32 ± 5.49	50.11 ± 3.54	19.88 ± 1.08	53.47 ± 1.91
$HCO_3^-(\mu mol\ kg^{-1})^{(i)}$	1680.44 ± 72.77	2113.83 ± 28.27	1663.57 ± 38.09	2074.59 ± 3.91	1633.56 ± 84.87	2091.45 ± 5.56
$HCO_3^-(\mu mol\ kg^{-1})_{(f)}$	1993.15 ± 36.41	2124.94 ± 21.19	2000.92 ± 34.03	2129.34 ± 15.25	1930.78 ± 12.72	2129.70 ± 15.94
$CO_3^{2-}(\mu mol\ kg^{-1})_{(i)}$	266.09 ± 15.24	83.57 ± 11.53	267.49 ± 15.50	100.43 ± 4.06	272.15 ± 30.47	88.15 ± 3.34
$CO_3^{2-}(\mu mol\ kg^{-1})_{(f)}$	118.19 ± 3.44	60.95 ± 10.16	105.26 ± 17.65	61.31 ± 3.43	133.17 ± 5.33	59.27 ± 1.23
Ω-Cal$_{(i)}$	6.30 ± 0.36	1.98 ± 0.27	6.34 ± 0.37	2.38 ± 0.10	6.46 ± 0.72	2.09 ± 0.08
Ω-Cal$_{(f)}$	2.80 ± 0.08	1.44 ± 0.24	2.51 ± 0.42	1.46 ± 0.08	3.16 ± 0.13	1.42 ± 0.03
Ω-Arg$_{(i)}$	4.05 ± 0.23	1.27 ± 0.18	4.10 ± 0.24	1.54 ± 0.06	4.21 ± 0.47	1.36 ± 0.05
Ω-Arg$_{(f)}$	1.80 ± 0.05	0.93 ± 0.15	1.62 ± 0.27	0.95 ± 0.05	2.06± 0.08	0.92 ± 0.02

4.2.4   Particulate carbon

Samples for the determination of total particulate carbon (TPC) and particulate organic carbon (POC) were collected on pre-combusted (12 hours, 500°C) silver capsules (Elemental Microanalysis, UK) and stored at -20°C. The POC capsules contained 50 larvae per triplicate and were fumed for 96 hours with a saturated HCl solution to remove all inorganic carbon. TPC and POC were then dried for 48 hours at 60°C and subsequently measured on a Thermo Finnegan flash EA1112 elemental analyser using acetanilide as the calibration standard (see Appendix 5). Particulate inorganic carbon (PIC) was calculated as the difference between TPC and POC (Riebesell *et al.*, 2000; Zondervan *et al.*, 2001).

4.2.5   Scanning electron microscopy (SEM) of larval skeletons

Larvae of *P. miliaris* were collected to examine skeletal abnormalities. Larval tissue was removed by using a mild solution of hyperchlorite diluted in a solution of distilled water which was saturated with sodium tetraborate (which acts as a buffer) for 15 minutes. The larvae were then rinsed three times for 5 minutes with distilled water to remove any remaining hyperchlorite solution. The skeletal rods were then mounted on SEM stubs, gold coated and analysed using a LEO 1455VP scanning electron microscope (Oxford Instruments, INCA) for evidence of atypical formation or erosion of the larval skeleton.

4.2.6   Statistical analyses

For the morphological data two-way ANOVA was used, with pH and temperature as fixed factors and the larval source as the dependent variable. The parametric Tukey post-hoc tests were carried out to assess the significant differences between treatment groups. Normality was confirmed by the One-Sample Kolmogorov-Smirnov test (POA, P >0.150; BL, P >0.150) to ensure that the distribution was homogeneous and normally distributed. All statistics were carried out using Statistica 9 (StatSoft, Inc. Oklahoma,

USA) and Minitab 15 (Minitab 15® Statistical Sotware for Windows®, 2007, Coventry, UK) software.

4.3 RESULTS

4.3.1 Carbonate chemistry

For all experiments, coastal water was collected in order to maintain (in the laboratory) the *in situ* seawater carbonate chemistry in which *P. miliaris* inhabit. The initial pCO_2 experimental conditions of coastal seawater varied from 193 µatm at 15.4°C, to 208 µatm at 18°C and to 220 µatm at 20°C. These values reflect the typical water carbonate chemistry fluctuations in the intertidal zone, owing to photosynthetic activity (e.g. pH 8.3- 7.5) (Menendez *et al.*, 2001; Wootton *et al.*, 2008), riverine inputs and upwelling events on daily and seasonal bases (Feely *et al.*, 2008).

4.3.2 Fertilization and mortality

There was a significant effect of temperature and pH on the percentage of fertilized eggs. Fertilization decreased by 20% at 15°C and 13% at 18°C for pH 8.2 and 7.7, but there was no significant effect under 20°C ($P = 0.999$). Results indicate that a rise in temperature increases the fertilization success tolerance to low pH condition (Fig. 4.1 A).

The development of *P. miliaris* echinopluteus larvae was investigated until the rudiment was visible and the larvae were considered competent to settle (on day 38). The percentage of larvae that did not survive the 38 days exposure period increased from 37% to 63% as temperature increased from 15°C to 20°C. Statistical analyses suggest that the increase in mortality was significantly different between temperatures but not significant for pH (see Table in Appendix 9).
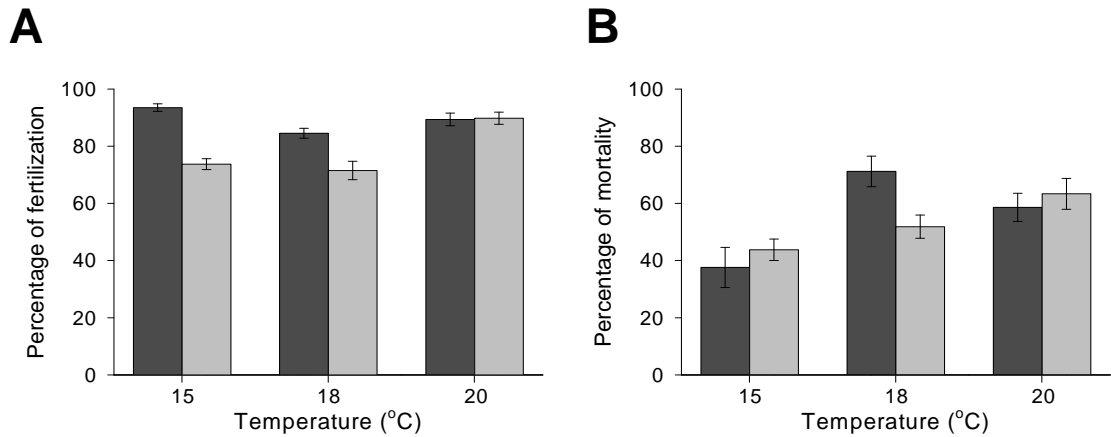
Figure 4.1 Effect of pH and temperature on the percentage of (A) fertilization and (B) mortality of *P. miliaris*. Dark grey bars represent control pH (8.2) and light grey bars low pH (7.7) conditions. The percentage of mortality was calculated on the last day of the experiment (day 38).

4.3.3   Larval growth and development

The pattern of larval growth was unaffected by changes in pH (control 8.2 and 7.7), with temperature being the dominant factor. The POA and BL growth of the larvae were significantly different between temperatures ($F_{2,61}$ = 20.95 $P < 0.001$) although this was not the case for pH ($F_{1, 61}$ = 1.04 P =0.311) treatments (see Table 4.2). There was no negative effect of high pCO_2 levels on the larval growth at the higher temperatures (18 and 20°C) compared to the control (15°C). In fact, the thermal increase was found to enhance larval growth of *P. miliaris* (Fig. 4.2 and Appendix 9).

At the initial time of development (day 3), the POA and BL length showed a significant difference ($P < 0.001$) between temperature treatments. However, there was no significant difference in POA and BL across temperature treatments when exposed to extended periods (in this study 38 days). The POA and BL parameters were no longer affected by temperature or pH after the larvae completed the 4-armed developmental stage.

The potential for differences in larval form related to temperature and/or pH as stressor factors, was tested by calculating the value of POA:BL for the entire sampling

period (days 3-38). Results show that there were no distinct patterns of growth. There was a linear increase of POA:BL but no abnormal growth for the higher temperature scenarios (18 and 20 ^{o}C) was observed (Fig. 4.2). The larvae appeared to acclimate to the temperature increase and showed no malformation or skewness at day 38 (Fig. 4.2).
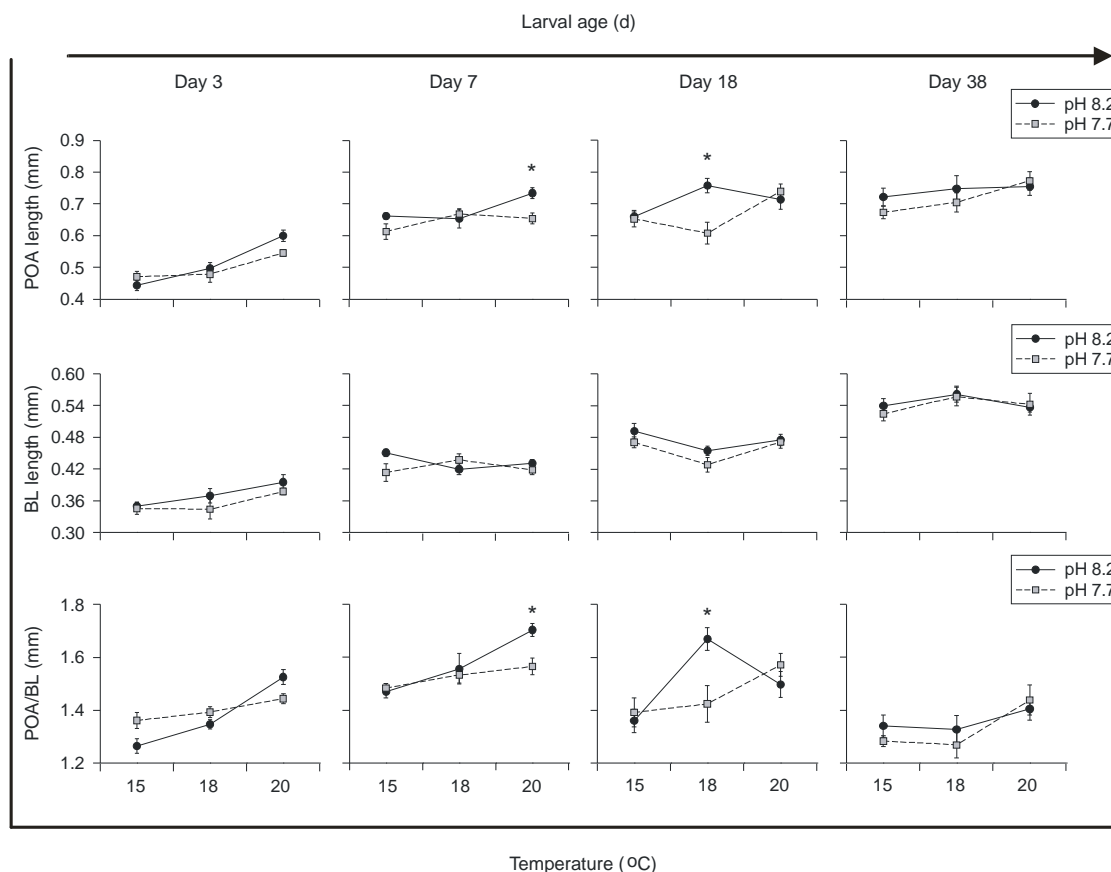
Figure 4.2 Changes in morphological parameters of the sea urchin larvae *P. miliaris* during 38 days of exposure to different temperatures and pH. POA (post oral arm length); BL (body length). Values are means ± SE, *n* = 3 replicates and * indicates significant differences (*p* < 0.01) between pH and temperature treatments.

The interactive effect of temperature and pH on the stomach size of the larvae was also analysed. Specimens were not fed for 24 hours before sampling was performed in order to homogenise the sample and select from individuals with an empty digestive system. The growth of the gut increased significantly in the temperature (15°C to 20°C) conditions ($F_{2,61}$ = 5.34 P < 0.01) although there was no significant change in gut size with pH (8.2 to 7.7) conditions ($F_{1,61}$ = 0.04 P = 0.842; Fig. 4.3).   There was a significant change in the POA:BL ratio of the species *P. miliaris* under increasing

temperature conditions, but no significant change under different pH treatments (see Table 4.2 for statistics).
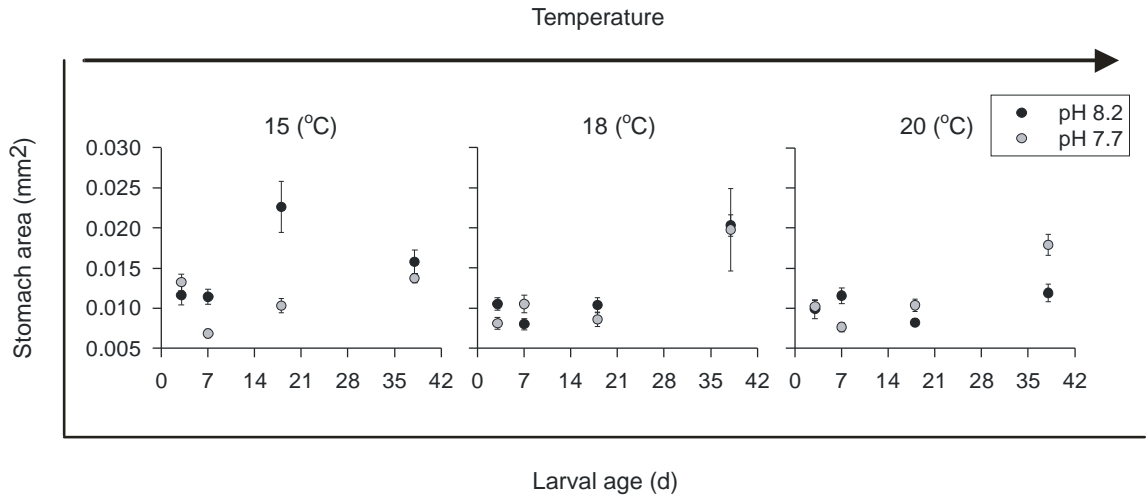
Figure 4.3 Effect of pH and temperature on the digestive system of *Psammechinus miliaris* larvae reared for 38 days in 3 temperature and 2 pH conditions. Values correspond to mean ± SE, *n* = 3 replicates for each experimental condition.

Table 4.2 Two-way ANOVA on the percentage of fertilized eggs, mortality and length of morphometric variables of the sea urchin *P. miliaris*. The morphological values are for day 0 (i) and day 38 (f).

Parameter	Source	*F* (df)	P
% Fertilization	pH	36.9 (1,90)	< 0.001
	Tempt.	14.17 (2,90)	< 0.001
	pH x Tempt.	11.2 (2,90)	< 0.001
% Mortality	pH	1.39 (1,12)	0.262
	Tempt.	9.36 (2,12)	< 0.01
	pH x Tempt.	5.04 (2,12)	0.026
Morphology			
Postoral arm (mm)[i]	pH	1.04 (1,61)	0.311
	Tempt.	20.95 (2,61)	< 0.001
	pH x Tempt.	2.49 (2,61)	0.091
Postoral arm (mm)[f]	pH	0.967 (1,65)	0.329
	Tempt.	2.64 (2,65)	0.078
	pH x Tempt.	0.78 (2,65)	0.458
Body length (mm)[i]	pH	2.21 (1,61)	0.142
	Tempt.	4.75 (2,61)	< 0.01
	pH x Tempt.	0.34 (2,61)	0.707
Body length (mm)[f]	pH	0.13 (1,65)	0.716
	Tempt.	1.52 (2,65)	0.226
	pH x Tempt.	0.24 (2,65)	0.784

POA/BL[i]	pH	0.95 (1,61)	0.332
	Tempt.	23.35 (2,61)	< 0.001
	pH x Tempt.	6.42 (2,61)	< 0.01
POA/BL[f]	pH	0.51 (1,65)	0.475
	Tempt.	4.24 (2,65)	< 0.01
	pH x Tempt.	0.66 (2,65)	0.517
Stomach area (mm^2)	pH	0.04 (1,61)	0.842
	Tempt.	5.34 (2,61)	< 0.01
	pH x Tempt.	2.04 (2,61)	0.138
Stomach area (mm^2)	pH	0.48 (1,65)	0.489
	Tempt.	3.98 (2,65)	< 0.05
	pH x Tempt.	2.31 (2,65)	0.106

4.3.4   Particulate carbon

The particular inorganic carbon (PIC) was measured as a proxy for biocalcification. Data showed the interactive effect of temperature and pH on calcification of the sea urchin larvae. Significantly there was a gradual increase in PIC production in larvae exposed to acidified waters under elevated temperatures (Fig. 4.4). In fact, echinoplutei larvae that were cultured at pH 8.2 (control) and pH 7.7 conditions had a greater percentage of PIC production at 20^oC compared with observed PIC in larvae incubated at the control temperature (15^oC). The interactive effect that pH and temperature had on the production of PIC was significantly different ($P < 0.05$) across treatments. Scanning electron micrographs of the larval rods revealed bigger skeletal structures at 18 and 20^oC compared to the control 15^oC in both pH treatments (8.2 and 7.7) (Fig. 4.5).

Additionally, the particulate organic carbon (POC) was tested as a comparison of larval growth of soft tissue (POA, BL). The results of POC per larva did not exhibit differences and were found to be not significant ($P = 0.097$) across treatments (Table 4.3). However, the PIC:POC ratio data revealed the effect that a lowering in pH had on the production of the larval endoskeleton. Larvae grew larger skeletons at higher temperatures, however low pH caused a negative effect on calcification and PIC production. At hypercanic conditions PIC was generally lower than at normocapnic conditions (Fig. 4.4).
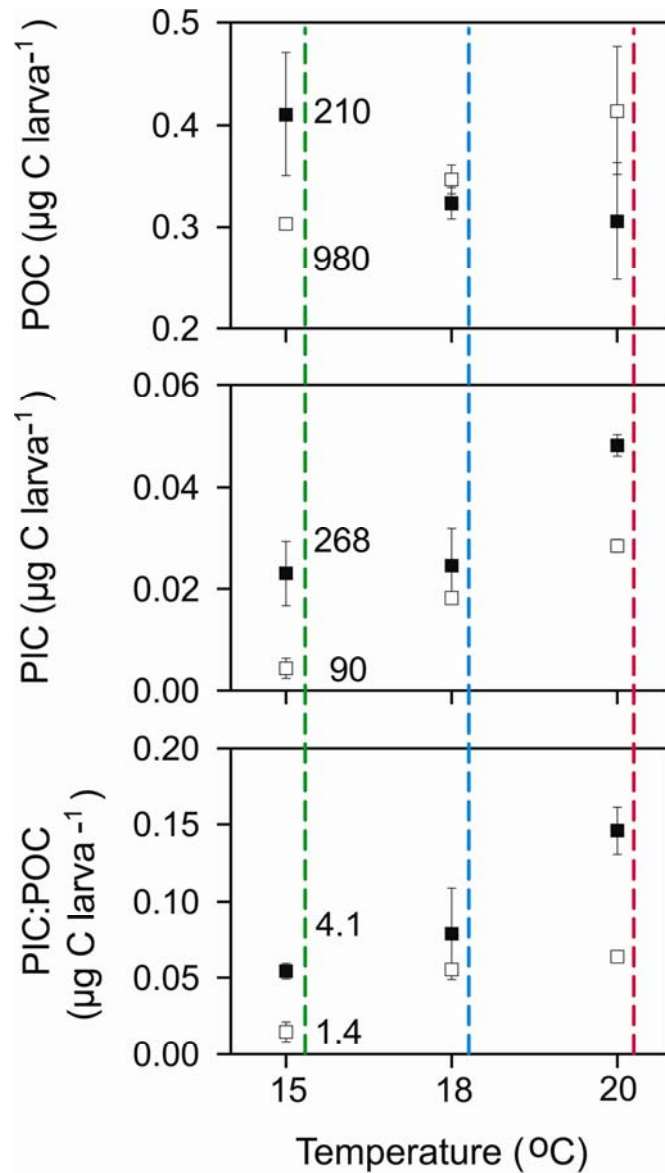
Figure 4.4 Particulate organic (POC) and inorganic (PIC) carbon per larva of the sea urchin *P. miliaris*. Lines indicated are corresponding ranges of pCO_2, $[CO_3^{2-}]$ and Ω_{Arg} as a function of temperature and pH. Larvae were incubated at three temperatures (15, 18 and 20 ^{o}C) and two pH (8.2, black squares and pH 7.7, white squares) conditions. A) POC, pCO_2 values; B) PIC, $[CO_3^{2-}]$ values; and C) PIC:POC ratio, Ω-Arg values. We note that values pCO_2, $[CO_3^{2-}]$ and Ω-Arg differed slightly between experimental sets for the three temperatures, therefore, the values are only approximates (see Table 4.1 for corresponding values). Bars denote ± SE (n =3).

Furthermore the rates of CO_3^{2-} : HCO_3^- uptake in seawater cultures of the larvae were investigated. The carbonates ion uptake (CO_3^{2-} : HCO_3^-) was significantly greater at the control pH (8.2) than at the reduced pH (7.7) for both sampling days (day 0 and

38). However, the CO_3^{2-} : HCO_3^- ratio was not significantly different between the three temperature treatments (Table 4.3 and Appendix 9).

Table 4.3 Two-way ANOVA of the effect of the particulate carbon and carbonate ratio among different levels of pH and temperature. The carbonate ratios are values for day 0 (i) and day 38 (f).

Paramete	Source	*F* (df)	P
Particulate carbon			
	pH	0.70 (1,11)	0.418
TPC (µg C)	Tempt.	0.37 (2,11)	0.693
	pH x Tempt.	4.26 (2,11)	< 0.05
	pH	0.04 (1,11)	0.837
POC (µg C)	Tempt.	0.15 (2,11)	0.855
	pH x Tempt.	2.90 (2,11)	0.097
	pH	21.78 (1,11)	< 0.05
PIC (µg C)	Tempt.	3.04 (2,11)	0.088
	pH x Tempt.	5.51 (2,11)	< 0.05
	pH	27.09 (1,11)	< 0.05
PIC:POC	Tempt.	2.87 (2,11)	0.098
	pH x Tempt.	1.56 (2,11)	0.251
Carbonate ratios			
	pH	309.89	< 0.001
CO_3^{2-} : $HCO_3^{-\,i}$	Tempt.	0.30 (2,12)	0.743
	pH x Tempt.	0.30 (2,12)	0.746
	pH	204.13	< 0.001
CO_3^{2-} : $HCO_3^{-\,f}$	Tempt.	3.56 (2,12)	0.061
	pH x Tempt.	5.40 (2,12)	0.021

4.4 DISCUSSION

4.4.1   Fertilization success under ocean acidification and ocean warming

It can be difficult to extrapolate ecosystem response from laboratory experiments because particular environmental conditions can both enhance or counteract the effect of stressor factors (e.g. temperature, CO_2) on marine biota (Hall-Spencer *et al.*, 2008).

Using oceanic water for laboratory experiments with intertidal organisms could bring about misleading results because the organism response will be tested with a different water chemistry compared to the *in situ* carbonate seawater conditions.

It is reported that in *P. miliaris,* fertilization and larval development tolerance is robust to temperatures well above ambient temperature and the increases expected for British coastal waters under predicted climate change scenarios (Sheppard, 2004; Hughes *et al.*, 2010). These results are in agreement with several studies that show thermotolerance in sea urchins (Fujisawa and Shigei, 1990; Byrne *et al.*, 2009). It has been suggested that the tolerance that the sea urchin exhibits is due to maternal acclimatisation that combines with the larval phenotypic plasticity enabling the organism to withstand high temperatures (Fujisawa and Shigei, 1990; Byrne *et al.*, 2009; Byrne *et al.*, 2010a).

The fundamental life history processes (reproduction, fertilization, embryogenesis, larval development and metamorphosis) are considered as very vulnerable and sensitive to environmental stressors (Royal Society, 2005). Studies have shown that temperature can affect the timing of developmental processes (Sewell and Young, 1999; Staver and Strathmann, 2002). Data revealed the interactive effect of temperature and pH on sea urchin fertilization success. When pCO$_2$ levels increase in seawater, dissolved CO_2 readily crosses biological membranes and enters intracellular spaces across animal surfaces (Fabry *et al.*, 2008). A reduction in fluid pH, due to elevated environmental pCO$_2$, has consequences for cellular metabolism and impacts on reproduction (Seibel and Fabry, 2003).

The dataset examined in this study showed a decrease in the fertilization success by 20% and 13% at temperatures of 15 and 18°C respectively, under the same pH 7.7 condition. As in seawater, CO_2 reacts with the internal fluids of the organism causing an internal pH decrease. This decline is detrimental for the fertilization process as it requires an intracellular increase in pH in order to initiate development (Johnson *et al.*, 1976). Therefore a new intracellular level, sufficient to compensate and equilibrate cellular metabolism to match pH demand, is needed. Results showed a negative impact on fertilization in low temperature conditions (15°C). However, this effect was reduced

when temperature increased (18 and 20°C), as a compensatory effect. Higher temperatures cause an increment in kinetic energy (thermodynamic effect), which increases the motion in molecules (e.g. CO_2) breaking intermolecular bonds and releasing CO_2 from solution. Warming decreases the level of CO_2 absorption, making the membrane structure act as a diffusion barrier. The results of these experiments showed no effect on fertilization under the highest temperature scenario (20°C) as opposed to the negative effect seen at the lowest temperature (15°C). The plasma membrane diffusion in the sea urchin eggs *Strongylocentrotus purpuratus* vary with ocean temperature by alterations in the membrane composition and structure (Weaver *et al.*, 2008). The increase in temperature from 15 to 20°C seems to counteract the negative effect that acidification of seawater has on fertilization.

In the tropical sea urchin *Echinometra lucunter* it has been observed that high water temperatures (between 23 to 34°C) appear to be more suitable for fertilization than lower temperatures (below 12°C) (Sewell and Young, 1999). A recent study also indicates that acidification does not affect fertilization success in the sea urchin species *Heliocidaris erythrogramma* (Byrne *et al.*, 2010b) at temperatures of 20, 24 and 26°C. These studies, in accordance with the results of this thesis, suggest that the susceptibility of fertilization to ocean acidification may be controlled by temperature tolerance, which adds weight to the idea of species-specivity.

Temperature and pH are limiting factors for eggs and early cleavage stages. However, both factors may be overcome during later developmental stages because of larval plasticity (Sewell and Young, 1999). Results showed a nullifying effect on the larval growth when exposed to extended periods (> 7 days) to changes in temperature and pH conditions of seawater. This emphasises that the duration to which organisms are exposed to stressor factors is crucial in understanding natural plasticity to ocean acidification and ocean warming. Studies have already shown that in the short term, species typically present a low adaptability tolerance to multiple stressors (Kurihara and Shirayama, 2004; Byrne *et al.*, 2009). Data showed that the sea urchin larvae followed a normal developmental process (Shearer *et al.*, 1914). The postoral arms, which appear first, are the best indicator of divergence of larval form (Strathmann *et al.*, 1992). Results show that there was no effect on the growth of POA and BL between

treatments, suggesting that the larvae can acclimate to changing environmental conditions with time.

There is a direct relationship between the growth of POA and stomach area throughout the experiment suggesting that echinoplutei grew long arms, in agreement with observations of plastic responses that enhance food capture by elongation of the ciliary band (Bertram and Strathmann, 1998; Sewell *et al.*, 2004; Strathmann, 2007), to sustain feeding. It is known that a reduction in arm size leads to reduced apparatus for feeding (Sewell *et al.*, 2004). An 8% decrease in the length of the ciliated band can decrease the amount of water cleared for food by 20% (Hart and Strathmann, 1994). It was observed that a reduction in the gut size is equivalent to a decrease in POA length, which represents an adaptation to compensate for environmental stresses (pH and temperature changes).

Synchrony between food and optimal environmental temperature is critical for planktotrophic larvae (Dupont *et al.*, 2010a) given that the life time of larvae as plankton rely on temperature and food as sources for development. The data presented may imply that temperature (as the dominant environmental factor) influences the rate of food intake which could lead to a delay in development to achieve metamorphosis. An ecological implication may be that by spending longer time periods at the planktonic stage, larvae are more vulnerable to higher predation (Staver and Strathmann, 2002; Strathmann, 2007) which could decrease the success of this well acclimated larvae.

4.4.2   Calcification of *Psammechinus miliaris* under environmental climate change scenarios

The sea urchin larvae have skeletal parts of magnesium-bearing calcite which is 30 times greater than the solubility of calcite without magnesium (Politi *et al.*, 2004). The larval spicules are more susceptible to dissolution than aragonite. Orr *et al.* (2005) suggested that calcification does not occur if waters became undersaturated with respect to both aragonite and calcite (ΩCal/Arg < 1). However, these data demonstrate that *P. miliaris* larvae can precipitate calcium carbonate at ΩCal/Arg values below 1. In

contrast to the general contemporary opinion that sea urchin larvae are greatly threatened by ocean acidification, *P. miliaris* seems to be not only resilient to elevated pCO_2, but temperature increases appear to enhance its calcification rate. These results would probably need to be taken into consideration in biocheochemical models, specifically those that model the future export flux of calcite.

It is known that suppression of metabolic mechanisms is not advantageous for the organisms (Seibel and Fabry, 2003) as it limits the survival of the species and causes lethal irreversible effects. Even though, echinoplutei can successfully calcify skeletal segments under acidified conditions (e.g. Kurihara and Shirayama 2004; Clark *et al.*; also see Chapters 2 and 3 in this thesis) the physiological capacity to tolerate temperature stress can affect skeletal formation.

In agreement with previous studies (Wootton *et al.*, 2008; Clark *et al.*, 2009; O'Donnell *et al.*, 2010), these results showed that there are disadvantageous effects of low pH on the development of the larval endoskeleton. The biological fixation of inorganic carbon (calcification) in marine organisms employs several mechanisms to compensate for hypercapnia. These mechanisms include: 1) compensation of the acid-base imbalance by passive chemical buffering of intra- and extra-cellular fluids (e.g. dissolution of biological $CaCO_3$ structures); 2) active ion transport, CO_2 and hydrogen ion transport by extracellular respiratory proteins (Seibel and Fabry, 2003). Intertidal species are adapted to environments with steep CO_2 gradients [similar to Antarctic species (Clark *et al.*, 2009)] and have developed a high capacity to buffer ion exchange and CO_2 transport (O'Donnell *et al.*, 2010). The acid/base homeostatic ability that the *P. miliaris* larvae showed suggests that it is sufficient to cope with changes in pH as seen in other organisms [e.g., amphipods (Hauton *et al.*, 2009); pteropods (Comeau *et al.*, 2010)].
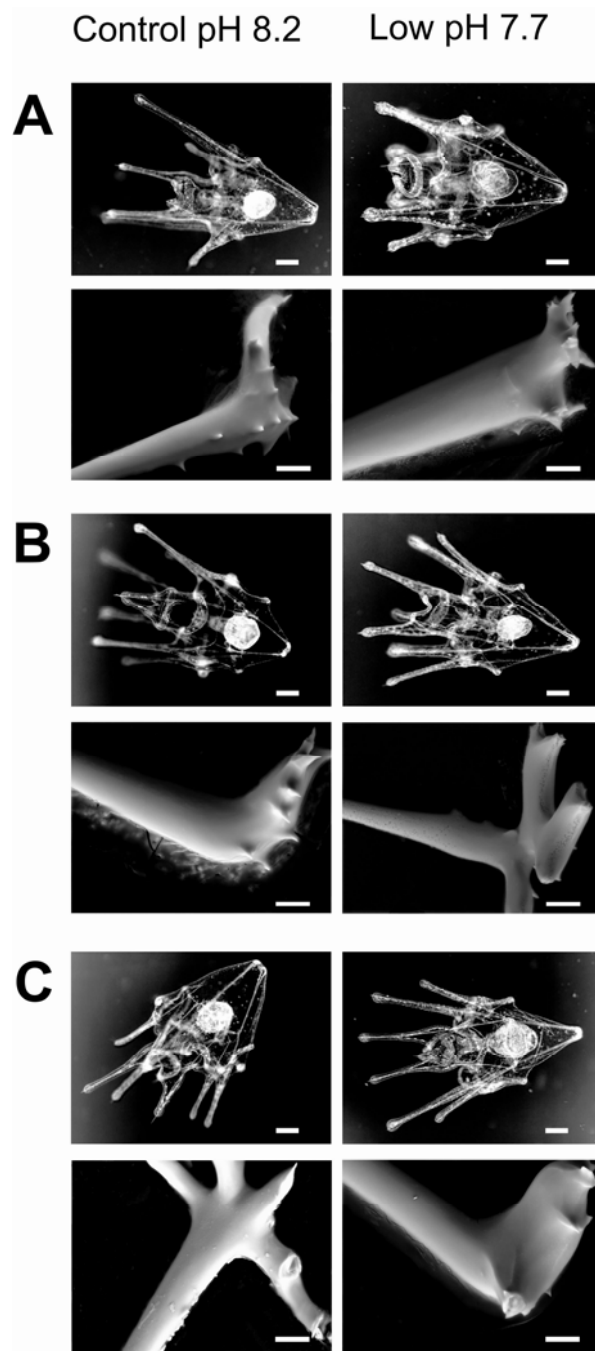
Figure 4.5 Scanning electron micrographs of larval skeletal rods of *Psammechinus miliaris* larvae grown under two pH levels. A) temperature control (15 °C), B) temperature condition 18 °C, and C) temperature effect at 20 °C. Scale bars in light microscopy image of the whole larvae represent 100 μm, and scale bars in SEM images represent 10 μm.

Decreasing calcification rates in coral reefs has been attributed to global warming (Gattuso *et al.*, 1998), which increases the risk of extinction of local species or ecosystems (Pörtner, 2008). Recent studies have demonstrated that intertidal/subtidal species are the most likely to be threatened by climate warming (Somero, 2002;

Somero, 2010). However, analyses show that species from mid-latitudes (e.g *P. miliaris*) are more likely to acclimate to changes in temperature because these species do not live at temperatures that are closer to their upper thermal tolerance limits (Somero, 2010). In this study, the temperature conditions under which the species were placed mirror the natural warming that this species experiences from the beginning of the spring (start of reproduction cycle) to the end of the summer. Moreover, experimental conditions have mimicked the gradual warming ($0.6^{o}C$ per decade) that southern and western UK coastal waters have experienced over the last 25 years (Hughes *et al.*, 2010). These conditions might have increased the larval thermal tolerance through gradual acclimation. The present data show that low pH reduces calcification rates but a rise in temperature appears to counteract this negative effect on the development of larval skeleton in sea urchin larvae.

Therefore, it is also important to design experiments which would permit organisms to remain under examination for extended periods of time. Longer perturbation experiments would likely allow investigation as to whether the organism can acclimate to hypercapnic and thermal water conditions.

4.4.3   Conclusions

The results of this study suggest that echinoderm larvae have adapted and possibly specialised in a range of ambient CO_2 conditions, from the high concentrations found in the deep sea (Suarez-Bosche *et al. in review*; see Appendix 1) to the widely fluctuating levels typical of the intertidal zone.

In summary, sea urchin larvae are likely to acclimate and survive to predicted ocean acidification and global warming scenarios by using a variety of physiological and biogeochemical responses intrinsic to their biology. The limits to acclimation are set by metabolic trade-offs at a calcification level, for example, through minimising energy to calcify their skeletons in relation to climate variability. Nevertheless, this study suggests that larval acclimation and tolerance to high pCO_2 and future ocean warming is likely to ensure the survival of the species.

CHAPTER 5

GROWING HALF OF THE BODY: DEVELOPMENT OF THE NERVOUS SYSTEM DURING REGENERATION IN SEASTAR LARVAE

5   GROWING HALF OF THE BODY: DEVELOPMENT OF THE NERVOUS SYSTEM DURING REGENERATION IN SEASTAR LARVAE

5.1   INTRODUCTION

5.1.1   Regeneration

Regeneration is the reactivation of developmental processes during postembryonic life in order to restore damaged or missing tissues. It is a process of cell turnover and tissue repair, replacement of lost parts or organs, and even complete re-growth of whole individuals from small body fragments (Carnevali, 2006). The growth of new tissues and structures could be from either non-differentiated (e.g. stem cells) or differentiated established cells in a differentiated environment. Growth may also be the result of new cell division, rearrangement and/or re-specification of existing cells (Thorndyke *et al.*, 1999).

Regeneration is a common occurrence among invertebrate phyla. It has been observed in all classes of echinoderms (Carnevali, 2006). Crinoids and asteroids regenerate appendages (arms, pinnulae, cirri), ophiuroids regenerate internal organs (stomach) and arms, echinoids exhibit regeneration of external appendages (spines) and holothuroids can regenerate the whole visceral mass (Vickery *et al.*, 2001; Carnevali, 2006). This distinctive and remarkable capacity characteristic of this phylum makes echinoderms ideal model organisms in which to investigate regeneration. It is worth noting that asteroids and ophiuroids are capable of asexual reproduction by means of fission (Mladenov *et al.*, 1983) and cloning processes (Carnevali, 2006). The seastar in particular is an ideal model organism because it is easy to grow in the laboratory and there has been extensive physiological and morphological characterisation of its development. In particular, asteroid larval development is well characterised, and although regeneration is documented it has so far been poorly explored.

5.1.2   The echinoderm larval nervous system

Aspects of neural organisation have been described for larvae of all classes of echinoderms, but there is a lack of detailed information on many aspects of their neuroanatomy (Reynolds *et al.*, 1992; Chee and Byrne, 1997; Moss *et al.*, 1998; Vickery *et al.*, 2001; Nakajima *et al.*, 2004a; Byrne *et al.*, 2006). One of the major problems has been the lack of clearly defined ultrastructural features of neurons in echinoderms. The known anatomy of the echinoderm larval nervous system is based on histochemistry, histology, electron microscopy, *in situ* hybridisation with nucleic acid probes, and immunostaining with antibodies (Burke *et al.*, 2006). The most widely used and successful approach has been the use of antibodies against neurotransmitters and neuropeptides (Chee and Byrne, 1997; Moss *et al.*, 1998; Nakajima *et al.*, 2004a). In particular, antibodies to serotonin (5-HT), dopamine and the SALMFamide peptide antibodies developed by Thorndyke and colleagues have proved to be excellent neural markers (Moss *et al.*, 1994; Beer *et al.*, 2001). Recently, Nakajima *et al.* (2004) developed a monoclonal antibody, 1E11, which is neuron specific and has been used in the identification of neural structures in larvae and adults of echinoderms, hemichordates, and urochordates.

The use of antibodies has revealed a number of interesting features of the echinoderm larval nervous system. In asteroids, the cells occur in pairs and appear to migrate extensively before they congregate near the ciliary band, in which the neurons project neurites to form a network. These organisms have ciliated sensory neurons, interneurons, and few ganglia (Bishop and Burke, 2007).

To date, there has been no detailed description of the nervous system during the regeneration of seastar larvae. For this reason, the aim of this project was to describe neural organisation and neural development during the process of regeneration of the larvae of Pacific seastar species *Pisaster ochraceus* and *Orthasterias koehleri* using the neuro-specific novel 1E11 and anti-serotonin antibodies. Furthermore, the ontogeny of the nervous system during re-growth of missing larval structures was investigated.

5.2   MATERIALS AND METHODS

5.2.1   General description

The seastar *Pisaster ochraceus* and *Orthasterias koehleri* were collected in Eastsound, Orcas Island and Pt. George, Shaw Island WA, USA, respectively (Fig. 5.1). They were maintained in the running seawater aquarium at ambient temperature (mean = $13^{o}C \pm 1.0$) at the Friday Harbor Laboratories, WA, USA.

Figure 5.1 Adult seastar *Pisaster ochraceus* (left side panel) and *Orthasterias koehleri* (right side panel).

Spawning was induced by the maturation promoting hormone 1-methyladenine (1-MA) (Sigma Chemical Co.). One ml of 100 µM 1-MA (in distilled water) was injected in the coelomic cavity of the seastars. Spawning began after approsimately 30 minutes or more. Fertilization and manipulation of the seastar embryos followed standard protocols for larval culture (Strathmann, 1987). Embryos were placed in filtered seawater (1 µm, Millipore) and were fed on the marine microalgae *Isochrysis galbana* and *Rhodomonas* sp. every second day, at a concentration of 6,000 and 3,000 cells ml^{-1} respectively. Temperature (mean = $12.5^{o}C \pm 1.0$) and salinity (mean = 35 ± 0.0) were both constant during the experiment.

The seastar species used in this study have planktotrophic larvae that go through a dipleurula stage before they reach the bipinnaria stage. The bipinnaria develops further into a brachiolaria stage with three preoral arms with attachment organs before

metamorphosis. The larvae were reared for 40 days until the brachiolaria stage. Micromanipulation was performed across the oesophagus (E) to dissect the brachiolaria larvae into anterior (preoral lobe) and posterior (postoral lobe) portions (Vickery *et al.*, 2001; Vickery *et al.*, 2002) (Fig. 5.2).

The bisected preoral and postoral lobes and non-bisected controls (in triplicates) were maintained separately for two weeks in fingerbowls placed in water tables with a circulating seawater system. The filtered seawater in each fingerbowl was changed every other day (Strathmann, 1987) and the bisected portions and controls were fed with the microalgae *Isochrysis galbana* and *Rhodomonas* sp every second day.
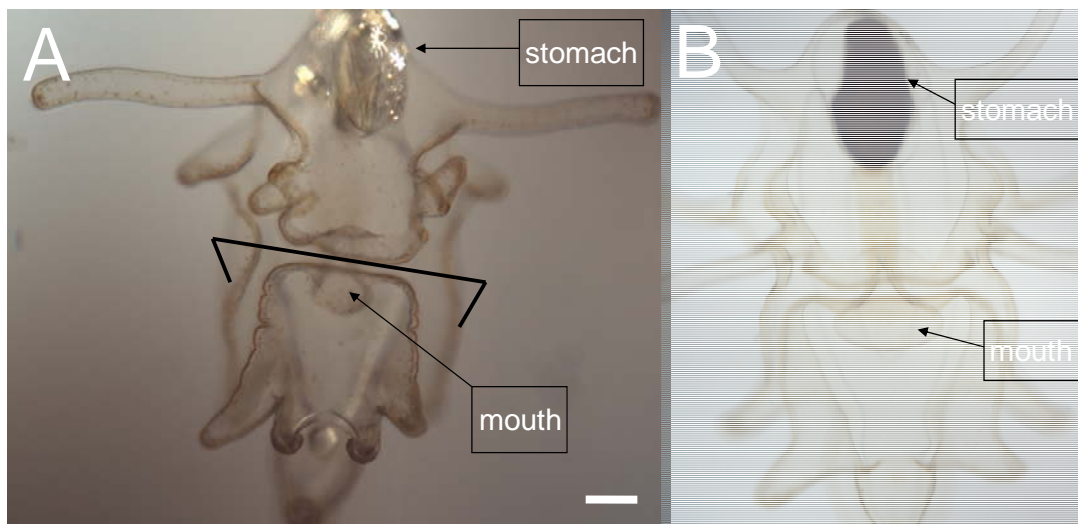
Figure 5.2 Brachiolaria larvae of the two seastar species *P. ochraceus* (A) and *O. koehleri* (B). Dissection into preoral lobe (anterior portion including mouth) and postoral lobe (posterior portion including stomach). Line of bisection is shown in panel A. Scale bar represents 100 μm.

5.2.2   Immunofluorescence protocol

A new protocol for indirect immunofluorescence was developed, with optimised fixation and dilution of the antibodies (1E11 and anti-serotonin), for immunostaining of seastar larvae during regeneration (see Appendix 10 for full details of the methodology). Larvae were collected and washed once with 0.22 μm filtered seawater. The specimens were gently fixed for 15 minutes by drop by drop addition of 4% paraformaldehyde in seawater. They were then post-fixed in ice-cold methanol (MeOH; the use of cold

methanol greatly improved larval morphology) for no more than 5 minutes at room temperature (RT). To reduce non-specific antibody binding the specimens were incubated for 30 minutes in phosphate-buffered saline (PBS) and blocked with PBS containing 0.05% Triton X-100 (PBST) plus 5% normal goat serum. The primary antibodies, anti-synaptotagmin (1E11, Nakajima *et al.,* 2004) and anti-serotonin (Invitrogen, USA), were diluted 1:200 and 1:50 in blocking buffer, respectively. After overnight incubation at 4°C the larvae were rinsed three times in PBST. They were then incubated with the respective secondary antibodies, Alexa Fluor 488 conjugated anti-mouse IgG and Alexa Fluor 568 conjugated anti-rabbit IgG (Molecular Probes, Invitrogen, USA; respectively), diluted 1:500 in PBST for two hours at RT. After rinsing three times with PBS, the specimens were mounted on a slide (LabScientific, Inc.) in Glycerol:PBS (1:1) and examined with a radiance confocal microscope (Nikon Eclipse E800). Images were adjusted and assembled using Image J software (NIH, USA).

5.2.3   Application of Stokes' theorem to estimate irregular areas

The areas of the larvae were calculated by using a practical result derived from the general Stokes' theorem of Integral Calculus (M.C. Suarez-Arriaga, *pers. comms.*). This particular result gives the area A of an irregular plane region of shape D delimited by a closed curve C as shown in the figure, and represented by the following equation:

$$A(D) = \int_D dA = \frac{1}{2} \int_C (x\,dy - y\,dx)$$

(1)
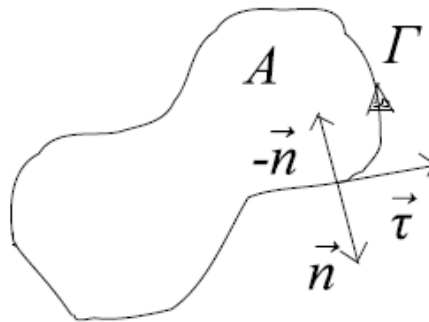
Figure 5.3 The shape of a seastar postoral lobe during regeneration. The area of each larva was calculated using matlab. A = area of the seastar larvae.

93

Where the circle on the second integral denotes that the integration must be performed over the entire curve C. Using this result for the particular case of linear splines, which are the union of n straight-lines S_i covering approximately the entire curve C (see Fig. 5.3), a practical algorithm is obtained to estimate any irregular area. The equation of each one of the lines y (x) defined by two points (x_i, y_i) and (x_{i+1}, y_{i+1}), for i = 1, n is given by:

$$y - y_i = \frac{y_{i+1} - y_i}{x_{i+1} - x_i}(x - x_i) \tag{2}$$

with the condition that the last point (x_{n+1}, y_{n+1}) is connected to the first one (x_1, y_1) it follows that:

$$A(D) \approx \frac{1}{2}\sum_{i=1}^{n}\oint_{S_i}(x\,dy - y\,dx) \cong \frac{1}{2}\sum_{i=1}^{n}x_i(y_{i+1} - y_i) - y_i(x_{i+1} - x_i) \tag{3}$$

Where the n integrals are performed over every linear spline S_i (i = 1, n).

The areas of the larvae investigated at different developmental stages of regeneration were calculated using equation 3 (program developed by M.C. Suarez-Arriaga) in Matlab R2009a (see Appendix 12 for Matlab code) (The MathWorks, Inc. 2009).

5.2.4   Volume estimation

The volumes of the larvae were calculated by multiplying the thickness of the confocal sections (approximately 2.5 µm) by the number of optical section taken for each image.

5.2.5   Statistical analyses

The regenerated portions and controls were examined and measured every other day for two weeks. All measurements were analysed statistically using one-way ANOVA, with day as the fixed factor and the area/volume as the dependent variable. The parametric Tukey post-hoc test was used to assess the significant differences between treatment groups, and values of $P < 0.001$, $P < 0.01$ and $P < 0.05$ were employed to assess statistical significance. All analyses were carried out using Statistica 9 (StatSoft, Inc. Oklahoma, USA) software.

5.3   RESULTS

5.3.1   Regeneration of seastar larvae after bisection

The larvae of the seastar species *P. ochraceus* and *O. koehleri* were surgically bisected 40 days after fertilization. This study reports for the first time the larval body mass and the thickness of the larval tissue (area and volume), as an indicator of growth during regeneration at various larval stages (Fig. 5.4). Before dissection the areas of brachiolaria larvae of *P. ochraceus* and *O. koehleri* were 1.55 ± 0.07 mm^2 ($n = 3$) and 2.13 ± 0.41 mm^2 ($n = 4$), respectively (see Appendix 11). After the larvae were bisected, both the anterior and posterior portions continued swimming by utilising the ciliary band and were able to feed on phytoplankton. Remarkably, the anterior portion continued to collect phytoplankton in the oral cavity even though the gut had been lost due to bisection. Meanwhile, the posterior portion collected phytoplankton directly through the oesophagus.

Immediately after bisection the preoral lobe of *O. koehleri* larvae decreased in size (bisected = 0.377 ± 0.012 mm^2 in area; 13 days later = 0.259 ± 0.013 mm^2 in area; $n = 6 \pm$ SE). The decrease in size of the postoral lobe (with a functional digestive system) continued until day 7, at which point the measured area appeared to plateau and then the lobe exhibited further growth (see Fig. 5.4 and Appendix 11).

Both the bisected preoral and postoral lobes of the *P. ochraceus* larvae decreased in size after bisection (preoral lobe area = 0.246 ± 0.042 mm^2; with a minimum in size 7 days later 0.114 ± 0.023 mm^2; $n = 7 \pm$ SE; postoral lobe area = 0.374 ± 0.030 mm^2; with a minimum size 7 days later 0.117 ± 0.040 mm^2; $n = 9 \pm$ SE).
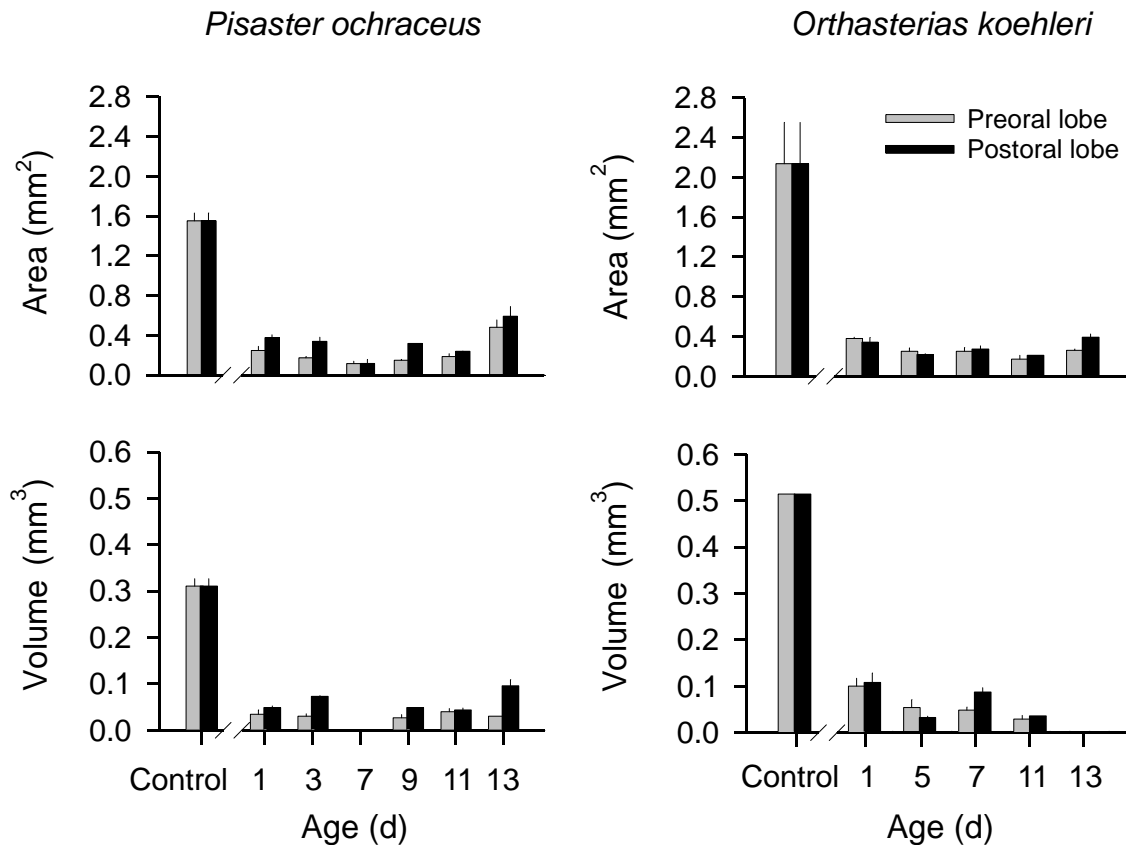
Figure 5.4 Development of *P. ochraceus* and *O. koehleri* larvae during regeneration after bisection. Measurement of the body area and volume of the preoral lobe (grey) and postoral lobe (black). Error bars indicate ± SE.

The resulting new postoral lobe of *P. ochraceus* had a significantly larger area at day 13 compared with the postoral portion immediately after bisection ($P < 0.001$). Conversely, the increase in size for the bisected *O. koehleri* larvae constituted a smaller area than the portions immediately after bisection ($P < 0.05$) (see Table 5.1 for statistical data).

Table 5.1 One-way ANOVA of estimates of the area and volume during re-growth of *P. ochraceus* and *O. koehleri* larvae from bisected preoral and postoral lobes.

	Source	SS	MS	*F (df)*	P
Pisaster ochraceus					
Preoral lobe	Day*Area	0.476266	0.095253	6.19 (5,16)	< 0.001
	Day*Volume	0.000245	0.000061	0.41 (4,8)	0.79
Postoral lobe	Day*Area	0.513986	0.102797	3.89 (5,18)	< 0.001
	Day*Volume	0.004718685	0.00118	10.24 (4,12)	< 0.001
Orthasterias koehleri					
Preoral lobe	Day*Area	0.067153123	0.016788	7.05 (4,13)	< 0.01
	Day*Volume	0.008074164	0.002691	13.25 (3,8)	< 0.001
Postoral lobe	Day*Area	0.080521913	0.02013	3.68 (4,11)	< 0.05
	Day*Volume	0.011737454	0.003912	4.58 (3,6)	< 0.05

The increase in size of the preoral lobe of the *P. ochraceus* larvae resulted in a significantly smaller area and volume measurements than those of the postoral lobe. Conversely, the growth of both the preoral and postoral lobes of *O. koehleri* larvae was broadly similar (Fig. 5.5). Overall, the postoral lobes of both species, which retaining a functional gut and with the ability to digest phytoplankton more rapidly, produced a larger area and volume than the preoral lobes. The smaller preoral lobes of *P. ochraceus* suggest that food limitation affected their growth. However, the preoral lobes were able to accumulate phytoplankton particles in the oral cavity while a functional digestive system regenerated. Furthermore, the bisected anterior lobe appeared to reabsorb some larval body tissue as a nutrient source during re-growth of a functional gut, thus explaining their decrease in area and volume.
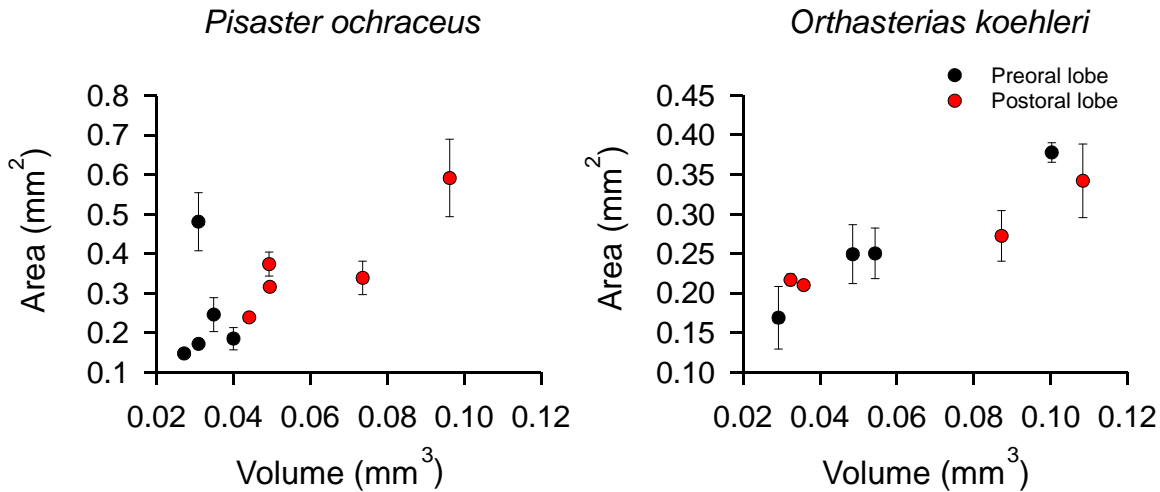
Figure 5.5 Development of the area and volume of the preoral (black) and postoral (red) lobes during regeneration of *P. ochraceus* and *O. koehleri* larvae. Data for area are means ± SE.

5.3.2   The larval nervous system in seastars

Immunofluorescent staining with the 1E11 and anti-serotonin antibodies revealed all known neural structures during regeneration of the *P. ochraceus* and *O. koehleri* larvae. The apical ganglion, oral ganglia, an array of neurons and neurites that extend into the ciliary bands, cell bodies in the oesophagus, and a network of neurites in the intestine were observed. In the brachiolaria stage, 1E11 and anti-serotonin antibodies labelled an elaborate array of neurons and neurites (Fig. 5.6). The cell bodies of the immunoreactive neurons of the ciliary band nerve varied in shape, which is a common feature of asteroids (Chee and Byrne, 1997; Nakajima *et al.*, 2004a; Elia *et al.*, 2009). Cell bodies and flask-shaped nerve cells, visible in the ciliary band in *P. ochraceus* and *O. koehleri* have previously been observed in echinoid larvae (Beer *et al.*, 2001; Burke *et al.*, 2006).
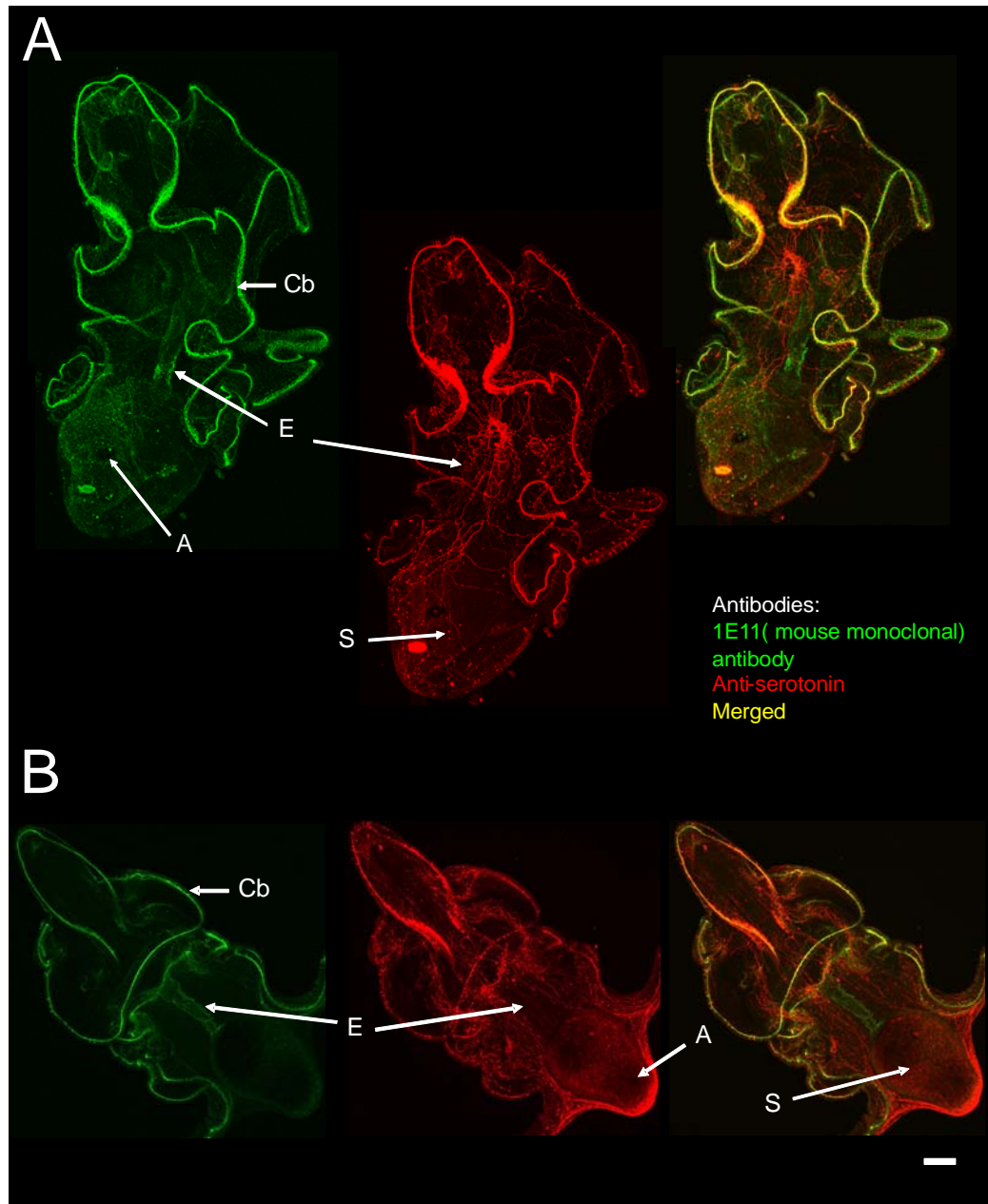
Figure 5.6. Nervous system of the *P. ochraceus* larva (A) and *O. koehleri* (B) revealed by immunofluorescent staining. The confocal stack shows details of the ciliary band (Cb) and neurons immunolabeled with 1E11 (green) and anti-serotonin (red) antibodies. The merged image of the two staining patterns (yellow) is shown to the right. Anus (A); Oesophagus (E); Stomach (S). Scale bar represents 100 μm.

The ciliary bands were broad and the cell bodies evenly spaced throughout the bands. The cells were interconnected by thin neurites that projected from the ciliary bands. Regularly spaced immunoreactive flask-shaped cells were observed within the ciliary bands (Fig. 5.7).
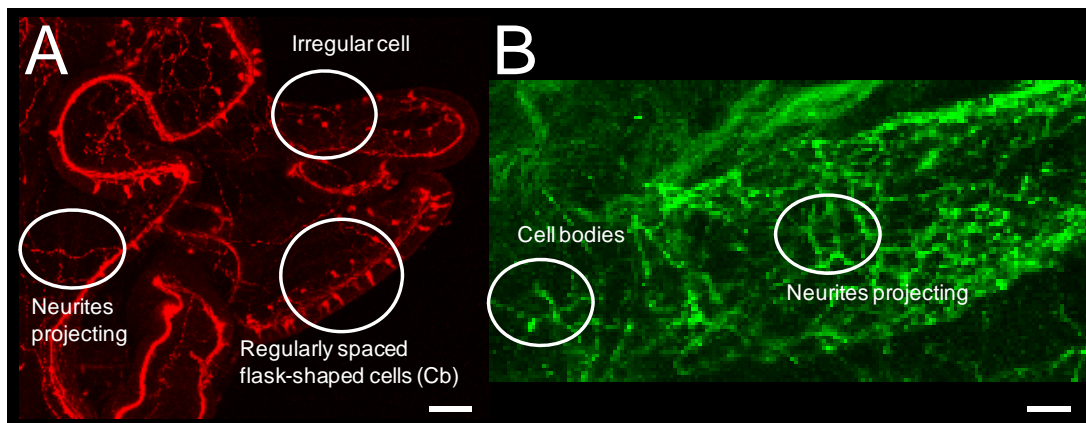
Figure 5.7 Immunoreactive cells and neurites in the *P. ochraceus* larva. A close up of the confocal image reveals different structures of the larval nervous system: (A) neurite projections, irregular cells between the ciliary band (Cb) and regularly spaced flask-shaped cells. Scale bar represents 50 µm. (B) Confocal stack of the oesophagus exposed neurite projections and cell bodies revealed by the 1E11 antibody. Scale bar represents 20 µm.

5.3.3   Nervous system during regeneration

The process of regeneration was followed for two weeks and larvae were fixed every other day for subsequent analysis of the regenerating region by immunofluorescent staining and confocal microscopy. An immunoreactive neuroblast appeared in the regenerating postoral larvae portion four days after bisection. When first observed, the serotonergic ganglion (formed by lateral clusters of serotonin-containing cells) was associated with the projections of neurites (Fig. 5.8).

Moreover, a large number of flask-shaped cell bodies with 5-HT-like immunoreactivity developed in the epithelium. Confocal sectioning into the larva from the ventral surface revealed axonal-like processes from the basal portion of these cells bodies extending inwards towards the buccal cavity and apical surface (Fig. 5.8). The immunoreactive cell bodies are associated with the larval mouth and what appear to be a fine neurites forming an intersection of nerves (plexus) surrounding the oesophagus (Fig. 5.10).
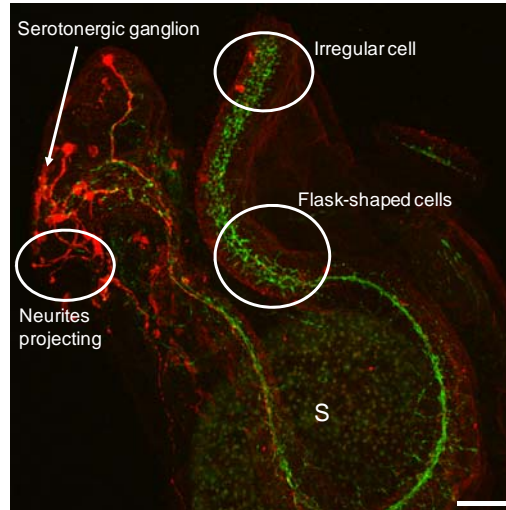
Figure 5.8 Posterior lobe of *P. ochraceus* after 4 days of regeneration. Lateral view revealed projection of neurites from the ciliary band (Cb) toward the oral ectoderm as in gastrulation. Imunostaining with the 1E11 (green) and anti-serotonin antibodies (red) revealed irregular cells and flask-shaped cells in between the Cb. Stomach (S). Scale bar represents 20 μm.

By the start of day 7, larval re-growth had produced a prominent cluster of neurite tracks throughout the length of the entire circumoral ciliary band. This cluster became more dense by day 9 (Fig. 5.9 and 5.10). Furthermore, the ganglion innervates the preoral and postoral ciliated bands interconnecting them during neurogenesis of the larvae.

Regeneration of the posterior lobe of *P. ochraceus* was completed after 11 days. Both the anterior and posterior lobes of the larvae were capable of regenerating the missing mouth and upper oesophagus. In the case of the anterior lobe, regeneration of the stomach was also observed. Internally, the larvae of both species had a well-developed gut and a distinct extension formed at the end of the larvae (e.g. both posterior and anterior) containing a complicated network of neurons and neurites (Fig. 5.10 and 5.11).
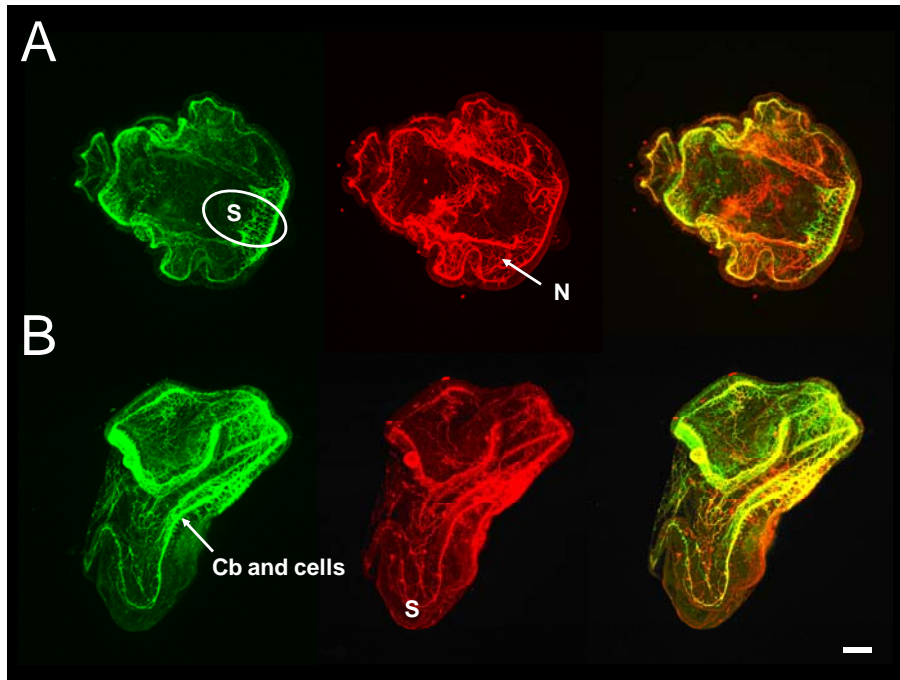
Figure 5.9. Anterior lobe of *P. ochraceus* after (A) 9 and (B) 11days of regeneration, showing completion of a net of neurons and neurites (N). Ciliary band (Cb), stomach (S). Ellipsoid highlights the stomach that was regenerated. Scale bar represents 100 μm.
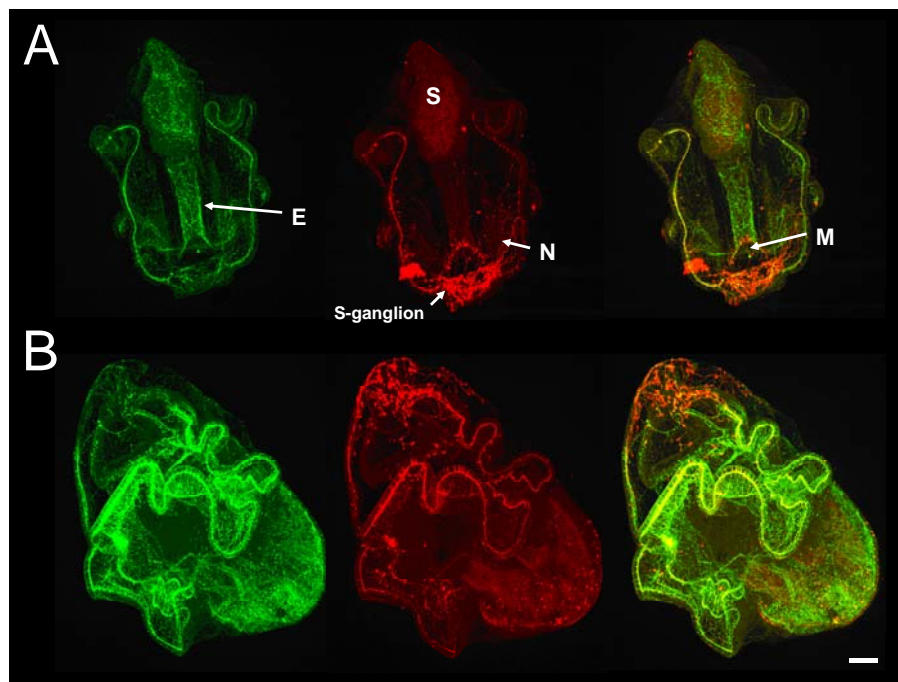
Figure 5.10 Posterior lobe of *P. ochraceus* after (A) 11 days and (B) after 13 days of regeneration. The serotonergic ganglion (S-ganglion) appears to be associated with the oral cavity. Oesophagus (E), stomach (S), neurites (N) and mouth (M). Scale bar represents 100 μm.
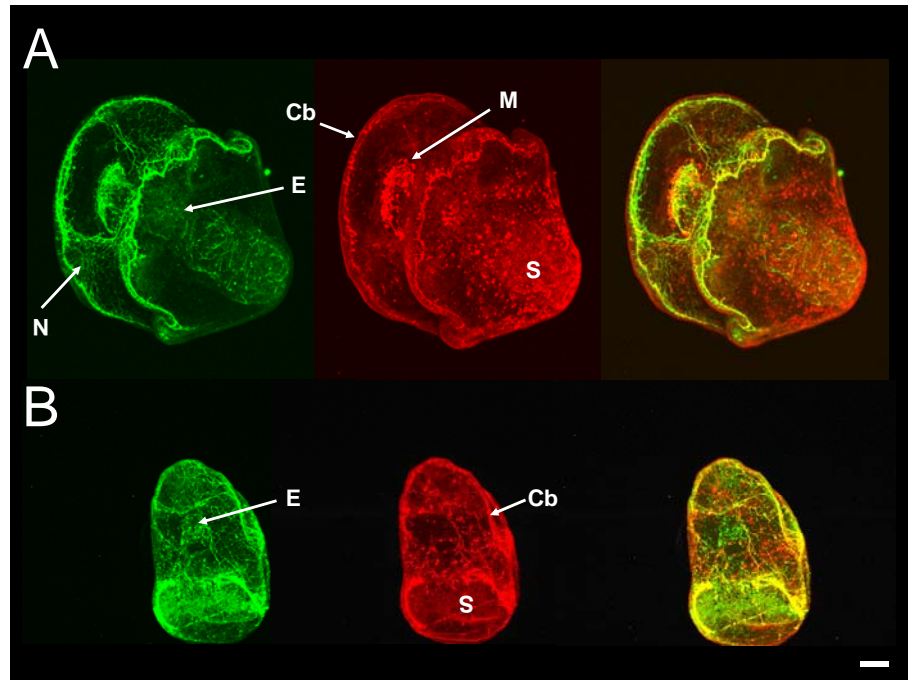
Figure 5.11   Regeneration of the posterior lobe (A) of *O. koehleri* larvae with the formation of a complicated net of neurons and neurites by day 7. Regeneration of the anterior lobe (B) by day 11. Ciliary band (Cb), neurites (N), mouth (M), stomach (S) and oesophagus (E). Scale bar represents 100 μm.

5.4 DISCUSSION

The results of this study demonstrate that the planktotrophic larvae of the seastar *P. ochraceus* and *O. Koehleri* possess extensive regeneration capabilities. The separated preoral and postoral lobes of both species regenerated missing body parts (with organogenesis) within two weeks; with no mortality due to bisection. The regeneration processes in the brachiolaria larva were similar to those described for *Luidia foliolata* and *Pisaster ochraceus* (Vickery and McClintock, 1998; Vickery *et al.*, 2002). It has also been demonstrated that following surgical bisection of *Luidia foliolata* and both bipinnaria and brachiolaria larvae of the seastar *Pisaster ochraceus* into anterior and posterior portions, both portions of the larva are able to regenerate all missing organs and tissues (Vickery and McClintock, 1998).

5.4.1   Ontogenesis during regeneration

During the re-growth of seastar larvae, both species showed a thickening of the former upper oesophagus/lower mouth in the anterior portion during the first 48 hours following surgical bisection. After the appearance of mesenchyme cells, an invagination of the body-thickened wall occurred to form a tube. In both seastar species the anterior portions of the bisected larvae lacked their functional gut and were unable to feed on phytoplankton (Fig. 5.12). This caused a reduction in the area and volume of the preoral lobes for 7 days until a functional digestive system had regenerated and the capacity to feed was restored (Fig. 5.12). Seven days after bisection, the newly formed digestive tube in the anterior portion elongated towards the posterior portion and formed the anus. By day 10 the anterior portion had completed the digestive tube and the new oesophagus, intestine and stomach were differentiated. In the mean time (by day 7), the posterior portion had almost completely regenerated the mouth. Conversely, the posterior portion with a functional digestive system continued to feed actively and increased in area and volume over the two week regeneration period. As a result of regeneration with organogenesis, two new, completely independent larvae were produced following surgical bisection of the original larvae of *P. ochraceus* and *O. koehleri*, after approximately 11-13 days.
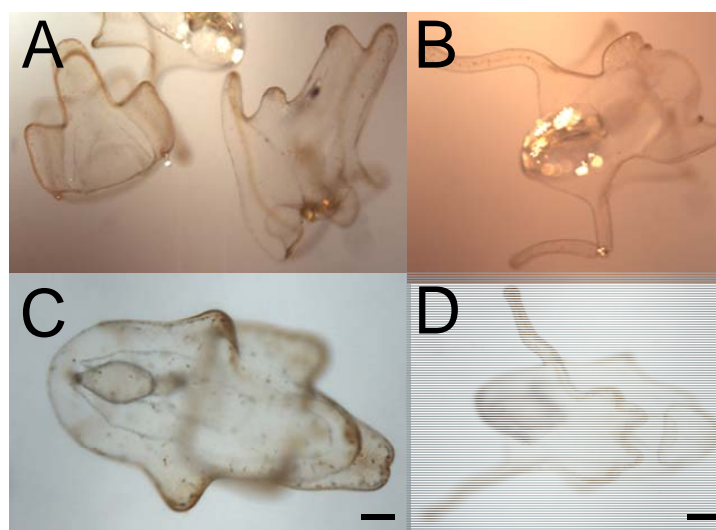
Figure 5.12 Light microscopy images showing the anterior lobe (A) and posterior lobe (B) after bisection (time zero of regeneration). After 13 days, regeneration of both the anterior lobe (C) and posterior lobe (D) was complete. Scale bars represent 50 μm (A and C) and 100 μm (B and D).

Mesenchyme cells played a regenerative role in the formation of a new pair of coelomic pouches, as previously documented during the regeneration of echinoid larvae (Vickery *et al.*, 2001). The coelomic structures are fundamental body components, and the coelomocytes participate in regenerative processes in adult echinoderms (Thorndyke *et al.*, 1999). Observations made in this study suggest that during re-growth, cell proliferation was initiated at the larval epithelium (ectoderm) near the site of bisection. Microscopic examination revealed that these cells appeared to de-differentiate into mesenchymal-like cells and then to re-differentiate into new types of cells that eventually gave rise to the regenerated body parts (Thorndyke *et al.*, 1999). However, further investigations are necessary to characterise this process.

Cell fate in echinoderm larvae has previously been thought to be pre-determined and irreversible once the larvae reach a certain developmental stage (Thorndyke *et al.*, 1999). However, the results of this study demonstrate that fully-differentiated larval body tissues had the same capacity to recapitulate their developmental process as that shown during gastrulation.

The plasticity of developmental pathways and organogenesis suggested that additional proliferation and apparent de-differentiation and re-differentiation takes place in order to restore missing body parts. These observations are in line with those of Vickery *et al.* (2002), who found that during larval regeneration of asteroids and echinoids, organogenesis could apparently re-grow new tissues (including the larval coelomic pouches) from previously differentiated cells. Taken together, these findings indicate that the fate of larval-specific cells is not fixed in planktotrophic echinoderm larvae, and cells are capable of re-forming the missing larval structures.

5.4.2   Neurogenesis during regeneration

This study has produced the first images of neurons undergoing regeneration in bisected seastar larvae. Neurogenesis was clearly revealed by immunostaining with 1E11 and anti-serotonin antibodies (Fig. 5.13). The appearance of the serotonergic ganglia, oral ganglia, intestinal and oesophagus plexus and the cells and neurites in the

ciliary band during regeneration comprised all the components previously described during the development of the larval nervous system (Chee and Byrne, 1997; Nakajima *et al.*, 2004a). Studies with the 1E11 antibody have revealed novel features of the asteroid larval nervous system, such as an extensive plexus in the intestine and oesophagus that was not serotonergic (Nakajima *et al.*, 2004a).
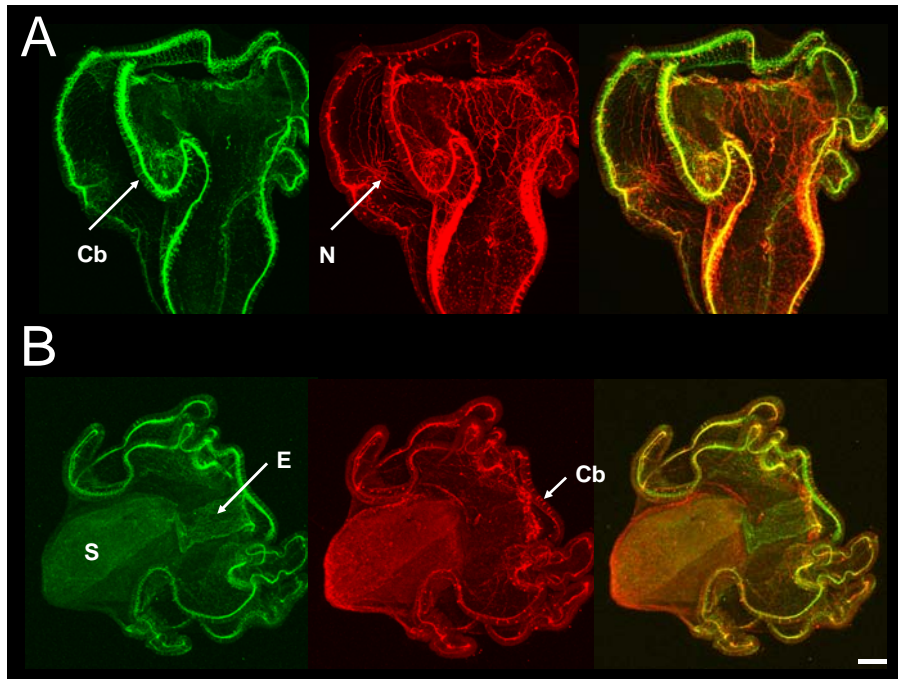
Figure 5.13 Immunostaining with 1E11 and anti-serotonin antibodies of the bisected *O. koehleri* larvae into anterior (A) and posterior (B) lobes (day 0). Ciliary band (Cb), neurites (N), stomach (S) and oesophagus (E). Scale bar represents 100 μm.

The results of the present study suggest that the developmental path of the nervous system followed by the bisected seastar larval portions is similar to those reported during gastrulation in echinoderm embryos [asteroids: (Chee and Byrne, 1997; Nakajima *et al.*, 2004a); holothurians: (Byrne *et al.*, 2006; Nakano *et al.*, 2006; Bishop and Burke, 2007); echinoids:(Vickery *et al.*, 2001; Morris *et al.*, 2004); crinoids: (Nakano *et al.*, 2009)]. The nervous system of the regenerating portions has a number of similarities to the neural structures formed during the process of gastrulation. Neurons and neurites are mostly within or associated with the ciliary band, the mouth, and the musculature in the regenerating portion. There is also a projection of neurites from the ciliary band towards the oral ectoderm as seen during gastrulation (Nakajima *et al.*, 2004a). As the regenerated portions elongated, serotonergic cells formed a

hemispherical array at the bisected end of the larvae (as in gastrulation), which indicates the migration and rearrangement of these cells. Both types of larvae regenerated paired oral ganglia associated with the larval mouth and with a network of immunoreactive cells (containing serotonin), furthermore the oesophagus started regeneration. Interestingly, the immunoreactive neuroblast appears during regeneration suggesting that the larvae recapitulate the growth of the nervous system as in gastrulation (Nakajima *et al.*, 2004a). Moreover, during neurogenesis of both bisected seastar species, cells of the ciliary band nerve gave rise to neurites that connected the surrounding neural network in the pre- and post-oral lobe.

It has been suggested that the neuronal cells connected to the ciliary band nerve play an important role in the coordination of the ciliary band activities (e.g. swimming and feeding; Chee and Byrne, 1997). It has also been proposed that planktotrophic larvae use the cilia of the ciliary band to carry food particles into the oesophagus (Strathmann, 1975) by muscle contractions. The ciliary band in *P. ochraceus* and *O. koehleri* larvae projected interconnecting neurites that were predominant in the oral ectoderm. The extensive plexus of neurites associated with the ciliary band system and digestive tract that was observed in this study is characteristic of feeding echinoderm larvae (Nakajima *et al.*, 2004a; Nakano *et al.*, 2006).

It has recently been proposed that the nervous system controls initiation of the retraction and resorption of larval tissue during echinoderm metamorphosis (Elia *et al.*, 2009). Since regeneration is essentially a developmental phenomenon that requires retraction and resorption of larval tissue, re-growth may be controlled in part by the larval nervous system.

Regardless of the seastar species, the process of regeneration of the nervous system observed in this study was strikingly similar to that described during gastrulation. This provides an insight into aspects of the nervous system that are essential for development and neurogenesis. This similarity also suggests conservation of neurogenesis mechanisms regardless of the developmental stage. The larvae regenerated their nervous system after bisection via the same path of neurogenesis used during gastrulation. Further investigation of neural development in earlier stages of

embryogenesis in both *P. ochraceus* and *O. koehleri* is required to add support to the hypothesis of neurogenic conservation.

5.4.3   Conclusions

Finally, the findings of this study indicate that the relationship between invertebrate deuterostomes and the chordates cannot be fully elucidated without a clear understanding of the organisation of their nervous systems. This study has highlighted the need for more research in the area of regeneration of echinoderm larvae and the mechanisms underlying regeneration of the nervous system. As echinoderms share many developmental traits with other deuterostomes, research into the neural repair processes in their larvae may lead to a better understanding of neurogenesis in many higher animals, including vertebrates.

CHAPTER 6

GENERAL DISCUSSION

6   GENERAL DISCUSSION

6.1   PROJECT SUMMARY

This thesis investigated environmental controls in echinoderm larval development. Echinoderms occupy a unique place in embryological studies as it possesses a number of features that makes it an excellent model organism. Firstly, they are extremely susceptible to changes in the chemistry of seawater and temperature, making them ideal subjects with which to examine environmental, ecological and evolutionary responses of marine biota to a changing world.

Furthermore they have several strategies to survive environmental stress (e.g. changes in temperature and carbonate chemistry, predations, long periods of starvation), including different reproduction modes. Echinoderm larvae have the capacity to undergo asexual reproduction, fission, cloning and regeneration of an entire organism from small body fragments. These remarkable abilities can be considered specific developmental strategies, during their larval life, that facilitate the species survival.

This research used two approaches to address the tolerance and abilities of echinoderm larvae to adapt to a changing ocean:

1) A study of the effect of ocean acidification and the changes it causes in carbonate chemistry on the development of sea urchin larvae *Psammechinus miliaris*.
2) A study of the nervous system of seastar larvae during regeneration.

Alterations to seawater carbonate chemistry caused by anthropogenic emissions of CO_2 are generating profound changes in the marine environment, which the scientific community is only beginning to understand. The response of marine biota to these environmental alterations is, however, highly complex and requires long-term experimental analyses to be fully understood. This study, unlike any other in the current literature, has provided an examination over time scales relevant to larval development

(fertilization to metamorphosis) rather than a few days or hours as has been investigated in the literature. Although recent studies have investigated the effect of ocean acidification on echinoderm larvae, they do not determine the impact of ocean acidification under "long-term" exposure (from the process of fertilization to larval metamorphosis) to high CO_2 conditions; this can lead to misguided conclusions (see review of Dupont *et al.*, 2010). The literature does not address either the impact of ocean acidification on larval development in naturally occurring CO_2-enriched waters.

This study addresses both knowledge gaps. Firstly, experiments lasted up to 38 days, compared to 13 days as the current maximum duration in the literature (Kurihara and Shirayama 2004; Dupont *et al.*, 2010). As a result of the extended time of exposure, my results revealed a different trend compared to that shown in the contemporary literature. In longer-term exposures, echinoderm larvae appear to adapt to increasing levels of CO_2 in the seawater. However in the shorter-term experiments undertaken in this study, the echinoderm response to CO_2-enriched waters is more mixed (negative effect on fertilization and calcification but no effect on general larval growth). It is suggested, therefore, that subsequent to experiencing an initial mixed response, echinoderm larvae start to build a tolerance to CO_2-enriched waters and acclimate.

This study used, for the first time, naturally-occurring CO_2 enriched waters for experimentation and did not rely on manual carbon chemistry manipulation. Naturally-occurring gradients in the carbonate saturation state (seawater from different depths) were obtained to analyse the effect of CO_2 changes on the model organism. These field data were then compared with laboratory experiments where echinoderms were analysed under tightly controlled conditions (pH, CO_2 and temperature). Trends from both environments (natural and controlled) suggested that *P. miliaris* larvae are capable of tolerating broad changes in carbonate chemistry and can be therefore be deemed an evolutionary success.

Additionally, an experiment to document the regeneration of the nervous system of echinoderm larvae was conducted. Although the nervous system and echinoderm regeneration have previously been described in the literature as separate topics (e.g.

Byrne *et al.,* 2006, Burke *et al.,* 2006, Nakahima *et al.,* 2004, Vickery *et al.,* 2001), this is the first time both have been studied simultaneously.

The following sections further detail findings from this thesis' major experimental themes, namely:

1. Fertilization success in near-future levels of ocean acidification and ocean warming
2. Mortality rates in near-future levels of ocean acidification and ocean warming
3. Larval growth and development of *Psammechinus miliaris*
4. Changes to calcification rates of *Psammechinus miliaris* under CO_2-induced ocean acidification and ocean warming
5. Development of the nervous system during regeneration in seastar larvae *Pisaster ochraceus* and *Orthasterias koehleri*

6.2   FERTILIZATION SUCCESS IN NEAR-FUTURE LEVELS OF OCEAN ACIDIFICATION AND OCEAN WARMING

6.2.1   Summary of findings

Elevated CO_2 conditions (hypercapnia) decreased the fertilization success of the sea urchin *P. miliaris* by approximately 20% to 30%. As dissolved CO_2 crosses the membranes, energy must be spent to maintain the ionic balance within the organism compartments. One concern is whether or to what extent organisms are able to maintain this balance under projected ocean acidification scenarios, and the consequences on fertilization and larval development remain an open question. In the present study it was demonstrated that elevated pCO$_2$ has an impact on the reproductive success of the sea urchin, because fertilization requires an intracellular increase in pH to initiate development (Johnson, 1976).

Importantly, this study showed that the effect is reduced when temperature increases, as warming decreases the level of CO_2 absorption and the cell membrane structure acts as a diffusion barrier. Therefore, the increase in temperature appears to counteract the negative effect that acidification of seawater has on fertilization (as shown in Fig. 6.1). This is reported in detail in Chapters 2 and 4.

6.2.2   Implications

In all experimental cases, the fertilization success of *P. miliaris* decreased in the presence of elevated environmental pCO$_2$ (Fig. 6.1). Since the oceans are expected to undergo changes in temperature, it is irrelevant to examine pCO$_2$ in isolation this stressor factor. As seen in this study, temperature is perhaps one of the most influential stressor factors to echinoderm larvae. Therefore, it is suggested that multifactorial experiments represent a more realistic scenario of an organism's responses to environmental selection pressure.

6.3   MORTALITY RATES IN NEAR-FUTURE LEVELS OF OCEAN ACIDIFICATION AND OCEAN WARMING

6.3.1   Summary of findings

Both laboratory experimental studies showed that an increase in the percentage of mortality was directly linked to higher pCO$_2$ values and higher temperatures (Fig. 6.1). Furthermore, higher calcification rates investigated in this study (enhanced with an increment in temperature) proved to be linearly correlated with higher mortality rates. It is suggested that, since larvae need to invest more energy in order to produce larger skeletons during growth, as they use more resources on calcification only those that can tolerate the stressing conditions survive.

The laboratory experiments showed that debris and contamination in the cultures are all factors that enhance larval sensitivity and lead to higher mortality rates (Fig. 6.1). It should be noted that the comparison in the percentage of mortality in Figure 6.1 is based on data from two different experiments. The first dataset was calculated at day 21 (different CO$_2$ levels experiment) while the second dataset was calculated at day 38 (combined CO$_2$ + temperature experiment). This will lead to some limitation in comparison, as the experiment that lasted longer will inevitably show higher rates of mortality.

6.3.2   Implications

The negative effect of an increase in mortality rates with ocean acidification and temperature will likely feed through to the wider marine ecosystem. For example, the abundance of commercially-important shellfish species (e.g. clams, oysters, sea urchins) may decline, having potentially serious consequences for marine food resources (Cooley *et al.,* 2009).

Furthermore, increases in oceanic temperature and CO_2 predicted for the global ocean over the next 50 and 100 years, are likely to impact echinoderm development and survival. For example, whilst marine calcifiers development would likely continue, the energy invested in metabolic trade-offs to compensate for climate variability might decrease survival success. Marine calcifiers, such as echinoderms, play a key role in maintaining the balance and energy flow in coastal ecosystems (e.g. grazing, burrowing, calcifying) (McClintock 1994, Turon *et al*. 1995) and so any decrease in survival success may potentially upset the balance of energy flow in the coastal zone. Another implication of changes to temperature, salinity and food availability is the forcing of species to migrate to areas with less extreme environments. It has been proposed that the higher latitudes would represent a threat to marine organisms, and most likely their marine biota would be displaced towards lower latitude environments (Doney, 2006).

However, echinoderm larvae presented a plastic response to climate stressors (e.g. high temperature and CO_2), that could enable the phylum to survive. The main reason is that these organisms inhabit waters that are increasing in CO_2 concentrations (e.g. deep ocean water, upwelling zones, CO_2 vents), allowing a physiological adaptation for many generations. The tolerance that echinoderms have for those environments would result in an evolutionary advantage. However, it is important to note that acclimation is hampered by a trade-off at the calcification level. If a decrease in skeleton production continues, mortality rates will increase as the formation of shell for these organisms is vital for development and survival. A consequential decrease in echinoderm populations would undoubtedly be felt well beyond their own species with likely knock on effects to various pelagic ecosystems.
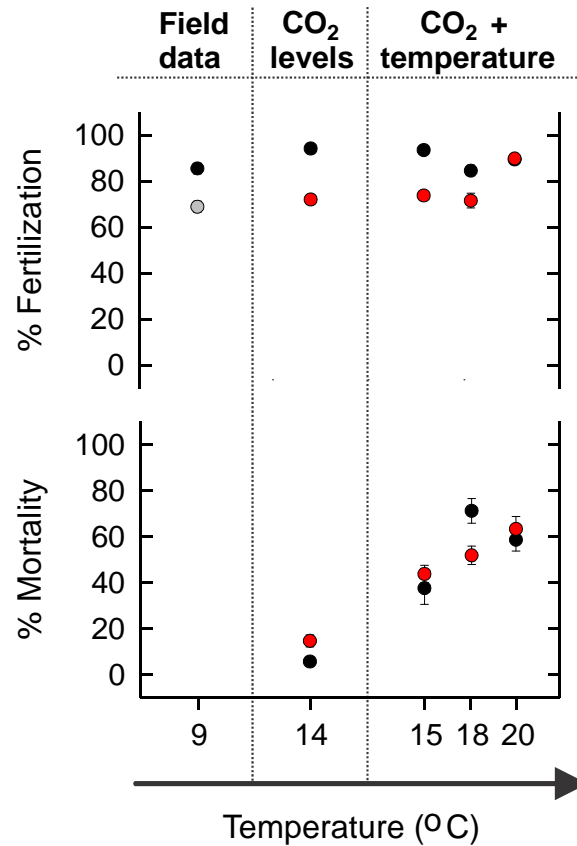
Figure 6.1 Sea urchin *P. miliaris* response to environmental stressors on the percentage of fertilization and mortality. Black circles indicate present pCO_2 values of ~ 250 ppmv, gray and red circles correspond to projected future concentrations of ~ 420 and ~ 920 ppmv respectively. Values are means ± SE. It should be noted that pCO_2 values differed slightly between experimental sets and are therefore only approximations. Percentage of mortality for the field data is not available due to the short culture time of this experiment. The CO_2 levels experiment represents mortality at day 21 and the experiment of CO_2 + temperature interaction indicates mortality at day 38.

6.4 LARVAL GROWTH AND DEVELOPMENT OF
PSAMMECHINUS MILIARIS

6.4.1 Summary of findings

Both data from the field and laboratory experiments highlight the ecological relevance of testing the CO_2 and temperature synergistic effects and the capacity of the larvae to tolerate climate stressors (as seen in Fig. 6.2). This study showed the

117

phenotypic plasticity of larval growth (POA and BL) under increments in pCO$_2$ and the associated changes in seawater carbonate chemistry. These data showed that the general growth of the larvae did not exhibit any detrimental effects, even in the presence of near and/or undersaturated conditions (where Ω-Cal = 1.16 and Ω-Arg = 0.75; this is addressed in Chapter 2). It is important to note that echinoderms typically experience fluctuations in water carbonate chemistry, characteristic of their habitat due to photosynthetic activity (e.g. pH 8.3- 7.5) (Menendez *et al.*, 2001; Wootton *et al.*, 2008), riverine inputs and upwelling events on daily and seasonal bases. This adds weight to the findings of this study that the early life history of *P. miliaris* is likely to adapt to a broad range of pH, as they are already experiencing these fluctuations in their natural environments.

6.4.2   Implications

Overall, these results suggest that echinoderm larvae have adapted and possibly specialised in a range of ambient CO$_2$ conditions, from the high concentrations found in the deep sea to the widely fluctuating levels typical of the intertidal zone (see Chapter 2, 3 and 4). From an evolutionary perspective, the ability of larvae to cope with broad changes in water chemistry conditions may have determined the ability of shallow water echinoderms to progressively colonise deeper environments early in their evolutionary history.
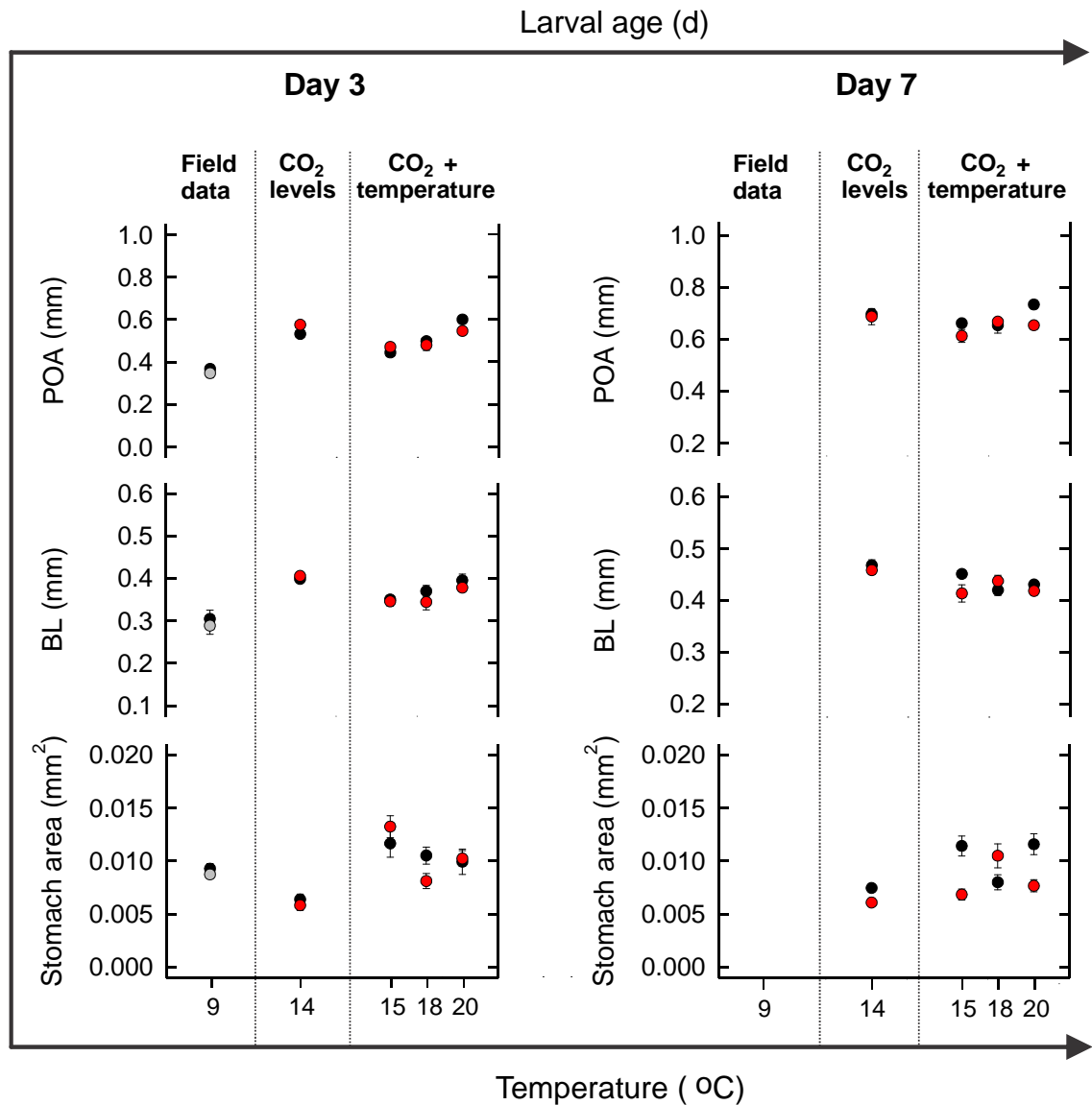
Figure 6.2 Morphological changes in the sea urchin larvae *P. miliaris* exposed for 3 days and 7 days to three different experimental conditions. Postoral arm length (POA), body length (BL). Values are means ± SE. Black circles indicate present pCO$_2$ values of ~ 250 ppmv, gray and red circles correspond to projected future concentrations of ~ 420 and ~ 920 ppmv respectively. Note that pCO$_2$ values differed slightly between experimental datasets and are therefore only approximations. Note that no field data are available for day 7 as the larvae were cultured until day 5 only (see Chapter 3).

6.5   CHANGES TO CALCIFICATION RATES OF
PSAMMECHINUS MILIARIS UNDER CO$_2$-INDUCED OCEAN
ACIDIFICATION AND OCEAN WARMING

6.5.1   Summary of findings

The impact of ocean acidification and ocean warming varies according to the process examined. As demonstrated in this study, calcification is one of the most sensitive processes along with fertilization. Previous studies have shown that echinoplutei can successfully calcify skeletal segments under acidified conditions (e.g. (Kurihara and Shirayama, 2004; Clark *et al.*, 2009; Suarez-Bosche *et al.*, 2010). Even though the widely accepted hypothesis is that ocean acidification will have the greatest impact on organisms that form highly soluble magnesium calcite to build their skeleton (e.g. echinopluteus larvae; Weber, 1969; Politi *et al.,* 2004) results from this study suggest that changes in rates of calcification do not have a major impact on larval fitness. This is important because the skeleton helps to maintain larvae body shape (fitness) for orientation, buoyancy and migration (Strathmann, 2000; Kurihara, 2008), for feeding (Bertram and Strathmann, 1998; Strathmann, 2007), as a defence against predators (Emlet, 1982) and as a pH regulation (Johnson and Epel, 1981).

The interactive effect of temperature and pH on calcification of the sea urchin larvae was investigated. Importantly, there was a gradual increase in PIC production seen in larvae exposed to acidified waters when there was an increment in temperature (Chapter 4). Results from this study suggest that temperature, and not CO$_2$-enriched seawaters, is the main limiting factor in determining the rate of larval calcification.

6.5.2   Implications

A fundamental understanding of the impact of ocean acidification and ocean warming on the process of calcification is necessary to elucidate realistic effects on

larval development and ecological implications. Echinoderms provide a major global contribution of $CaCO_3$ with more than 5% of total ocean biological pump (0.1 Pg C yr^{-1} to global carbon export; see Lebrato *et al.,* 2010). Any changes to their rates of calcification could therefore have important consequences for carbon cycling.

6.6   DEVELOPMENT OF THE NERVOUS SYSTEM DURING REGENERATION IN SEASTAR LARVAE

6.6.1   Summary of findings

This study demonstrated that the planktotrophic larvae of the asteroids *Pisaster ochraceus* and *Orthasterias Koehleri* possess extensive regeneration capacities. Both species regenerated missing body parts (with organogenesis) within two weeks and no mortality occurred due to bisection. For the first time, an area and volume estimation of larvae mass during regeneration was presented. This was important because this approach allowed a more comprehensive study on the fate of the growing tissue during regeneration (see Chapter 5).

Most importantly, this research has shed light on the cell fate during re-growth in echinoderm larvae. It was demonstrated that fully-differentiated larval body tissues have the capacity to recapitulate their developmental process as during gastrulation. Moreover, neurogenesis during the regeneration process was clearly followed by immunostaining with 1E11 and anti-serotonin antibodies. For the first time, images of immunoreactive neurons undergoing regeneration in seastar larvae were presented. Thus results suggested that in planktotrophic asteroid larvae the developmental path of the nervous system was strikingly similar to those described during gastrulation in echinoderm embryos (see Chapter 5 for details).

6.6.2 Implications

Echinoderms share many developmental traits with other deuterostomes. Therefore, a clear understanding of the organisation of their nervous systems in these organisms could reveal the relationship of invertebrate deuterostomes with the chordates. Research into the neural repair processes in echinoderm larvae may lead to a better understanding of neurogenesis in many higher animals, including vertebrates. Asteroid larvae provide a valuable experimental model, which opens new possibilities for exploring the fundamental mechanisms underlying regeneration of the nervous system in deuterostomes, with potential biomedical applications.

6.7 LIMITATIONS AND UNCERTAINTIES

6.7.1 Differences in experimental organisms and seawater conditions

Limitations to experimental work are inherent in most studies involving marine organisms. Sea urchins were collected at Torbay, England and transported to the National Oceanography Centre (a 4.5 hours journey) for the experiments performed during 2007, 2008 and 2009. However, in the late summer of 2009 sea urchins from the Torbay area were no longer ripe and so instead organisms were collected from North Wales as their spawning period start and finishes later in the year.

Although the same species was collected from both sites, their habitat, carbonate seawater chemistry, temperature and diet varied. This may have affected comparison of larval development rates under the controlled conditions. Measurements of larvae tolerance between different sea urchin populations (e.g. fertilization success, larval growth, calcification rates) imply errors as their development differs due to external factors (such as food intake, thermal sensitivity, exposure to light and oxygen, tolerance to handling). Even at the cellular level, diversity in gamete quality has an effect on the growth and development of the organism.

For the majority of the experimental work the local seawater (in which the sea urchins inhabit) was used, but this was not possible for the experiment carried out with the sea urchins collected from North Wales. Due to local hydrographic conditions, the carbonate chemistry and temperature in which the sea urchins are found is different to the experimental local seawater used from Torbay. Instead, the Torbay seawater was used for all experiments including the experiment with the sea urchins from North Wales. For this reason the tolerance developed to changes in seawater carbonate chemistry by the sea urchin from North Wales may have been different to those collected from Torbay.

6.7.2   Experimental set-up and organism manipulation

Although sea urchin larvae are easy to rear and sea urchin adults are abundant in coastal communities, they are in general highly sensitive to changes in temperature and handling. It was especially difficult to set the right bubbling of CO_2 and to maintain a constant temperature. The growth of echinoderm larvae is affected by high rates of bubbling, especially at the initial developmental stages. The disruption of the embryos by high rates of bubbling affects their survival and development as previous workers have noted (Svetlana Maslakova and Eugenio Carpizo; *pers. comms.*). This made assessment of fertilization success and gastrulation more difficult.

6.7.3   Limitations of field experimentation

During the PAP cruise it was crucial to maintain the sea urchin in a healthy state until the experiment was conducted. Timing was crucial, and it was imperative to start the experiments before deep seawater equilibrated with ambient CO_2. For this reason, gametes of sea urchin were spawned before the CTD was on board. As gametes deteriorate with age, all experimental manipulations needed to be conducted rapidly.

6.7.4   New protocol development

For this study a new protocol were developed. This research made the first measurements of particulate inorganic carbon (PIC) in larvae. The PIC estimated calcification in sea urchin larvae cultured at different seawater carbonate chemistry. Although this method has previously been used in coccolithophores (Riebesell, 2000) this is the first time this proxy has been used as a calcification measurement in echinoderm larvae. This protocol is as yet unverified by comparison with alternative techniques.

Samples for *in situ* hybridisation and gene expression were taken to access the development of skeletogenesis under different carbonate chemistries and temperature. Unfortunately these samples were not analysed due to limited amount of time and funding.

CHAPTER 7

FINAL CONCLUSIONS AND
RECOMENDATIONS FOR FURTHER RESEARCH

7   FINAL CONCLUSIONS AND RECOMMENDATIONS FOR FURTHER RESEARCH

7.1   FINAL CONCLUSIONS

This research has investigated two main projects using echinoderms as model organisms. A summary of the main conclusions and findings is as follows:

7.1.1   Ocean acidification, changes in carbonate chemistry, the effect of temperature/CO_2 interactions and their impact on the development of sea urchin larvae *Psammechinus miliaris*

Trade-offs between thermal and hypercapnia adaptation processes had an impact on the fertilization success and larval calcification, with potential consequences for growth, development, performance and metamorphosis. However, the larvae already experience natural variations in carbon chemistry and temperature in their natural environment that is within and even exceeds predicted climate scenarios. Therefore, these ecologically versatile larvae may be an evolutionary success in the face of future projected climate scenarios.

General larval growth (defined by POA and BL) was unaffected by changes in pCO_2 and the related changes in carbonate chemistry, with temperature being the dominant factor. Temperature increases were found to enhance larval growth of *P. miliaris.*

This study confirms the need to look beyond the first developmental stages in echinoderm larvae as a single endpoint when considering the effect of ocean acidification that may occurs in the 21st century and instead investigate larval adaptation on a molecular level. This may shed further light on interesting evolutionary responses.

127

The limits to acclimation are set by metabolic trade-offs through balancing energy in the required functions to adapt to climate variability. Nevertheless, this study shows that *P. miliaris* larvae acclimate to high pCO$_2$ and future ocean warming.

Since the oceans are expected to undergo changes in temperature, it is irrelevant to isolate CO$_2$ as a single stressor factor. Therefore it is suggested that multifactorial experiments, like those undertaken in this study, represent a more realistic scenario of organisms' responses to environmental selection pressure.

This thesis emphasises that the duration to which organisms are exposed is crucial in understanding natural adaptation to ocean acidification and global warming. Studies have shown that in the short term, species present a low tolerance to multiple stressors. Results of this thesis show that they are able to adapt to stressful conditions with time.

7.1.1.1 Implications of research findings

Implications of the findings that echinoderms may acclimate to increasingly acidic coastal waters reach beyond the scientific community, and are applicable to a range of stakeholders that use the coastal zone. Models of biochemical cycles will need to take these findings into consideration when making projections of climate change scenarios. Environmental managers and policy-makers in turn base local and national scale policy decisions of marine conservation and fisheries on the projections of these models. Results of this study, disseminated through various media channels (e.g. http://www.bbc.co.uk/news/science-environment-11511624), will also be of interest to the general public when forming decisions about the impact of carbon emissions on their coastline. It will help the public think about new areas of impact of climate change, especially when they can relate these impacts to a familiar sight at many English seaside resorts – the sea urchin.

There is however a danger that popularisation of these findings may fuel political opinion to discredit the seriousness of anthropogenic climate change. Communicating the

true results of climate change science to the public is an important, but often complicated task. It is therefore necessary to emphasise that, although these findings suggest sea urchins may acclimate to a changing ocean, it does not mean there would be no negative effect of a warmer and more acidic environment on the wider marine ecosystem. Indeed, detrimental impacts are still likely as a result of behavioural and developmental changes and geographic re-distribution of the echinoderm under climate stressors.

7.1.2 A study of the nervous system of the seastar larvae *Pisaster ochraceus* and *Orthasterias koehleri* during regeneration

This study demonstrates that the planktotrophic larvae of the asteroids *P. ochraceus* and *O. Koehleri* possess extensive regeneration capacities. The bisected portions of both species regenerated missing body parts (with organogenesis) within two weeks. No mortality occurred due to bisection.

Neurogenesis during the regeneration process was clearly revealed by immunostaining with 1E11 and anti-serotonin antibodies. The results of this study suggest that in planktotrophic seastar larvae the developmental path of the nervous system followed by the bisected larval portion is similar to those reported during gastrulation in echinoderm embryos.

7.2 RECOMMENDATIONS FOR FURTHER RESEARCH

As with the majority of research studies, results gained through experimentation raise more questions and highlight the need for further study to address uncertainties. This is particularly pertinent in a novel and developing research area such as ocean acidification where the scientific community is only beginning to grasp the effect of the climate stressor on the development of marine biota.

7.2.1   The effect of changes in carbonate chemistry on the development of sea urchin larvae *P. miliaris*

Havenhand (2008) demonstrated that sperm speed and motility in high pCO_2 conditions decrease. It would also be useful to measure the sperm performance in high CO_2 environments with a temperature increment. Another important aspect of fertilization would be to assess the internal pH increment at different seawater carbonate chemistry.

Further recommendations include the examination of the energetic cost of a thinner skeleton cultured at different carbon chemistry by using molecular tools. Recently, new gene-encoding proteins that are specifically involved in spicule matrices have been identified (Killian 2008). These were isolated using polyclonal antibodies which would be of great use in examining the larval skeleton. It is essential to follow the development of marine calcifiers before, during and after metamorphosis. As this research suggests, echinopluteus larvae can adapt to carbonate chemistry changes. Comparisons of the internal anatomy and survival of juveniles resulting from different changes in temperature and CO_2 would be of great interest.

In addition to the phenotypic plasticity of larval arm growth analysis presented in this study, it would be of great use to implement molecular tools to address the evolutionary (genetic) adaptation of the larvae to changes in seawater carbonate chemistry.

This research concludes that to fully understand the impact of ocean acidification and ocean warming on the health, distribution and function of echinoderm populations the natural CO_2 gradients would be an ideal laboratory to test this effect. The natural environments which exhibit carbonate gradients are deep ocean water, upwelling areas, CO_2 vents and oxygen minimum zones. These areas present higher levels of CO_2 than predicted by ocean models and investigations based on these zones would yield realistic and worst-case scenario results. Results from studies based on these areas would allow the scientific community, policy makers and the general public to better protect and regulate

the coastal zone with more accurate projections of marine invertebrate behavioural changes in the face of climate change.

The above suggestion of possible future work is by no means exhaustive but aims to cultivate ideas in order to expand potential future research concerning the effect of ocean acidification in marine invertebrates.

7.2.2   Regeneration of the nervous system of seastar larvae

7.2.2.1 Gene expression

Our understanding of the biology of echinoderm regeneration cannot be complete without the inclusion of molecular studies. This is because the genes involved in the regenerating process of echinoderm larvae could help explain some of the gene behaviour in other chordate organisms with biomedical implications. In spite of the widespread and successful employment of echinoderms for molecular studies based on embryonic or larval development, there is at present a large gap in our knowledge of regeneration and few data are available.

The understanding of developmental mechanisms is a crucial part of modern embryology. In recent years considerable research effort has been focused on identifying novel genes that direct developmental processes. However, direct observation of the morphological development of organisms, which generates fundamental knowledge, has been neglected. The focus on the regeneration of the seastar nervous system in this study aimed to understand both the morphological changes that larvae undergo during regrowth and the genes involved in this process. Future potential work for this study includes three key genes involved in development:

1) Bone Morphogenetic Proteins (BMP) genes

Activation of BMP genes are correlated with cell division and future growth of specific regions of the embryo. The absence of BMP signalling turns cells into nerve cells spontaneously (Nakajima *et al.*, 2004b). Genes regulating gastrulation, such as BMP-4, have been shown to be involved in cell division and growth of specific regions in early embryonic development in frogs and sea urchins (Reynolds *et al.*, 1992).

2) *Wnt* gene

The *Wnt* gene is part of a gene family that encodes secreted signaling molecules that control cell fate in animal development and human diseases (Kusserow *et al.*, 2005).

3) Afuni gene

Thorndyke (2005) reported the molecular cloning of a BMP from regenerating arms of the ophiuroid *Amphiura filiformis*. Cellular expression of this Afuni gene occurs in migratory cells (Bannister *et al.*, 2005).

7.2.2.2 Gene expression analysis

A preliminary investigation optimised PCR conditions for amplification of the *Wnt* (~250bp) and afuni (~400bp) genes (Fig. 7.1). Sufficient RNA for RT-PCR could be isolated from a small amount of material (15 larvae). These first steps could enable future gene expression analysis using QPCR.
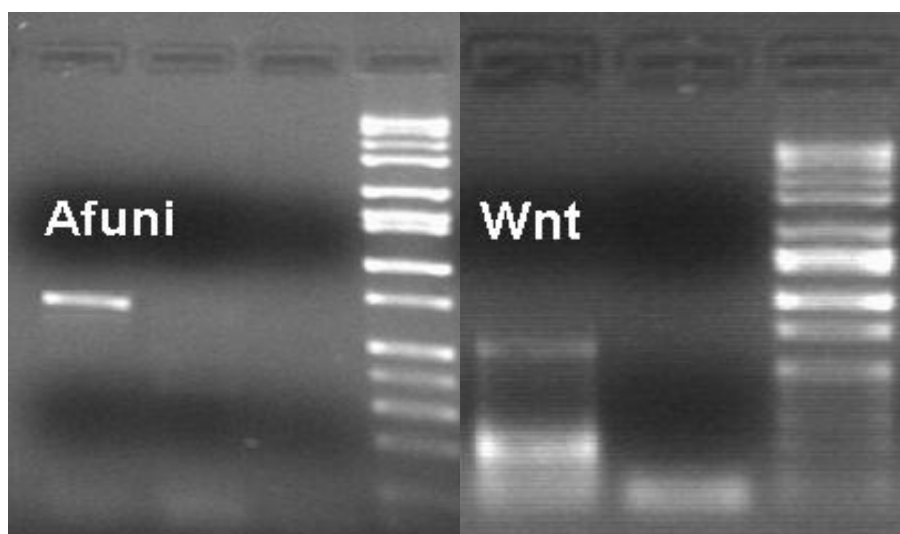
Figure 7.1 Agarose gel image showing DNA fragments amplified by RT-PCR using primers specific for the developmental regulator genes Wnt and afuni (expressed in migratory cells). Empty lines are the negative control and the last columns of both agarose gels represent the molecular weight ladders (each line represents 50bp).

REFERENCES

Aquino-Souza R, Hawkins SJ, Tyler PA (2008) Early development and larval survival of *Psammechinus miliaris* under deep-sea temperature and pressure conditions. *Journal of the Marine Biological Association of the United Kingdom* 88: 453-461

Balch WM, Drapeau DT, Bowler BC, Booth E (2007) Prediction of pelagic calcification rates using satellite measurements. *Deep-Sea Research* II: 478-495

Bannister R, McGonnell IM, Graham A, Thorndyke MC, Beesley PW (2005) Afuni, a novel transforming growth factor-beta gene is involved in arm regeneration by the brittle star Amphiura filiformis. *Development Genes and Evolution* 215: 393-401

Beer AJ, Moss C, Thorndyke M (2001) Development of serotonin-like and SALMFamide-like immunoreactivity in the nervous system of the sea urchin *Psammechinus miliaris. Biological Bulletin,* Marine Biological Laboratory, Woods Hole 200: 268-280

Bertram DF, Strathmann RR (1998) Effects of maternal and larval nutrition on growth and form of planktotrophic larvae. *Ecology* 79: 315-327

Bishop C, Burke R (2007) Ontogeny of the holothurian larval nervous system: evolution of larval forms. *Development Genes and Evolution* 217: 585-592

Bulling MT, Hicks N, Murray L, Paterson DM, Raffaelli D, White PCL, Solan M (2010) Marine biodiversity-ecosystem functions under uncertain environmental futures. *Philosophical Transactions of the Royal Society B-Biological Sciences* 365: 2107-2116

Burke RD, Osborne L, Wang D, Murabe N, Yaguchi S, Nakajima Y (2006) Neuron-specific expression of a synaptotagmin gene in the sea urchin *Strongylocentrotus purpuratus. The Journal of Comparative Neurology* 496: 244-251

Byrne M, Ho M, Selvakumaraswamy P, Nguyen HD, Dworjanyn SA, Davis AR (2009) Temperature, but not pH, compromises sea urchin fertilization and early development under near-future climate change scenarios. *Proceedings of the Royal Society B-Biological Sciences*

Byrne M, Selvakumaraswamy P, Ho MA, Woolsey E, Nguyen HD (2010a) Sea urchin development in a global change hotspot, potential for southerly migration of thermotolerant propagules. *Deep Sea Research Part II: Topical Studies in Oceanography* In Press, Corrected Proof

Byrne M, Sewell MA, Prowse TAA (2008) Nutritional ecology of sea urchin larvae: influence of endogenous and exogenous nutrition on echinopluteal growth and phenotypic plasticity in Tripneustes gratilla. *Functional Ecology* 22: 643-648

Byrne M, Sewell MA, Selvakumaraswamy P, Prowse TAA (2006) The Larval Apical Organ in the Holothuroid *Chiridota gigas* (Apodida): Inferences on Evolution of the Ambulacrarian Larval Nervous System. *Biological Bulletin* 211: 95-100

Byrne M, Soars N, Selvakumaraswamy P, Dworjanyn SA, Davis AR (2010b) Sea urchin fertilization in a warm, acidified and high pCO$_2$ ocean across a range of sperm densities. *Marine Environmental Research* 69: 234-239

Caldeira K, Wickett ME (2003) Anthropogenic carbon and ocean pH. *Nature* 425: 365-365

Caldeira K, Wickett ME (2005) Ocean model predictions of chemistry changes from carbon dioxide emissions to the atmosphere and ocean. *Journal of Geophysical Research. C. Oceans* 110

Carnevali C (2005) Regeneration response and *Endocrine disrupters* in crinoid echinoderms: An old experimental model, a new ecotoxicological test. In: Matranga V. (ed) Echinodermata. Springer, Germany, pp 167-200

Carnevali C (2006) Regeneration in Echinoderms:repair, regrowth, cloning. *Invertebrate Survival Journal*: 64-76

Chee F, Byrne M (1997) Visualization of the developing serotonergic nervous system in the larvae of the sea star, *Patiriella regularis* using confocal microscopy and computer generated 3-D reconstructions. *Invertebrate Reproduction and Development* 31: 151-158

Cigliano M, Gambi MC, Rodolfo-Metalpa R, Patti FP, Hall-Spencer JM (2010) Effects of ocean acidification on invertebrate settlement at volcanic CO2 vents. *Marine Biology* (Berlin) 157:2489-2502

Clark AM (1968) Starfishes and their relations. British Museum (Natural History), London, pp 119

Clark D, Lamare M, Barker M (2009) Response of sea urchin pluteus larvae (Echinodermata: Echinoidea) to reduced seawater pH: a comparison among a tropical, temperate, and a polar species. *Marine Biology* 156: 1125-1137

Comeau S, Jeffree R, Teyssie JL, Gattuso JP (2010) Response of the Arctic Pteropod Limacina helicina to Projected Future Environmental Conditions. *PLoS one* 5: 7

Cooley SR, Kite-Powell HL, Doney SC (2009) Ocean acidification's potential to alter global marine ecosystem services. *Oceanography* 22: 172-181

Dickson AG, Millero FJ (1987) A comparison of the equilibrium constants for the dissociation of carbonic acid in seawater media. *Deep-Sea Research* 34:1733-1743

Doney SC (2006) The dangers of ocean acidification. *Scientific American* (International Edition) 294:38-45

Doney SC, Balch WM, Fabry VJ, Feely RA (2009a) Ocean acidification a critical emerging problem for the ocean sciences. *Oceanography* 22: 16-25

Doney SC, Fabry VJ, Feely RA, Kleypas JA (2009b) Ocean Acidification: The Other CO2 Problem. *Annual Review of Marine Science* 1: 169-192

Dupont S, Havenhand J, Thorndyke W, Peck L, Thorndyke M (2008) Near-future level of CO_2-driven ocean acidification radically affects larval survival and development in the brittlestar *Ophiothrix fragilis*. *Marine Ecology-Progress Series* 373: 285-294

Dupont S, Lundve B, Thorndyke M (2010a) Near Future Ocean Acidification Increases Growth Rate of the Lecithotrophic Larvae and Juveniles of the Sea Star Crossaster papposus. *Journal of Experimental Zoology Part B-Molecular and Developmental Evolution* 314B: 382-389

Dupont S, Ortega-Martinez O, Thorndyke M (2010b) Impact of near-future ocean acidification on echinoderms. *Ecotoxicology* 19: 449-462

Elia L, Selvakumaraswamy P, Byrne M (2009) Nervous System Development in Feeding and Nonfeeding Asteroid Larvae and the Early Juvenile. *Biological Bulletin* 216: 322-334

137

Emlet RB (1982) Echinoderm calcite: A mechanical analysis from larval spicules. *Biological Bulletin*: 264-275

Emlet RB, Crain CM, George SB (2002) Atlas of Marine Invertebrate Larvae. In: Young C. M. (ed) *Journal of Experimental Marine Biology and Ecology*. Academic Press, USA, pp 531-551

Engel A, Zondervan I, Aerts K, Beaufort L, Benthien A, Chou L, Delille B, Gattuso JP, Harlay J, Heemann C, Hoffmann L, Jacquet S, Nejstgaard J, Pizay MD, Rochelle-Newall E, Schneider U, Terbrueggen A, Riebesell U (2005) Testing the direct effect of CO_2 concentration on a bloom of the coccolithophorid Emiliania huxleyi in mesocosm experiments. *Limnology and Oceanography* 50: 493-507

Fabry VJ, Seibel BA, Feely RA, Orr JC (2008) Impacts of ocean acidification on marine fauna and ecosystem processes. *ICES Journal of Marine Science* 65: 414-432

Feely RA, Sabine CL, Hernandez-Ayon JM, Ianson D, Hales B (2008) Evidence for upwelling of corrosive "acidified" water onto the continental shelf. *Science* 320: 1490-1492

Feely RA, Sabine CL, Lee K, Berelson W, Kleypas J, Fabry VJ, Millero FJ (2004) Impact of Anthropogenic CO_2 on the $CaCO_3$ System in the Oceans. *Science* 305: 362-366

Fujisawa H, Shigei M (1990) Correlation of embryonic temperature sensitivity of sea urchins with spawning season. *Journal of Experimental Marine Biology and Ecology* 136: 123-139

Gage JD, Tyler PA (1991) Deep-Sea Biology: A Natural History of Organisms at the Deep-Sea Floor. Cambridge University Press United Kingdom

Gage JD, Tyler PA (1981) Non-viable seasonal settlement of larvae of the upper bathyal brittle star *Ophiocten gracilis* in the Rockall Trough abyssal. *Marine Biology* 64:153-161

Gattuso JP, Frankignoulle M, Bourge I, Romaine S, Buddemeier RW (1998) Effect of calcium carbonate saturation of seawater on coral calcification. *Global and Planetary Change* 18: 37-46

Gazeau F, Gattuso JP, Dawber C, Pronker AE, Peene F, Peene J, Heip CHR, Middelburg JJ (2010) Effect of ocean acidification on the early life stages of the blue mussel Mytilus edulis. *Biogeosciences* 7:2051-2060

Gazeau F, Quiblier C, Jansen JM, Gattuso JP, Middelburg JJ, Heip CHR (2007) Impact of elevated CO_2 on shellfish calcification. *Geophysical Research Letters* 34

Gilbert SF, Raunio AM (1997) Embryology Constructing the Organism. Copyright 1997 by Sinauer Associates, Inc., Canada

Grainger JL, Winkler MM, Shen SS, Steinhardt RA (1979) Intracellular pH controls protein synthesis rate in the sea urchin egg and early embryo. *Developmental Biology* 68:396-406

Guillard, RRL (1975) Culture of phytoplankton for feeding marine invertebrates. pp 26-60. *In* Smith W.L. and Chanley M.H (Eds.) *Culture of Marine Invertebrate Animals*. Plenum Press, New York, USA.

Gutowska MA, Portner HO, Melzner F (2008) Growth and calcification in the cephalopod Sepia officinalis under elevated seawater pCO(2). *Marine Ecology-Progress Series* 373: 303-309

Hall-Spencer JM, Rodolfo-Metalpa R, Martin S, Ransome E, Fine M, Turner SM, Rowley SJ, Tedesco D, Buia MC (2008) Volcanic carbon dioxide vents show ecosystem effects of ocean acidification. *Nature* 454: 96-99

Hart MW, Strathmann RR (1994) Functional consequences of phenotypic plasticity in echinoid larvae. *Biological Bulletin* 186: 291-299

Hauton C, Tyrrell T, Williams J (2009) The subtle effects of sea water acidification on the amphipod Gammarus locusta. *Biogeosciences* 6: 1479-1489

Havenhand JN, Buttler F-R, Thorndyke MC, Williamson JE (2008) Near-future levels of ocean acidification reduce fertilization success in a sea urchin. *Current Biology* 18

Hermans J, Borremans C, Willenz P, Andre L, Dubois P (2010) Temperature, salinity and growth rate dependences of Mg/Ca and Sr/Ca ratios of the skeleton of the sea urchin Paracentrotus lividus (Lamarck): an experimental approach. *Marine Biology* (Berlin) 157:1293-1300

Hilton, J, Lishman, JP, Mackness, S, Heaney, SI, (1986). An automated method for the analysis of particulate carbon and nitrogen in natural waters. *Hydrobiologica* 141, 269 – 271.

Howell KL, Billett DSM, Tyler PA (2002) Depth-related distribution and abundance of seastars (Echinodermata : Asteroidea) in the Porcupine Seabight and Porcupine Abyssal Plain, NE Atlantic. *Deep-Sea Research Part I-Oceanographic Research Papers* 49: 1901-1920

Hughes SL, Holliday NP, Kennedy J, Berry DI, Kent EC, Sherwin T, Dye S, Inall M, Shammon T, T. S (2010) Temperature (Air and Sea) *in* MCCIP Annual Report Card 2010-11 *MCCIP Science Review* 16 pp

Hyman LH (1995) The invertebrates. Echinodermata, the Coelomate Bilateria. McGraw-Hill, New York

Iglesias-Rodriguez MD, Halloran PR, Rickaby REM, Hall IR, Colmenero-Hidalgo E, Gittins JR, Green DRH, Tyrrell T, Gibbs SJ, von Dassow P, Rehm E, Armbrust EV, Boessenkool KP (2008) Phytoplankton calcification in a high-CO_2 world. *Science* 320: 336-340

IPCC (2007) Intergovernmental Panel on Climate Change. The Fourth Assessment Report of the IPCC

Johnson CH, Epel D (1981) Intracellular pH of Sea Urchin Eggs Measured by the Dimethyloxazolidinedione (DMO) Method. *The Journal of Cell Biology* 89: 284-291

Johnson JD, Epel D, Paul M (1976) Intracellular pH and activation of sea urchin eggs after fertilization. *Nature* 262

Kelly MS, Brodie CC, McKenzie JD (1998) Somatic and gonadal growth of the sea urchin *Psammechinus miliaris* maintained in polyculture with the Atlantic salmon. *J. Shellfish Res.*: 1557-1562

Kelly MS, Hunter AJ, Scholfield CL, McKenzie JD (2000) Morphology and survivorship of larval *Psammechinus miliaris* (Gmelin) (Echinodermata: Echinoidea) in response to varying food quantity and quality. *Aquaculture* 183: 223-240

Key RM, Kozyr A, Sabine CL, Lee K, Wanninkhof R, Bullister JL, Feely RA, Millero FJ, Mordy C, Peng TH (2004) A global ocean carbon climatology: Results from Global Data Analysis Project (GLODAP). *Global Biogeochemical Cycles* 18

Kleypas JA, Feely RA, Fabry VJ, Langdon C, Sabine CL, Robbins LL (2006) Impact of ocean acidification on coral reefs and other marine calcifiers: a guide for future research. Report of a workshop held 18-20 April 2005, St. Petersburg, FL, sponsored by NSF, NOAA, and the US Geological Survey

Kump LR, Bralower TJ, Ridgwell A (2009) Ocean acidification in deep time. *Oceanography* 22: 94-107

Kurihara H (2008) Effects of CO_2-driven ocean acidification on the early developmental stages of invertebrates. *Marine Ecology-Progress Series* 373: 275-284

Kurihara H, Matsui M, Furukawa H, Hayashi M, Ishimatsu A (2008) Long-term effects of predicted future seawater CO2 conditions on the survival and growth of the marine shrimp Palaemon pacificus. *Journal of Experimental Marine Biology and Ecology* 367: 41-46

Kurihara H, Shirayama Y (2004) Effects of increased atmospheric CO2 on sea urchin early development. *Marine Ecology-Progress Series* 274: 161-169

Kusserow A, Pang K, Sturm C, Hrouda M, Lentfer J, Schmidt HA, Technau U, von Haeseler A, Hobmayer B, Martindale MQ, Holstein TW (2005) Unexpected complexity of the Wnt gene family in a sea anemone. *Nature* 433: 156-160

Langdon C, Takahashi T, Sweeney C, Chipman D, Goddard J, Marubini F, Aceves H, Barnett H, Atkinson MJ (2000) Effect of calcium carbonate saturation state on the calcification rate of an experimental coral reef. *Global Biogeochemical Cycles* 14: 639-654

Langer G, Geisen M, Baumann KH, Klas J, Riebesell U, Thoms S, Young JR (2006) Species-specific responses of calcifying algae to changing seawater carbonate chemistry. *Geochemistry Geophysics Geosystems* 7

Lebrato M, Iglesias-Rodriguez D, Feely R, Greeley D, Jones D, Suarez-Bosche N, Lampitt R, Cartes J, Green D, Alker B (2010) Global contribution of echinoderms to the marine carbon cycle: a re-assessment of the oceanic $CaCO_3$ budget and the benthic compartments. *Ecological Monographs e-View*

References

Leclercq N, Gattuso JP, Jaubert J (2002) Primary production, respiration, and calcification of a coral reef mesocosm under increased CO2 partial pressure. *Limnology and Oceanography* 47: 558-564

Lewis E, Wallace DWR (1998) Program Developed for CO_2 System Calculations. Program Developed for CO_2 System Calculations. Carbon Dioxide Information Analysis Center, Oak Ridge National Laboratory, U.S. Department of Energy, Oak Ridge, Tennessee

Mann KH, Lazier JRN (1991) Dynamics of Marine Ecosystems Biological-Physical Interactions in the Oceans. Blackwell Scientific Publications Inc.: Cambridge, Massachusetts, USA; Oxford, England, Uk.

Matranga V (2005) Echinodermata. Springer, Germany.

McClintock JB (1994) Trophic biology of antarctic shallow-water echinoderms. *Marine Ecology-Progress Series* 111:191-202

McEdward LR, Jaeckle WB, Komatsu M (2002) Atlas of Marine Invertebrate Larvae. In: Young C. M. (ed) *Journal of Experimental Marine Biology and Ecology*. Academic Press, USA, pp 499-512

Melzner F, Gutowska MA, Langenbuch M, Dupont S, Lucassen M, Thorndyke MC, Bleich M, Pörtner HO (2009) Physiological basis for high CO2 tolerance in marine ectothermic animals: pre-adaptation through lifestyle and ontogeny? *Biogeosciences* 6: 2313-2331

Menendez M, Martinez M, Comin FA (2001) A comparative study of the effect of pH and inorganic carbon resources on the photosynthesis of three floating macroalgae species of a Mediterranean coastal lagoon. *Journal of Experimental Marine Biology and Ecology* 256: 123-136

Mestre NC, Thatje S, Tyler PA (2009) The ocean is not deep enough: pressure tolerances during early ontogeny of the blue mussel *Mytilus edulis*. *Proceedings of the Royal Society B-Biological Sciences* 276: 717-726

Miles H, Widdicombe S, Spicer JI, Hall-Spencer J (2007) Effects of anthropogenic seawater acidification on acid-base balance in the sea urchin *Psammechinus miliaris*. *Marine Pollution Bulletin* 54: 89-96

Mladenov PV, Emson RH, Colpit LV, Wilkie IC (1983) Asexual reproduction in the west indian brittle star *Ophiocomella ophiactoides* (H.L. Clark) (Echinodermata: Ophiuroidea). *Journal of Experimental Marine Biology and Ecology* 72: 1-23

Morris VB, Zhao J-T, Shearman DCA, Byrne M, Frommer M (2004) Expression of an Otx gene in the adult rudiment and the developing central nervous system in the vestibula larva of the sea urchin Holopneustes purpurescens. *International Journal of Developmental Biology* 48: 17-22

Morse JW, Andersson AJ, Mackenzie FT (2006) Initial responses of carbonate-rich shelf sediments to rising atmospheric pCO_2 and "ocean acidification": Role of high Mg-calcites. *Geochimica et Cosmochimica Acta* 70: 5814-5830

Mortensen T (1927) Handbook of the echinoderms of the British Isles. Oxford University Press, U. K.

Moss C, Burke RD, Thorndyke MC (1994) Immunocytochemical localization of the neuropeptide S1 and serotonin in larvae of the starfish *Pisaster ochraceus* and *Asterias rubens. Journal of Marine Biological Association* 74: 61-71

Moss C, Hunter AJ, Thorndyke MC (1998) Patterns of bromodeoxyuridine incorporation and neuropeptide immunoreactivity during arm regeneration in the starfish *Asterias rubens. Philosophical Transactions of the Royal Society* 353: 421-436

Mucci A (1983) The Solubility of Calcite and Aragonite in Seawater at Various Salinities, Temperatures, and One Atmosphere Total Pressure. *American Journal of Science* 283: 780-799

Nakajima Y, Kaneko H, Murray G, Burke RD (2004a) Divergent patterns of neural development in larval echinoids and asteroids. *Evolution & Development* 6: 95-104

Nakajima Y, Kaneko H, Murray G, Burke RD (2004b) Divergent patterns of neural development in larval echinoids and asteroids. *Evolution and Development* 6: 95-104

Nakano H, Murabe N, Amemiya S, Nakajima Y (2006) Nervous system development of the sea cucumber *Stichopus japonicus. Developmental Biology* 292: 205-212

Nakano H, Nakajima Y, Amemiya S (2009) Nervous system development of two crinoid species, the sea lily *Metacrinus rotundus* and the feather star *Oxycomanthus japonicus*. *Development Genes and Evolution* 219: 565-576

Nielsen C (1998) Origin and evolution of animal life cycles. *Biological Reviews* 73: 125-155

O'Donnell MJ, Todgham AE, Sewell MA, Hammond LM, Ruggiero K, Fangue NA, Zippay ML, Hofmann GE (2010) Ocean acidification alters skeletogenesis and gene expression in larval sea urchins. *Marine Ecology Progress Series* 398

Orr JC, Fabry VJ, Aumont O, Bopp L, Doney SC, Feely RA, Gnanadesikan A, Gruber N, Ishida A, Joos F, Key RM, Lindsay K, Maier-Reimer E, Matear R, Monfray P, Mouchet A, Najjar RG, Plattner GK, Rodgers KB, Sabine CL, Sarmiento JL, Schlitzer R, Slater RD, Totterdell IJ, Weirig MF, Yamanaka Y, Yool A (2005) Anthropogenic ocean acidification over the twenty-first century and its impact on calcifying organisms. *Nature* 437: 681-686

Orton JH (1914) On the breeding habitats of *Echinus miliaris*, with a note ont eh feeding habits of *Patella vulgata*. *Journal of the Marine Biological Association U.K.*: 254-257

Passaro M, Ziveri P, Milazzo M, Rodolfo-Metalpa R, Hall-Spencer JM (2011) Exploring CO_2 volcanic vents at Vulcano Island, Mediterranean Sea, to study the planktonic calcifier response to long-term changes in carbonate chemistry. *Geophysical Research Abstracts* 13

Paulmier A, Ruiz-Pino D, GarÃ§on V (2011) CO_2 maximum in the oxygen minimum zone (OMZ). *Biogeosciences* 8:239-252

Payan P, Girard J-P, Ciapa B (1983) Mechanisms regulating intracellular pH in sea urchin eggs. *Developmental Biology* 100: 29-38

Politi Y, Arad T, Klein E, Weiner S, Addadi L (2004) Sea urchin spine calcite forms via a transient amorphous calcium carbonate phase. *Science* 306: 1161-1164

Politi Y, Levi-Kalisman Y, Raz S, Wilt F, Addadi L, Weiner S, Sagi I (2006) Structural characterization of the transient amorphous calcium carbonate precursor phase in sea urchin embryos. *Advanced Functional Materials* 16: 1289-1298

Pörtner HO (2008) Ecosystem effects of ocean acidification in times of ocean warming: a physiologist's view. *Marine Ecology Progress Series*: 203-217

Pörtner HO, Reipschläger A (1996) Ocean Storage of CO_2. In: Ormerod B., Angel M. (eds) Environmental Impact, MIT and International Energy Agency, Boston/Cheltenham, pp 57-81

Reynolds SD, Angerer LM, Palis J, Nasir A, Angerer RC (1992) Early mRNAs, spatially restricted along the animal-vegetal axis of sea urchin embryos, include one enconding a protein related to tolloid and BMP-1. *Development* 114: 769-786

Riebesell U., Fabry V. J., L. H, (Eds.) GJ-P (2010) Guide to best practices for ocean acidification research and data reporting. *Luxembourg: Publications Office of the European Union*: 260

Riebesell U, Zondervan I, Rost B, Tortell PD, Zeebe RE, Morel FMM (2000) Reduced calcification of marine plankton in response to increased atmospheric CO_2. *Nature* 407: 364-367

Ries JB (2010) Review: geological and experimental evidence for secular variation in seawater Mg/Ca (calcite-aragonite seas) and its effects on marine biological calcification. *Biogeosciences* 7:2795-2849

Ries JB (2009) Review: the effects of secular variation in seawater Mg/Ca on marine biocalcification. *Biogeosciences Discussions*: 7325-7452

Royal Society (2005) Ocean acidification due to increasing atmospheric carbon dioxide. Policy Document 12/05. The Royal Society, London p.60

Sabine CL, Feely RA, Gruber N, Key RM, Lee K, Bullister JL, Wanninkhof R, Wong CS, Wallace DWR, Tilbrook B, Millero FJ, Peng T-H, Kozyr A, Ono T, Rios AF (2004) The Oceanic Sink for Anthropogenic CO_2. *Science* 305: 367-371

Schiebel R (2002) Planktic foraminiferal sedimentation and the marine calcite budget. *Global Biogeochemical Cycles*: 13-21

Seibel BA, Fabry VJ (2003) Marine biotic response to elevated carbon dioxide. *Advances in Applied Biodiversity Science*: 59-67

Sewell MA, Cameron MJ, McArdle BH (2004) Developmental plasticity in larval development in the echinometrid sea urchin Evechinus chloroticus with varying food ration. *Journal of Experimental Marine Biology and Ecology* 309: 219-237

Sewell MA, Hofmann GE (2010) Antarctic echinoids and climate change: a major impact on the brooding forms. *Global Change Biology* "Accepted Article"

Sewell MA, Young CM (1999) Temperature limits to fertilization and early development in the tropical sea urchin Echinometra lucunter. *Journal of Experimental Marine Biology and Ecology* 236: 291-305

Shearer C, de Morgan W, Fuchs HM (1914) On the Experimental Hybridization of Echinoids. *Philosophical Transactions of the Royal Society of London. Series B* 204: 255-362

Sheppard Brennand H, Soars N, Dworjanyn SA, Davis AR, Byrne M (2010) Impact of Ocean Warming and Ocean Acidification on Larval Development and Calcification in the Sea Urchin *Tripneustes gratilla. PLoS one* 5

Sheppard C (2004) Sea surface temperature 1871-2099 in 14 cells around the United Kingdom. *Marine Pollution Bulletin* 49: 12-16

Shi D, Xu Y, Morel FMM (2009) Effects of the pH/pCO2 method on medium chemistry and phytoplankton growth. *Biogeosciences* 6

Smith WHF, Wessel P (1990) Gridding with continuous curvature splines in tension. *Geophysics* 55: 293-305

Somero GN (2002) Thermal physiology and vertical zonation of intertidal animals: Optima, limits, and costs of living. *Integrative and Comparative Biology* 42: 780-789

Somero GN (2010) The physiology of climate change: how potentials for acclimatization and genetic adaptation will determine 'winners' and 'losers'. *Journal of Experimental Biology* 213: 912-920

Stanley SM, Ries JB, Hardie LA (2005) Seawater chemistry, coccolithophore population growth, and the origin of Cretaceous chalk. *Geology* 33: 593-596

Staver JM, Strathmann RR (2002) Evolution of fast development of planktonic embryos to early swimming. *Biological Bulletin* 203: 58-69

Strathmann MF (1987) Reproduction and development of marine invertebrates of the Northern Pacific coast. University of Washington Press, Seattle

Strathmann RR (1975) Larval feeding in echinoderms. *American Zoologist* 15: 717-730

Strathmann RR (2000) Functional design in the evolution of embryos and larvae. *Seminars in Cell & Developmental Biology* 11: 395-402

Strathmann RR (2007) Time and extent of ciliary response to particles in a non-filtering feeding mechanism. *Biological Bulletin* 212: 93-103

Strathmann RR, Fenaux L, Strathmann MF (1992) Heterochronic Developmental Plasticity in Larval Sea Urchins and Its Implications for Evolution of Nonfeeding Larvae. *Evolution* 46: 972-986

Suarez-Bosche N, Lebrato M, Iglesias-Rodriguez D, Tyler PA (2010) *in review*

Sumida PYG, Tyler PA, Lampitt RS, Gage JD (2000) Reproduction, dispersal and settlement of the bathyal ophiuroid Ophiocten gracilis in the NE Atlantic Ocean. *Marine Biology* 137:623-630

Swalla BJ (2006) Building divergent body plans with similar genetic pathways. *Heredity* 97: 235-243

Takahashi T, Broecker WS, Bainbridge AE (1979) The Alkalinity and Total Carbon Dioxide Concentration in the World Oceans. *Carbon Cycle Modelling*: 271-286

Thomsen J, Gutowska MA, Saphörster J, Heinemann A, Trübenbach K, Fietzke J, Hiebenthal C, Eisenhauer A, Körtzinger A, Wahl M, Melzner F (2010) Calcifying invertebrates succeed in a naturally CO_2 enriched coastal habitat but are threatened by high levels of future acidification. *Biogeosciences Discuss* 7:5119-5156

Thorndyke MC, Chen WC, Moss C, Candia Carnevali MD, Bonasoro F (1999) Regeneration in echinoderms: Cellular and molecular aspects. *Echinoderm research, 1998*: 159-164

Turon X, Giribet G, Lopez S, Palacin C (1995) Growth and populations-structure of Paracentrotus lividus (Echinodermata: Echinoidea) in two contrasting habitats. *Marine Ecology-Progress Series* 122:193-204

Tyler PA, Young CM (1998) Temperature and pressure tolerances in dispersal stages of the genus *Echinus* (Echinodermata : Echinoidea): prerequisites for deep-sea invasion and speciation. *Deep-Sea Research Part II-Topical Studies in Oceanography* 45: 253-277

Tyler PA, Young CM, Clarke A (2000) Temperature and pressure tolerances of embryos and larvae of the Antarctic sea urchin *Sterechinus neumayeri* (Echinodermata : Echinoidea): potential for deep-sea invasion from high latitudes. *Marine Ecology-Progress Series* 192: 173-180

Verardo, DJ, Froelich, PN, McIntyre, A, (1990) Determination of organic carbon and nitrogen in marine sediments using the Carlo Erba NA-1500 analyzer. *Deep-Sea Research I* 37, 157 – 165.

Vickery MCL, Vickery MS, Amsler CD, McClintock JB (2001) Regeneration in echinoderm larvae. *Microscopy Research and Technique* 55: 464-473

Vickery MS, McClintock JB (1998) Regeneration in metazoan larvae. *Nature* 394: 140-140

Vickery MS, Vickery MCL, McClintock JB (2002) Morphogenesis and organogenesis in the regenerating planktotrophic larvae of asteroids and echinoids. *Biological Bulletin* 203: 121-133

Villalobos FB, Tyler PA, Young CM (2006) Temperature and pressure tolerance of embryos and larvae of the Atlantic seastars *Asterias rubens* and *Marthasterias glacialis* (Echinodermata : Asteroidea): potential for deep-sea invasion. *Marine Ecology-Progress Series* 314: 109-117

Walter LM, Morse JW (1985) The dissolution kinetics of shallow marine carbonates in seawater: A laboratory study. *Geochimica et Cosmochimica Acta* 49: 1503-1513

Watson SA, Southgate PC, Tyler PA, Peck LS (2009) Early larval development of the Sydney rock oyster Saccostrea glomerata under near-future predictions of CO2-driven ocean acidification. *Journal of Shellfish Research* 28: 431-437

Weaver FE, Shaikh SR, Edidin M (2008) Plasma membrane lipid diffusion and composition of sea urchin egg membranes vary with ocean temperature. *Chemistry and Physics of Lipids* 151: 62-65

Weber JN (1969) The incorporation of magnesium into the skeletal calcites of echinoderms. *American Journal of Science* 267: 537-566

Widdicombe S, Spicer JI (2008) Predicting the impact of ocean acidification on benthic biodiversity: What can animal physiology tell us? *Journal of Experimental Marine Biology and Ecology* 366: 187-197

Wood HL, Spicer JI, Widdicombe S (2008) Ocean acidification may increase calcification rates, but at a cost. *Proceedings of the Royal Society B-Biological Sciences* 275: 1767-1773

Wootton JT, Pfister CA, Forester JD (2008) Dynamic patterns and ecological impacts of declining ocean pH in a high-resolution multi-year dataset. *Proceedings of the*

National Academy of Sciences of the United States of America 105: 18848-18853

Young CM (2002) Atlas of Marine Invertebrate Larvae. Academic Press, USA

Young CM, Tyler PA, Fenaux L (1997) Potential for deep sea invasion by Mediterranean shallow water echinoids: Pressure and temperature as stage-specific dispersal barriers. *Marine Ecology-Progress Series* 154: 197-209

Zeebe RE, Wolf-Gladrow DA (2001) CO2 in Seawater: Equilibrium, Kinetics, Isotopes. Elsevier Oceanography Series, Amsterdan

Zondervan I, Zeebe RE, Rost B, Riebesell U (2001) Decreasing marine biogenic calcification: A negative feedback on rising atmospheric pCO_2. *Global Biogeochemical Cycles* 15: 507-516

References

<div align="right">**APPENDIX 1**</div>

Submitted manuscript entitled: "The adaptive response of echinoderm larvae to CO_2-enriched deep ocean waters". Authors: Suarez-Bosche, N. E., Lebrato, M., Tyler, P., and Iglesias-Rodriguez, M.D. 21st of September 2010.

Acclimation of echinoid larvae to CO₂-enriched deep ocean waters

Nadia Suárez-Bosche [1*], Mario Lebrato [2], Paul Tyler [1], M. Débora Iglesias-Rodríguez [1]

[1] School of Ocean and Earth Science, University of Southampton, National Oceanography Centre, Southampton, Southampton SO14 3ZH, UK

[2] IFM-GEOMAR, Department of Marine Biogeochemistry, Leibniz Institute of Marine Science. Kiel, 24105, Germany

[*] Correspondance: nesubo@noc.soton.ac.uk

Running head: Echinoid larval tolerance to CO₂ rich waters

Acknowledgments

We would like to thank Richard Lampitt and Colin Day, the crew and scientists of RRS *James Cook* cruise 034, for the opportunity to conduct incubations during the research expedition. We thank Darryl Green for elemental analysis of the seawater composition, Mark Stinchcombe for nutrient analysis and Robert Head for particulate carbon analysis. Dana Greely advised and enabled access to WOCE data for the Atlantic Ocean. This work was supported by the "European Project on Ocean Acidification" (EPOCA) for M. Lebrato's PhD. The National Council of Science and Technology of Mexico (CONACyT) funded this work as part of N. E. Suarez-Bosche's PhD.

Abstract

Oceanic uptake of anthropogenic carbon dioxide causes an increase in dissolved CO_2 with an associated decrease in the saturation state with respect to carbonate mineral phases (Ω). A decrease in the Ω is known to affect a variety of calcifying organisms physiologically and, in turn, biogeochemically. Paradoxically, many areas in the deep ocean that are near undersaturation or undersaturated harbour calcifying organisms such as echinoderms. Artificial manipulations in laboratory incubations are traditionally used to assess the impact of different seawater carbonate chemistries on marine biota. However, natural carbonate chemistry gradients (e.g. deep ocean water, upwelling areas, CO_2 vents) offer the possibility to work with organisms avoiding manipulation of the medium chemistry. Little is known about how exposure to deep-sea waters affects meroplankton life cycle stages, morphology, elemental composition, physiology, dispersal and health. Using larvae from the sea urchin species *Psammechinus miliaris*, we conducted incubations in the North Atlantic Ocean, using seawater from different depths. By using the natural carbonate chemistry gradient we assessed larval physiological and ecological plasticity. We show that naturally low Ω-Cal water (below 4000 m) had no effect on larval morphology and organic matter content but calcification decreased compared with shallow waters (250 m). The plasticity of *P. miliaris* to deep-sea water chemistry conditions suggests that the species can tolerate variable CO_2 conditions and changing environmental selection pressure. This represents an ecological advantage in maintaining stability and survival of populations.

Key words

Echinoderms, larvae, morphology, calcification, deep-sea colonization, CO_2 enriched waters.

Introduction

In the marine environment, organisms with alternating pelagic and benthic life stages populate distinct parts of the water column during their life history, therefore encountering variable carbonate chemistry conditions. In particular, many echinoderms have a meroplanktonic life stage, entering pelagic waters until they settle at the seabed (where they undergo metamorphosis), and develop to adult stages. They have a wide distribution, from shallow waters in the continental shelf to the deep-sea in all oceans and at all latitudes. Echinoids are one of the five classes of echinoderms, playing a key role in maintaining the balance and energy flow in marine ecosystems (e.g. grazing, burrowing, calcifying) (McClintock 1994, Turon *et al*. 1995). Additionally, they channel elements and export carbon, in some cases more than 1000 g $CaCO_3$ m^{-2} yr^{-1}, contributing to the global echinoderms carbonate export (> 0.1 Pg C yr^{-1}) (Lebrato *et al*. 2010). These organisms inhabit waters that are increasing in CO_2 concentration at a rate that is already measurable (Sabine *et al.* 2004), as a consequence of anthropogenic carbon emissions. The accelerated dissolution of CO_2 in seawater or "ocean acidification" (Caldeira & Wickett 2005) results in an increased concentration of hydrogen ions (H^+), bicarbonate ions (HCO_3^-), and a decrease of carbonate ions (CO_3^{2-}). This is important because CO_3^{2-} largely controls the saturation state of calcium carbonate (Ω-Cal $= [CO_3^{2-}][Ca^{2+}]/K_{sp}$) ($< 1=$ undersaturation; $> 1=$ supersaturated) where K_{sp} is the solubility constant for the $CaCO_3$ biomineral (Mucci 1983). The chemical changes induced by increasing CO_2 are known to affect the physiology of pelagic and benthic organisms including corals (Langdon *et al*. 2000), coccolithophores (Riebesell et al. 2000, Zondervan et al. 2001, Iglesias-Rodriguez et al. 2008), molluscs (Gazeau et al. 2007, Gazeau et al. 2010) and echinoderms (including echinoid larvae)

156

(Dupont et al. 2008, Clark et al. 2009). Recent concern about the ongoing decrease in Ω -Cal caused by ocean acidification has raised questions about the future of echinoderm populations, and their contribution to the marine carbon cycle.

Echinoderms may be susceptible to changes in the water carbonate chemistry, including changes in CO_2 and Ω-Cal, which they encounter during their life history from larvae (pelagic) to adult stages (benthic). These changes have been mainly assessed in laboratory enclosures where controlled environmental conditions allow the exploration of individual responses (e.g. morphological, developmental, and biochemical) to high CO_2 conditions. However, laboratory incubations heavily depend on artificial manipulations of the medium chemistry (Riebesell et al. 2010), thus they are necessarily an abstraction from the ocean.

Natural carbonate chemistry gradients provide the opportunity to incubate organisms without interfering with the medium chemistry. These gradients are experienced in the oceans as a consequence of different processes. Firstly, water column stratification/ventilation. In the water column, CO_2 increases with increasing depth as a result of *in situ* pressure, but it is also induced by the water masses respiration of sinking and decomposing biogenic material. Therefore, CO_2 concentrations increase (Ω-Cal decreases) at shallower depths from the Atlantic to the Pacific Ocean (Feely et al. 2004). The calcite compensation depth (CCD), below which the rate of production of $CaCO_3$ is exceeded by its rate of dissolution, is critical to organisms such as echinoderms that form $CaCO_3$ skeleton during their life cycle (Feely et al. 2004, Fabry et al. 2008), controlling the magnitude of exported biomineral to the ocean's interior. The CCD has moved closer to the surface and nearer to the coast owing to

anthropogenic emissions and the increasing oceanic uptake of CO_2 (Feely et al. 2004, Feely et al. 2008). Recent research on echinoderms suggests that deep-sea populations (in the Southern Ocean) are already at the boundaries of the CCD undersaturated waters at 3000 m, and organisms below those depths have weakly calcified skeletons (Sewell & Hofmann 2010). Secondly, gradients are experienced in the oceans as a result of natural upwelling events whereby deep CO_2-rich and low Ω-Cal waters surface in seasonal processes associated with major coastal currents such as the Canary Current (off northwest Africa), the Benguela Current (off Namibia), the Humboldt Current (off Peru and Chile), the Somali Current (off Somalia) and the California Current (off California and Oregon) (Mann & Lazier 1991). Oxygen minimum zones (OMZs) are associated with some upwelling events (e.g. Humboldt Current and the Arabian sea) and provide a field opportunity to test natural carbonate chemistry gradients (Paulmier et al. 2011). In shelf seas, seasonal upwelling (from shallow depths) of low oxygen and high CO_2 water masses (e.g. Baltic Sea) could also be used as a natural testing site (Thomsen et al. 2010). Thirdly, geophysical features (e.g. volcanic CO_2 vents); natural venting sites occur at the seabed as a consequence of volcanic activity, which emits CO_2 (> 90%), among other gases. These sites have been used to test natural gradients of CO_2 on benthic communities (Hall-Spencer et al. 2008, Cigliano et al. 2010) and also on pelagic calcifyers (Passaro et al. 2011).

At present, little is known about the effect of naturally high CO_2 and low Ω-Cal waters on the ecological success and physiological performance of marine biota. Therefore, we used for the first time the natural vertical gradient of the water column in ~5000 m of water in the North Atlantic Ocean to investigate the effects on development and biogeochemical features of the larvae of the sea urchin species *Psammechinus*

miliaris. The waters used have distinct carbonate chemistries that allow for testing short term responses and the biological plasticity of sea urchins to physico-chemical changes in a natural medium.

Methods

Study site

The experiment was carried out during May 2009 aboard RRS *James Cook* in the region of the Porcupine Abyssal Plain (PAP) (49 °N, 16 °W; ~ 4840 m water depth). A conductivity-temperature-depth (CTD) rosette at 49 01.559 °N, 015 10.226 °W was used to retrieve water from different depths (250, 2000, 4000, 4600 and 4710 m) representing water masses with different carbonate chemistries (Table 1).

Experimental conditions

The echinoid species *Psammechinus miliaris* were hand-collected in the intertidal at Torbay, UK (50° N 3°33′ W) and maintained in aerated seawater aboard RRS *James Cook* until the experiment was conducted. The specimens collected were in healthy condition, and stress was minimized by using the same intertidal seawater, temperature and salinity that the organisms had in their natural environment until the experiments were conducted. All onboard experiments were conducted at 9 ±1°C in a temperature controlled room.

Fertilization and larval culture

The sea urchins were induced to spawn by injection of 1 ml of 0.5 M KCl just before the CTD water was recovered on deck. In the fertilization experiment, the gametes from 4 males and 2 females were collected and the quality of each gamete source was analyzed with a microscope. The sperm motility and the eggs appearance/shape were checked. The eggs were placed in filter-sterilized seawater (0.22 μm filters, Millipore® Steriup™, Sigma-Aldrich) and the sperm were collected dry. The

total numbers of eggs used in the experiment were counted from a 20 ml suspension determined through counts of 100 μl aliquots. In the experiment, the eggs were split into 20 beakers containing 200 ml of experimental water at a density of ~3-4 eggs per ml in each treatment with water from different depths. Fertilization was performed by inoculating 1 μl of the combined sperm from all males. Sperm was activated directly in the vessels containing eggs that had been pre-acclimated to each experimental condition (water from different depths) for ~20 minutes. Sperm was counted using a haemocytometer and a final concentration of 10^3 sperm per ml was calculated, which typically yields high fertilization success and development. After 3 hours, fertilization success was determined as the eggs that had a fertilization envelope or showed cleavage at the 2 to 4 cell stage. Fertilization counts were taken from 4 replicates in each treatment (~60 eggs were taken from the eggs in suspension). To monitor the embryonic and larval morphology, an independent source of gametes was fertilized and placed in triplicate 2.5 litre vessels at densities of 3-4 eggs per ml, for each experimental condition (15 sealed containers to minimize atmospheric CO_2 exchange). The gastrula stage (~24 hours after fertilization) and four-armed pluteus larvae stage (5 days after fertilization) were sampled to assess developmental changes among treatments. Oxygen (mean = 352.1 μM ± 5.4) and temperature (mean = 8.9 ^{o}C ± 0.15) were recorded daily with an Oxygen Optode/Temperature sensor (AANDERAA 3830) in each of the experimental vessels.

Larval development and morphology

We performed morphological analyses on larval postoral arm length (POA) and body length (BL) in specimens incubated in waters from each depth that were fixed in 4% paraformaldehyde (EM GRADE, Science Services), and cleaned 3 times through

filtered sea water. The larvae were mounted on a microscope slide and photographed for analysis. The larval characters were measured using the software Image J (available at http://rsb.info.nih.gov/ij; developed by Wayne Rasband, National Institutes of Health, Bethesda, MD).

Particulate carbon analyses and calcification

Total particulate carbon (TPC) and particulate organic carbon (POC) were analyzed in triplicate using 50 larvae from each experiment. Larvae were isolated and washed 3 times in phosphate buffered saline (PBS) buffer to rinse off seawater. The larvae were pipetted into pre-combusted silver capsules (Elemental Microanalysis, UK) and stored at -20 °C for further analysis. For POC analysis, inorganic carbon was removed by acidification using a concentrated HCl solution under vacuum for 96 hours. The capsules for both POC and TPC were dried at 60 °C for 48 hours, and analyzed on a Thermo Finnegan flash EA1112 elemental analyzer using acetanilide as the calibration standard. Particulate inorganic carbon (PIC) was calculated by subtracting the POC from the TPC values (Riebesell et al. 2000). This method reduces uncertainties in the measurement of carbon per larvae, since we used an exact number of larvae to ascertain precisely the bulk carbon averaged per 50 larvae, which was not previously available in larval experiments conducted in the laboratory.

Natural seawater carbonate chemistry

Water sample aliquots for *in situ* dissolved inorganic carbon (DIC) and total alkalinity (TA) were collected directly from the CTD Niskin bottles 15 minutes before starting the experiment (immediately upon recovery of the CTD, to avoid aeration). The second sample point was 24 hours and 120 hours after the start of the experiment to

assess the changes in carbonate chemistry of the seawater during the development of the sea urchin larvae. The samples were taken at each experimental depth (in triplicate) and stored in sealed borosilicate glass bottles. An aliquot of $HgCl_2$ (0.4 mM) was added to the samples to prevent microbial growth. The Versatile INstrument for the Determination of Titration Alkalinity (VINDTA) was used to measure TA and DIC. The carbonate system [aragonite and calcite saturation (Ω-Arg and Ω-Cal), seawater pH_{total}, partial pressure of CO_2 (pCO_2), CO_2, HCO_3^-, CO_3^{2-} concentration] was calculated from measurements of TA, DIC, temperature, salinity, and nutrients using CO2 System Calculation Program (Lewis & Wallace 1998) [using the constants of Dickson and Millero (Dickson & Millero 1987); KSO_4 Dickson; pH: total scale; cited in Lewis and Wallace, 1998] and corrected for density in Matlab R2009a (The MathWorks, Inc. 2009). The temperature and pressure effects on the water carbonate chemistry were taken into account in the measurements of DIC and TA at the start and end of the experiment.

Calculation and representation of Ω-Cal from the WOCE A16 transect line

Oceanographic data in the Atlantic Ocean from 60°N to 60°S used in Figure 1 were accessed on the Global Ocean Data Analysis Project (GLODAP) (Key et al. 2004) from the World Ocean Circulation Experiment (WOCE) from cruise line A16N (04 June 2003 to 11 August 2003) and A16S (11 January 2005 to 24 February 2005). The Ω-Cal was calculated using the software CO2 System Calculations (Lewis & Wallace 1998). In the calculations we used the input parameters: total carbon (TC), total alkalinity (TA), temperature, salinity, pressure, silicate, and phosphate *in situ*. To construct the transect line profile the data were gridded using the minimum curvature method (Smith & Wessel 1990) with 62 field lines (spacing of 3°) in the x-axis (latitude) and 129 field lines (spacing of 50 m) in the y-axis (depth) from 60°N to 60°S and from 0 to 6000 m. The seabed is included (grey) and it is plotted from latitude and

pressure data inside a polygon. All data were plotted with the software Surfer v8 ^{TM} (Golden Software 2002, Colorado, USA).

Scanning electron microscopy of larval skeleton

Larval tissue was removed in a mild solution of hyperchlorite diluted with a solution of distilled water saturated with sodium tetraborate (which acts as a buffer) and filtered to remove any particles in suspension. Samples (skeletal rods) were washed three times with distilled water, mounted in SEM stubs and gold coated. Images were obtained with a Leo 1450VP scanning electron microscope.

Natural seawater elemental composition

The concentrations of calcium (Ca^{2+}) and magnesium (Mg^{2+}) in water samples from all depths were measured to rule out seawater effects on calcification (Table 1) following (Ries 2010). Elemental seawater composition was determined in triplicate by inductively coupled plasma optical emission (ICP-OES) using a Perkin Elmer optima 4300DV. The material for the samples was acid cleaned with nitric acid (HNO_3) to avoid contamination. Samples were diluted in 0.3M HCl and calibrated against multi-element standard solutions that bracketed the concentration ranges in the sample solutions. Standards were prepared gravimetrically using certified and traceable VWR Aristar single-element standard solutions, Romil UpA nitric acid and Milli-Q water. A standard seawater solution (IAPSO) and Certified Reference Materials (CRM) were analyzed for cross-reference.

Statistical analyses

Data analyses were performed in Minitab 15 (Minitab 15® Statistical Software for Windows®, 2007, Coventry, UK) and Statistica 9 (StatSoft, Inc. Oklahoma, USA) software. The experimental data were analyzed with one-way ANOVA (water source as

a fixed factor) with four replicates for the fertilization experiment (20 in total) and triplicates for the larval growth (15 containers in total) for every experimental condition to increase accuracy. The morphology data were normally distributed and a One-Sample Kolmogorov-Smirnov test (P >0.150) was used to ensure that the distribution was homogeneous. Fertilization success, morphometric data and particulate carbon (POC and PIC) were analyzed with a one-way ANOVA. The parametric Tukey test for multiple comparisons was used for *post hoc* analyses.

Appendix

Results

Natural seawater carbonate chemistry

At the PAP site (North Atlantic Ocean), as in most ocean basins (Takahashi et al. 1979), there is a gradient of increasing bicarbonate ions (HCO_3^-) and dissolved inorganic carbon (DIC), and a decrease in carbonate ions (CO_3^{2-}) and Ω-Cal with depth, while total alkalinity (TA) remains constant (Fig. 1b, Table 1). The measured samples (corrected for pressure and *in situ* temperature effect at depth) agreed well with the WOCE A16 transect line data in the region 40 °N-50 °N (Fig. 1b). Under the experimental conditions on board at ~9 °C and with surface pressure (1 atm), the water carbonate chemistry gradients were maintained for the water from 250 to 4710 m but with different concentrations (see Table 1). DIC and HCO_3^- increased from 2116 and 1940 μmol kg^{-1} at 250 m to 2175 and 2024 μmol kg^{-1} at 4710 m. The CO_3^{2-} and Ω-Cal varied from 161 μmol kg^{-1} and 3.84 (at 250 m) to 132 μmol kg^{-1} and 3.15 at 4710 m respectively. These changes reflect the increase in atmospheric CO_2 and the ocean's interior respiration that changes the chemistry of the deep-sea, resulting in a transition of the carbonate system from a predominately calcite saturated water column above 4000 m to undersaturated conditions below this depth in the Atlantic Ocean.

Fertilization and larval development

The average number of fertilized eggs (monitored 2 hours post-fertilization) was significantly different across treatments ($F_{4, 59} = 14.34$ $P < 0.001$), from 250 m to 4710 m (Fig. 2a). Results showed a decrease in fertilization success of 68 % in the deepest seawater samples (4000 m, 4600 m and 4710 m) compared to 85 % in the shallowest

water (250 m). Development and tissue morphology of *P. miliaris* larvae was not affected by deep water incubations (elevated HCO_3^- conditions and low CO_3^{2-} and Ω-Cal between 4000 and 4710 m). The null effect of the deep water on larval development (POA; $F_{4, 45} = 1.75$, $P = 0.157$ and BL; $F_{4, 45} = 1.15$, $P = 0.347$) was comparable across treatments over the 5 days of the incubations (Fig. 2b and Table 1). The data were especially variable in the incubations with water from below 4000 m.

Particulate carbon and calcification

The incubations allowed investigation of the effect of changes in carbon chemistry on calcification in early stages of *P. miliaris* larvae. Particulate inorganic carbon (PIC) was used as an indicator of calcium carbonate content per larvae. There was a doubling in larval PIC ($F_{4, 13} = 201.26$ $P < 0.01$) in the incubation with water from 250 m in agreement with observations of larger skeletons (Fig. 2c) and the same trend was observed in PIC:POC (Fig. 3a). A decline in calcification was observed in all incubations except from 250 m (the control). Scanning electron microscopy examinations revealed a decrease in size of the larval skeletons with decreasing Ω-Cal, although there was no evidence of corrosion. The effect of CO_3^{2-} availability (reduced in deeper waters) on the growth of the larval skeleton revealed an uptake of 15% of CO_3^{2-}:HCO_3^- in the surface 250 m (Ω-Cal= 3.84) compared to a 5-7% in incubations with water below 4000 m (Ω-Cal = 3.15) (Fig. 3b). The reduction in calcification (decrease in PIC and uptake of CO_3^{2-}) was confirmed by observations of smaller spicules as seen by the smaller skeleton rods (Fig. 4). Particulate organic carbon (POC) content per larvae was not significantly different across treatments ($F_{4, 13} = 1.04$ $P > 0.05$; Fig. 2c. See Table 1 in Appendix for the raw data).

Discussion

Fertilization and larval development

The phenotypic plasticity of *P. miliaris* in the water carbon chemistry gradients presented here shows that shallow water echinoids have the potential to adapt to a distinct gradient of carbon chemistry conditions during early development. This tolerance has been reported for early larval development in Antarctic echinoderms (Clark et al. 2009). This is a direct consequence of echinoids evolving in a habitat where pH changes can exceed up to 0.1 units on a daily basis (Menendez et al. 2001), and 0.4 units in months (Wootton et al. 2008). Our results indicate a ~20% decrease in fertilization success at Ω-Cal values near 3. This is in agreement with some laboratory studies showing that low pH seawater affects sperm motility and speed (Havenhand et al. 2008) and the low intracellular pH of the oocyte may prevent a successful fertilization (Grainger et al. 1979). However, recent studies indicate that acidification does not affect fertilization success in the sea urchin species *Heliocidaris erythrogramma* (Byrne et al. 2010). This suggests that the susceptibility of fertilization to ocean acidification may be species-specific. The tolerance of the larvae seems to be higher as they already encounter large variations in carbonate chemistry conditions during the larval stage (e.g. the sporadic exposure to deep CO_2 rich water associated with coastal upwelling events, and the diverse chemistry of the ocean currents on which they are transported).

Particulate carbon and calcification

Particulate organic carbon (POC) in the larval body remained almost constant over all depths tested, which is consistent with the lack of change in larval size. However, the decline in larval PIC observed in all treatments compared to the 250 m incubation suggests that under deep seawater conditions the larvae divert energy towards growing soft tissue rather than producing long skeletal rods (inorganic carbon, PIC). The growth of long arms (tissue) explain the increased efficiency of food collection by the larvae because of the extension of the ciliated bands along the arms (Strathmann 2007). A decrease in calcification resulting in weaker skeletons has been suggested to increase potential larval mortality (Staver & Strathmann 2002) given that the skeletal rods play important roles in larval feeding, motility and settling. However, the larvae may compensate this PIC loss by allocating energy to other vital functions. The decrease in calcification may also be a consequence of dissolution of Mg phases (incorporated as $MgCO_3$, thus contributing to the total PIC), which occur in the skeleton of sea urchins (Weber 1969, Hermans et al. 2010). This is caused by the greater susceptibility to dissolution of calcite with Mg, compared to that of calcite alone (Morse et al. 2006). However it is not clear whether and to what extent $MgCO_3$ is incorporated in early larval stages, and therefore if dissolution is an important process affecting skeleton formation during the first 5 days of development.

Seawater collected from different depths typically has different chemical characteristics, and therefore we cannot ignore the possibility of water properties other than carbonate chemistry affecting larval physiology. The elemental composition of seawater (especially Mg:Ca) is known to drive calcification and the net inorganic

carbon content of many organisms (Stanley et al. 2005, Ries 2010). Under all the experimental conditions tested, $[Ca^{2+}]$ and $[Mg^{2+}]$ remained near constant with a slight decrease with depth, yielding a Mg:Ca of 5.27 (mol:mol), which is on the upper limit of the Ries (2010) dataset for a variety of calcifying species. Therefore an effect of seawater Mg:Ca ratios on development and carbon acquisition can be eliminated.

Evolutionary adaptation to the deep-sea

The tolerance of *P. miliaris* larvae to the deep-sea water chemistry supports the notion that larval and juvenile stages of organisms are more resilient to environmental changes than adults given the varied hydrographic conditions and chemistry they experience when transported in the water column (Howell et al. 2002). This contrasts with laboratory incubations, where often larvae/juveniles are seen as the most susceptible to ocean acidification (Kurihara & Shirayama 2004, Dupont et al. 2008). Field studies indicate that larvae and juveniles [in species with planktotrophic and lecithotrophic reproduction mode (Sumida et al. 2000)] normally inhabit much deeper depths than the adults (> 1000 m deeper in some cases) (Gage & Tyler 1981, Howell et al. 2002). This is irrevocable evidence that they encounter (at least in the Atlantic Ocean) carbon chemistries similar to our study, and that they tolerate them. However, juveniles settling out of adult ranges tend not to survive (Gage & Tyler 1981), leading to the hypothesis that pressure and temperature shape the bathymetric distribution. We suggest that there may also be an ontogenic tolerance change to distinct carbon chemistries determining the niches for settlement and development. From an evolutionary perspective, the ability of larvae to cope with broad changes in seawater carbonate chemistry may have determined the ability of shallow water echinoderms to

progressively colonize deeper environments early in their evolutionary history (Villalobos et al. 2006, Mestre et al. 2009) (Fig. 1a). Previous studies on deep-sea colonization indicate that the genus *Echinus* spp. may have originated in shallow waters in the North Atlantic (Tyler & Young 1998), while the genus *Sterechinus* spp. is restricted to Antarctica (Tyler et al. 2000). This suggests that those species might have undergone bathymetric migration and speciation from a shallow-water ancestor, helped by favourable hydrographic conditions (with the formation of deep-water masses both in the North Atlantic and in Antarctica), and also tolerated extreme carbon chemistry variations. We argue that the different carbonate chemistry conditions that echinoderms naturally encounter in the water masses of the North Atlantic Ocean may not be a limiting factor in the colonization of deep-sea habitats. It is known that larval tolerance increases with age (Young et al. 1997), the swimming stage being the most likely invaders of the deep-sea and also the most tolerant to deep-sea conditions. The data suggest that larvae of this species could colonize and adapt to new carbon chemistry conditions in the future and that they could have done the same with a step-wise invasion in the past. Data for temperature and pressure effects on the later stages of larval development in *P. miliaris* suggest that they are more tolerant than at early embryo stages (Aquino-Souza et al. 2008). The present results are in accordance with previous studies of deep-sea invasion of this species (Aquino-Souza et al. 2008), suggesting that the depth distribution of *P. miliaris* cannot be explained by either physiological or chemical frontiers during planktonic stages. Deep-sea echinoids may have evolved the ability to cope with profound seawater chemical changes from a distant tolerant ancestor inhabiting a shallower ocean, which may make them resilient to carbonate changes over the next century.

References

Aquino-Souza R, Hawkins SJ, Tyler PA (2008) Early development and larval survival of *Psammechinus miliaris* under deep-sea temperature and pressure conditions. Journal of the Marine Biological Association of the United Kingdom 88:453-461

Byrne M, Soars N, Selvakumaraswamy P, Dworjanyn SA, Davis AR (2010) Sea urchin fertilization in a warm, acidified and high pCO_2 ocean across a range of sperm densities. Marine Environmental Research 69:234-239

Caldeira K, Wickett ME (2005) Ocean model predictions of chemistry changes from carbon dioxide emissions to the atmosphere and ocean. J Geophys Res (C Oceans) 110

Cigliano M, Gambi MC, Rodolfo-Metalpa R, Patti FP, Hall-Spencer JM (2010) Effects of ocean acidification on invertebrate settlement at volcanic CO2 vents. Marine Biology (Berlin) 157:2489-2502

Clark D, Lamare M, Barker M (2009) Response of sea urchin pluteus larvae (Echinodermata: Echinoidea) to reduced seawater pH: a comparison among a tropical, temperate, and a polar species. Marine Biology 156:1125-1137

Dickson AG, Millero FJ (1987) A comparison of the equilibrium constants for the dissociation of carbonic acid in seawater media. Deep-Sea Research 34:1733-1743

Dupont S, Havenhand J, Thorndyke W, Peck L, Thorndyke M (2008) Near-future level of CO_2-driven ocean acidification radically affects larval survival and development in the brittlestar *Ophiothrix fragilis*. Marine Ecology-Progress Series 373:285-294

Fabry VJ, Seibel BA, Feely RA, Orr JC (2008) Impacts of ocean acidification on marine fauna and ecosystem processes. ICES J Mar Sci 65:414-432

Feely RA, Sabine CL, Hernandez-Ayon JM, Ianson D, Hales B (2008) Evidence for upwelling of corrosive "acidified" water onto the continental shelf. Science 320:1490-1492

Feely RA, Sabine CL, Lee K, Berelson W, Kleypas J, Fabry VJ, Millero FJ (2004) Impact of Anthropogenic CO_2 on the $CaCO_3$ System in the Oceans. Science 305:362-366

Gage JD, Tyler PA (1981) Non-viable seasonal settlement of larvae of the upper bathyal brittle star *Ophiocten gracilis* in the Rockall Trough abyssal. Marine Biology 64:153-161

Gazeau F, Gattuso JP, Dawber C, Pronker AE, Peene F, Peene J, Heip CHR, Middelburg JJ (2010) Effect of ocean acidification on the early life stages of the blue mussel Mytilus edulis. Biogeosciences 7:2051-2060

Gazeau F, Quiblier C, Jansen JM, Gattuso JP, Middelburg JJ, Heip CHR (2007) Impact of elevated CO_2 on shellfish calcification. Geophysical Research Letters 34

Grainger JL, Winkler MM, Shen SS, Steinhardt RA (1979) Intracellular pH controls protein synthesis rate in the sea urchin egg and early embryo. Developmental Biology 68:396-406

Hall-Spencer JM, Rodolfo-Metalpa R, Martin S, Ransome E, Fine M, Turner SM, Rowley SJ, Tedesco D, Buia MC (2008) Volcanic carbon dioxide vents show ecosystem effects of ocean acidification. Nature 454:96-99

Havenhand JN, Buttler F-R, Thorndyke MC, Williamson JE (2008) Near-future levels of ocean acidification reduce fertilization success in a sea urchin. Current Biology 18

Hermans J, Borremans C, Willenz P, Andre L, Dubois P (2010) Temperature, salinity and growth rate dependences of Mg/Ca and Sr/Ca ratios of the skeleton of the sea urchin Paracentrotus lividus (Lamarck): an experimental approach. Marine Biology (Berlin) 157:1293-1300

Howell KL, Billett DSM, Tyler PA (2002) Depth-related distribution and abundance of seastars (Echinodermata : Asteroidea) in the Porcupine Seabight and Porcupine Abyssal Plain, NE Atlantic. Deep-Sea Research Part I-Oceanographic Research Papers 49:1901-1920

Iglesias-Rodriguez MD, Halloran PR, Rickaby REM, Hall IR, Colmenero-Hidalgo E, Gittins JR, Green DRH, Tyrrell T, Gibbs SJ, von Dassow P, Rehm E, Armbrust EV, Boessenkool KP (2008) Phytoplankton calcification in a high-CO_2 world. Science 320:336-340

Key RM, Kozyr A, Sabine CL, Lee K, Wanninkhof R, Bullister JL, Feely RA, Millero FJ, Mordy C, Peng TH (2004) A global ocean carbon climatology: Results from Global Data Analysis Project (GLODAP). Global Biogeochemical Cycles 18

Kurihara H, Shirayama Y (2004) Effects of increased atmospheric CO2 on sea urchin early development. Marine Ecology-Progress Series 274:161-169

Langdon C, Takahashi T, Sweeney C, Chipman D, Goddard J, Marubini F, Aceves H, Barnett H, Atkinson MJ (2000) Effect of calcium carbonate saturation state on the calcification rate of an experimental coral reef. Global Biogeochemical Cycles 14:639-654

Lebrato M, Iglesias-Rodriguez D, Feely R, Greeley D, Jones D, Suarez-Bosche N, Lampitt R, Cartes J, Green D, Alker B (2010) Global contribution of echinoderms to the marine carbon cycle: a re-assessment of the oceanic $CaCO_3$ budget and the benthic compartments. Ecological Monographs e-View

Lewis E, Wallace DWR (1998) Program Developed for CO_2 System Calculations. Program Developed for CO_2 System Calculations.

Carbon Dioxide Information Analysis Center, Oak Ridge National Laboratory, U.S. Department of Energy, Oak Ridge, Tennessee

Mann KH, Lazier JRN (1991) Dynamics of Marine Ecosystems Biological-Physical Interactions in the Oceans, Vol. Blackwell Scientific Publications Inc.: Cambridge, Massachusetts, USA; Oxford, England, Uk.

McClintock JB (1994) Trophic biology of antarctic shallow-water echinoderms. Marine Ecology-Progress Series 111:191-202

Menendez M, Martinez M, Comin FA (2001) A comparative study of the effect of pH and inorganic carbon resources on the photosynthesis of three floating macroalgae species of a Mediterranean coastal lagoon. Journal of Experimental Marine Biology and Ecology 256:123-136

Mestre NC, Thatje S, Tyler PA (2009) The ocean is not deep enough: pressure tolerances during early ontogeny of the blue mussel *Mytilus edulis*. Proceedings of the Royal Society B-Biological Sciences 276:717-726

Morse JW, Andersson AJ, Mackenzie FT (2006) Initial responses of carbonate-rich shelf sediments to rising atmospheric pCO_2 and "ocean acidification": Role of high Mg-calcites. Geochimica et Cosmochimica Acta 70:5814-5830

Mucci A (1983) The Solubility of Calcite and Aragonite in Seawater at Various Salinities, Temperatures, and One Atmosphere Total Pressure. American Journal of Science 283:780-799

Passaro M, Ziveri P, Milazzo M, Rodolfo-Metalpa R, Hall-Spencer JM (2011) Exploring CO_2 volcanic vents at Vulcano Island, Mediterranean Sea, to study the planktonic calcifier response to long-term changes in carbonate chemistry. Geophysical Research Abstracts 13

Paulmier A, Ruiz-Pino D, Garçon V (2011) CO_2 maximum in the oxygen minimum zone (OMZ). Biogeosciences 8:239-252

Riebesell U, Fabry VJ, Hansson L, Gattuso J-PE (2010) Guide to best practices for ocean acidification research and data reporting. Luxembourg: Publications Office of the European Union:260

Riebesell U, Zondervan I, Rost B, Tortell PD, Zeebe RE, Morel FMM (2000) Reduced calcification of marine plankton in response to increased atmospheric CO_2. Nature 407:364-367

Ries JB (2010) Review: geological and experimental evidence for secular variation in seawater Mg/Ca (calcite-aragonite seas) and its effects on marine biological calcification. Biogeosciences 7:2795-2849

Sabine CL, Feely RA, Gruber N, Key RM, Lee K, Bullister JL, Wanninkhof R, Wong CS, Wallace DWR, Tilbrook B, Millero FJ, Peng T-H, Kozyr A, Ono T, Rios AF (2004) The Oceanic Sink for Anthropogenic CO_2. Science 305:367-371

Sewell MA, Hofmann GE (2010) Antarctic echinoids and climate change: a major impact on the brooding forms. Global Change Biology "Accepted Article"

Smith WHF, Wessel P (1990) Gridding with continuous curvature splines in tension. Geophysics 55:293-305

Stanley SM, Ries JB, Hardie LA (2005) Seawater chemistry, coccolithophore population growth, and the origin of Cretaceous chalk. Geology 33:593-596

Staver JM, Strathmann RR (2002) Evolution of fast development of planktonic embryos to early swimming. Biological Bulletin 203:58-69

Strathmann RR (2007) Time and extent of ciliary response to particles in a non-filtering feeding mechanism. Biological Bulletin 212:93-103

Sumida PYG, Tyler PA, Lampitt RS, Gage JD (2000) Reproduction, dispersal and settlement of the bathyal ophiuroid Ophiocten gracilis in the NE Atlantic Ocean. Marine Biology 137:623-630

Takahashi T, Broecker WS, Bainbridge AE (1979) The Alkalinity and Total Carbon Dioxide Concentration in the World Oceans. Carbon Cycle Modelling:271-286

Thomsen J, Gutowska MA, Saphörster J, Heinemann A, Trübenbach K, Fietzke J, Hiebenthal C, Eisenhauer A, Körtzinger A, Wahl M, Melzner F (2010) Calcifying invertebrates succeed in a naturally CO_2 enriched coastal habitat but are threatened by high levels of future acidification. Biogeosciences Discuss 7:5119-5156

Turon X, Giribet G, Lopez S, Palacin C (1995) Growth and populations-structure of Paracentrotus lividus (Echinodermata: Echinoidea) in two contrasting habitats. Marine Ecology-Progress Series 122:193-204

Tyler PA, Young CM (1998) Temperature and pressure tolerances in dispersal stages of the genus *Echinus* (Echinodermata : Echinoidea): prerequisites for deep-sea invasion and speciation. Deep-Sea Research Part II-Topical Studies in Oceanography 45:253-277

Tyler PA, Young CM, Clarke A (2000) Temperature and pressure tolerances of embryos and larvae of the Antarctic sea urchin *Sterechinus neumayeri* (Echinodermata : Echinoidea): potential for deep-sea invasion from high latitudes. Marine Ecology-Progress Series 192:173-180

Villalobos FB, Tyler PA, Young CM (2006) Temperature and pressure tolerance of embryos and larvae of the Atlantic seastars *Asterias rubens* and *Marthasterias glacialis* (Echinodermata : Asteroidea): potential for deep-sea invasion. Marine Ecology-Progress Series 314:109-117

Weber JN (1969) The incorporation of magnesium into the skeletal calcites of echinoderms. American Journal of Science 267:537-566

Wootton JT, Pfister CA, Forester JD (2008) Dynamic patterns and ecological impacts of declining ocean pH in a high-resolution multi-year dataset. Proceedings of the National Academy of Sciences of the United States of America 105:18848-18853

Young CM, Tyler PA, Fenaux L (1997) Potential for deep sea invasion by Mediterranean shallow water echinoids: Pressure and temperature as stage-specific dispersal barriers. Marine Ecology-Progress Series 154:197-209

Zondervan I, Zeebe RE, Rost B, Riebesell U (2001) Decreasing marine biogenic calcification: A negative feedback on rising atmospheric pCO_2. Global Biogeochemical Cycles 15:507-516

Appendix

Table 1. Carbonate chemistry, oceanographic experimental conditions and seawater elemental composition. Water sampled obtained with a CTD and Niskin bottles [a]. Water carbon chemistry calculated from TA and DIC values and nutrients [b]. The CO_2 concentrations correspond to the different depths for the Porcupine Abyssal Plain (PAP) site. SD indicates the standard deviation of triplicate measurements.

	Depth (water sample)				
	250 m	2000 m	4000 m	4600 m	4710 m
A) Oceanographic parameters [a]					
Temperature (°C)	11.67	3.44	2.53	2.54	2.55
Salinity	35.60 ± 0.0	34.91± 0.0	34.91± 0.0	34.91± 0.0	34.92 ± 0.0
Oxygen (µM)	357.04 ± 2.8	357.64 ± 1.2	349.25 ± 3.5	347.16 ± 5.6	349.55 ± 3.66
B) Water carbon chemistry [b]					
TA ($\mu mol\ kg^{-1}$)	2344.55 ± 4.56	2307.63 ± 3.64	2351.76 ± 4.77	2356.22 ± 1.01	2356.34 ± 4.56
DIC ($\mu mol\ kg^{-1}$)	2116.13 ± 3.06	2130.66 ± 5.09	2175.37 ± 3.77	2176.41 ± 3.83	2175.83 ± 0.94
pCO_2 (µatm)	314.49 ± 6.35	404.55 ± 1.47	407.27 ± 7.12	414.58 ± 6.29	412.91 ± 9.50
CO_2 ($\mu mol\ kg^{-1}$)	14.16 ± 0.52	18.29 ± 0.07	19.31 ± 0.71	18.74 ± 0.51	18.67 ± 0.43
HCO_3^- ($\mu mol\ kg^{-1}$)	1940.03 ± 6.51	1982.96 ± 1.36	2028.54 ± 6.71	2025.83 ± 6.06	2024.90 ± 2.46
CO_3^{2-} ($\mu mol\ kg^{-1}$)	161.95 ± 4.87	129.70 ± 1.25	128.42 ± 4.40	131.83 ± 2.76	132.27 ± 2.76
Ω_{Cal}	3.84 ± 0.06	3.08 ± 0.01	3.09 ± 0.06	3.14 ± 0.03	3.15 ± 0.03
Ω_{Arg}	2.44 ± 0.07	1.96 ± 0.00	1.94 ± 0.04	2.00 ± 0.04	2.00 ± 0.04
pH_{total}	8.14 ± 0.01	8.04 ± 0.00	8.03 ± 0.02	8.04 ± 0.01	8.04 ± 0.01
C) Seawater elemental composition					
Ca^{2+} ($\mu g\ g^{-1}$)	10.59 ± 0.41	10.22 ± 0.10	10.34 ± 0.02	10.46 ± 0.14	10.36 ± 0.07
Mg^{2+} ($\mu g\ g^{-1}$)	33.95 ± 1.28	32.74 ± 0.36	33.03 ± 0.01	33.42 ± 0.43	33.04 ± 0.29
Mg:Ca (molar)	5.29 ± 0.00	5.27 ± 0.01	5.25 ± 0.00	5.25 ± 0.01	5.25 ± 0.00

Figure legends

Figure 1. (a) The vertical distribution of Ω-Cal along the WOCE A16 (from the GLODAP atlas) transect line in the Atlantic Ocean (map on the right corner) from 0 to 1000 m (top plot) and from 0 to 6000 m (bottom plot). The black line in the bottom plot indicates where Ω-Cal values equal 1 (drawn from an interpolation of the nearest Ω-Cal = 1). PAP denotes the location of the Porcupine Abyssal Plain and the conditions of the current study. Arrows indicate past (vertical gradient and colonization in the water column), present (the possibility of horizontal dispersion/migration), and future (a possible adaptation to environmental change) events involving echinoderm larvae. (b) Ω-Cal and HCO_3^- profiles from 40 °N to 50 °N [using the WOCE A16 transect line data from the GLODAP atlas (Key et al. 2004)] and *in situ* data at the Porcupine Abyssal Plain (PAP; 49 °N, 16 °W).

Figure 2. Development and growth conditions of *Psammechinus miliaris* larvae. (a) Effects on fertilization success, (b) larval morphology [Postoral arm (black) and Body length (grey)], (c) particulate carbon [PIC (black) and POC (grey) in triplicates per larva at day 5 of development], and (d) major elements (Ca^{2+} in light grey and Mg^{2+} in dark grey) of seawater (Mg:Ca = 5.27 ± 0.01 from 250 to 4710 m).

Figure 3. Carbon production and chemistry of *Psammechinus miliaris* larvae. (a) Organic, and inorganic carbon (values are per larva). (b) Carbonate:bicarbonate ratio. Note that grey bars correspond to the beginning of the experiment (day 0) and black

bars to the end (day 5) showing a maximum uptake of 15% of CO_3^{2-}:HCO_3^- during larval development. Error bars denote SD (n = 3). Also indicated are corresponding values of Ω-Cal, Ω-Arg, $[HCO_3^-]$ and $[CO_3^{2-}]$ against depth.

Figure 4. Morphometrics and skeletal rods of *Psammechinus miliaris* larvae. The whole skeleton of an incubated 5 day pluteus larvae using the shallowest water 250 m (a, b, c) and the deepest 4710 m (d, e, f), scale bar represents 100 μm. Both images have superimposed white rectangles that indicate magnified areas from the tip of the rod (c and f respectively), scale bar refers to 10 μm.
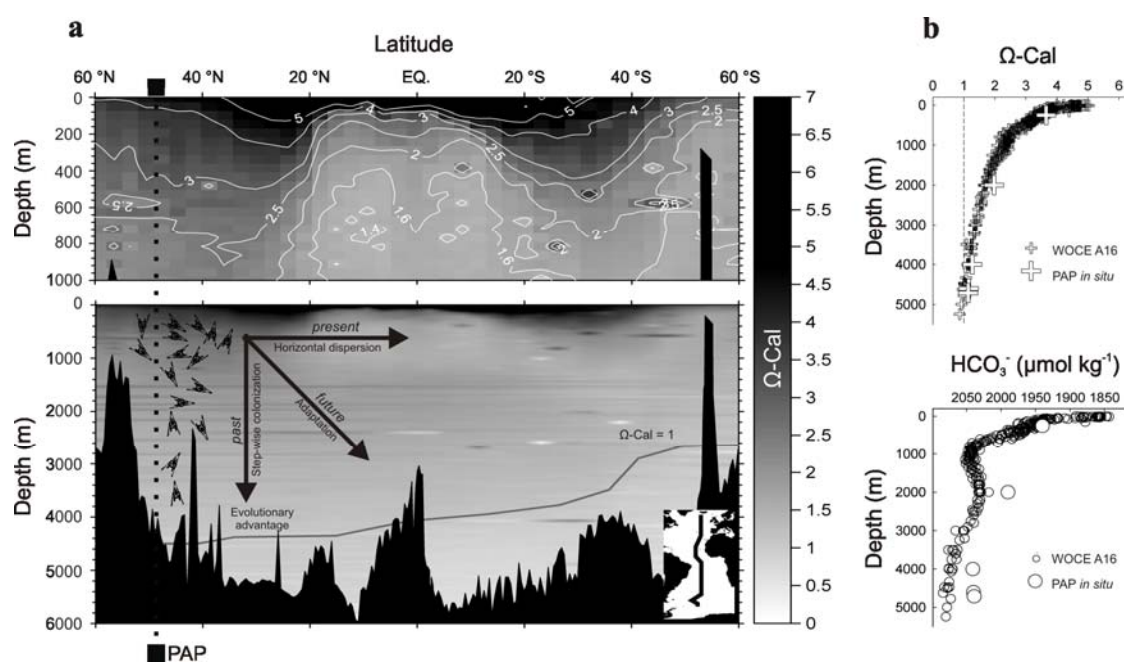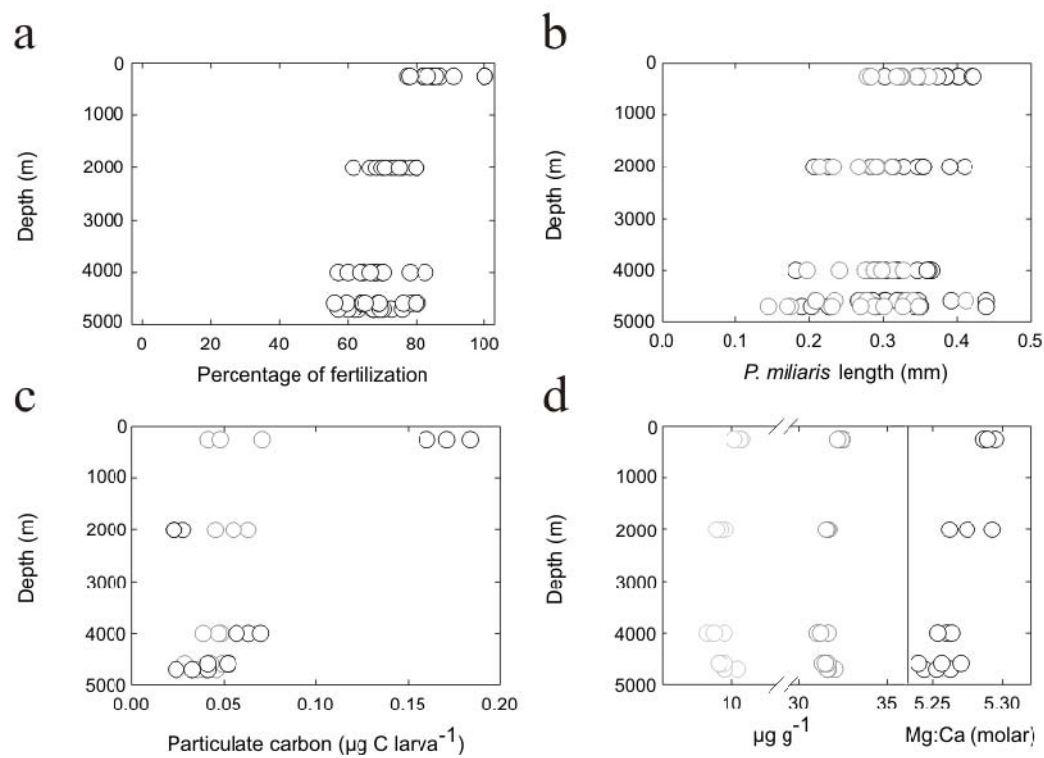
Figure 1

Figure 2

Figure 3
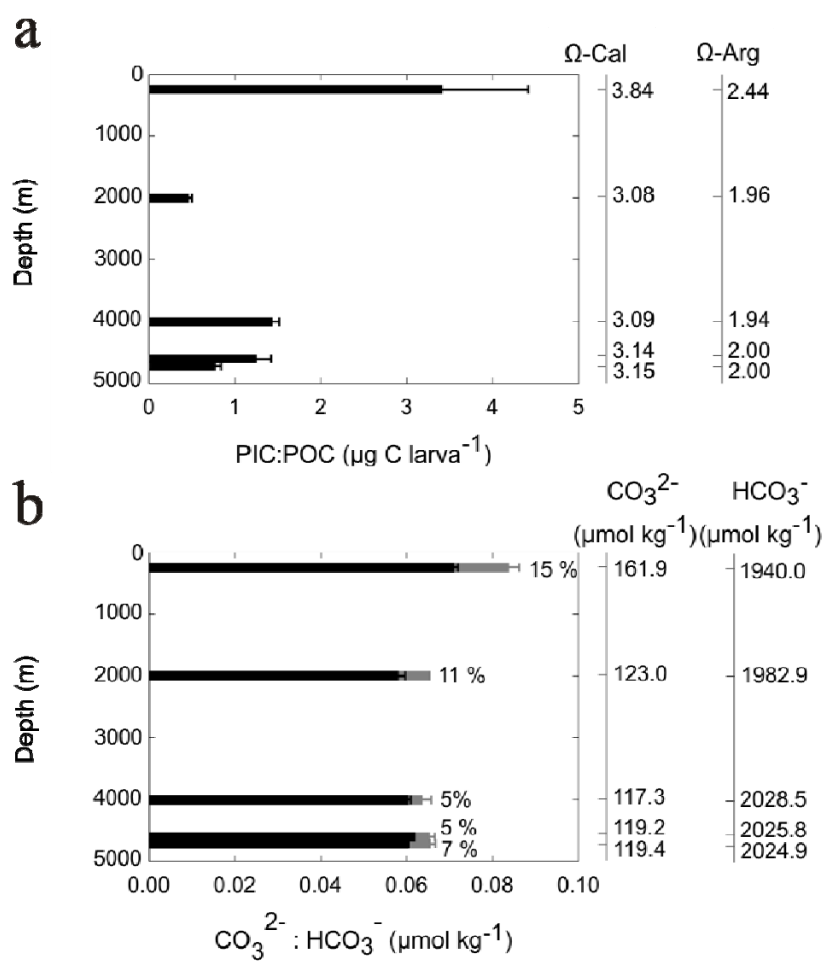
Figure 4
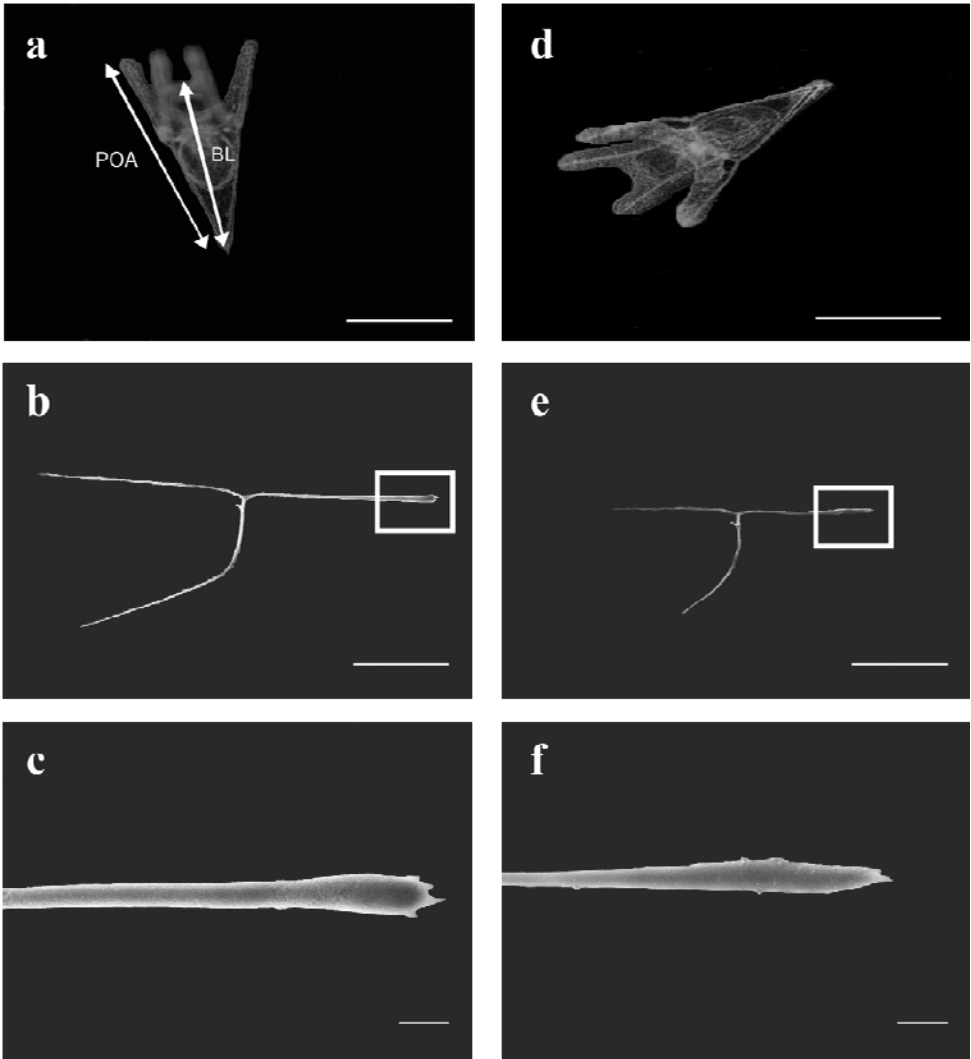
Appendix

Table 1. *Psammechinus miliaris* biological measurements for fertilization, morphological traits, and particulate carbon chemistry.

	Depth (water sample)					
	250 m	2000 m	4000 m	4600 m	4710 m	Statistics
	Mean ± SD / n	Mean ± SD / n	Mean ± SD / n	Mean ± SD / n	Mean ± SD / n	One-way ANOVA
A) Fertilization						
Fert. Success (%)	85.5 ± 7.83 / 12 *	72.73 ± 5.58 / 12 **	68.15 ± 7.34 / 11 **	68.88 ± 8.18 / 12 **	66.86 ± 5.4 / 12 **	$F_{4, 53} = 16.14$ $P < 0.001$
B) Morphology [a]						
Postoral arm (mm) [b]	0.366 ± 0.061 / 10**	0.321 ± 0.066 / 10**	0.318 ± 0.054 / 11**	0.346 ± 0.073 / 9**	0.291 ± 0.085 / 9**	$F_{4, 45} = 1.75$ $P= 0.157$
Body length (mm) [b]	0.304 ± 0.064 / 10**	0.280 ± 0.033 / 10**	0.283 ± 0.037 / 11**	0.282 ± 0.066 / 9**	0.250 ± 0.073 / 9**	$F_{4, 45} = 1.15$ $P = 0.347$
C) Particulate carbon[c]						
TPC	0.2248 ± 0.0168 / 3*	0.0791 ± 0.0114 / 3**	0.1080 ± 0.0111 / 3**	0.0886 ± 0.0163 / 3**	0.0733 ± 0.0135 / 3**	$F_{4, 14} = 59.9$ $P < 0.001$
POC	0.0533 ± 0.0154 / 3**	0.0545 ± 0.0089 / 3**	0.0446 ± 0.0051 / 3**	0.0401 ± 0.0102 / 3**	0.0455 ± 0.0076 / 3**	$F_{4, 10} = 1.51$ $P = 0.273$

PIC	0.1714 ± 0.0116 / 3	0.0245 ± 0.0028 / 3	0.0633 ± 0.0065 / 3	0.0485 ± 0.0063 / 3	0.0344 ± 0.0022 / 3	$F_{4, 10}$ = 177.41 P < 0.001
						250-2000, P < 0.001
						250-4000, P <0.001
Treatment pairs for PIC that are significantly different* (numbers represent p-values):						250-4600, P < 0.001
						250-4710, P < 0.001
						2000-4000, P < 0.001
						2000-4710, P = 0.02
						4000-4710, P = 0.004
PIC:POC	3.3989 ± 1.0117 / 3*	0.4528 ± 0.0471 / 3**	1.4226 ± 0.0952 / 3**	1.2386 ± 0.1789 / 3**	0.7625 ± 0.0802 / 3**	$F_{4, 10}$ = 18.27 P < 0.001

[a] 12 to 15 larvae were analyzed for each parameter

[b] Measurements taken during the fifth day of development 4-armed pluteus larvae.

[c] 50 larvae in triplicates were analysed, the particulate carbon values are per larva.

SD indicates the standard deviation of triplicate measurements. Tukey test * stands for a significant difference and ** for a non-significant difference.

APPENDIX 2

Part of this work have been published as Contributor: Lebrato M, Iglesias-Rodriguez D, Feely R, Greeley D, Jones D, **Suarez-Bosche N**, Lampitt R, Cartes J, Green D, Alker B (2010) Global contribution of echinoderms to the marine carbon cycle: a re-assessment of the oceanic $CaCO_3$ budget and the benthic compartments. *Ecological Monographs e-View.*

Abstract

The contribution of carbonate-producing benthic organisms to the global marine carbon budget has been overlooked, the prevailing view being that calcium carbonate ($CaCO_3$) is predominantly produced and exported by marine plankton in the "biological pump." Here, we provide the first estimation of the global contribution of echinoderms to the marine inorganic and organic carbon cycle, based on organism-level measurements from species of the five echinoderm classes. Echinoderms' global $CaCO_3$ contribution amounts to ~0.861 Pg $CaCO_3$/yr (0.102 Pg C/yr of inorganic carbon) as a production rate, and ~2.11 Pg $CaCO_3$ (0.25 Pg C of inorganic carbon) as a standing stock from the shelves, slopes, and abyssal depths. Echinoderm inorganic carbon production (0.102 Pg C/yr) is less than the global pelagic production (0.4–1.8 Pg C/yr) and similar to the estimates for carbonate shelves globally (0.024–0.120 Pg C/yr). Echinoderm $CaCO_3$ production per unit area is ~27.01 g $CaCO_3.m^{-2}.yr^{-1}$ (3.24 g $C.m^{-2}.yr^{-1}$ as inorganic carbon) on a global scale for all areas, with a standing stock of ~63.34 g $CaCO_3/m^2$ (7.60 g C/m^2 as inorganic carbon), and ~7.97 g C/m^2 as organic carbon. The shelf production alone is 77.91 g $CaCO_3.m^{-2}.yr^{-1}$ (9.35 g $C.m^{-2}.yr^{-1}$ as inorganic carbon) in contrast to 2.05 g $CaCO_3.m^{-2}.yr^{-1}$ (0.24 g $C.m^{-2}.yr^{-1}$ as inorganic carbon) for the slope on a global scale. The biogeography of the $CaCO_3$ standing stocks of echinoderms showed strong latitudinal variability. More than 80% of the global $CaCO_3$ production from echinoderms occurs between 0 and 800 m, with the highest contribution attributed to the shelf and upper slope. We provide a global distribution of echinoderm populations in the context of global calcite saturation horizons, since undersaturated waters with respect to mineral phases are surfacing. This shallowing is a direct consequence of ocean acidification, and in some places it may reach the shelf and upper slope permanently, where the highest $CaCO_3$ standing stocks from echinoderms originate. These organism-level data contribute substantially to the assessment of global carbonate inventories, which at present are poorly estimated. Additionally, it is desirable to include these benthic compartments in coupled global biogeochemical models representing the "biological pump" and its feedbacks, since at present all efforts have focused on pelagic processes, dominated by coccolithophores.
The omission of the benthic processes from modeling will only diminish the understanding of elemental fluxes at large scales and any future prediction of climate change scenarios.

Key words

Benthic compartments; CaCO₃ budget; carbon cycle; carbonate production; echinoderms; ocean acidification; standing stock.

Appendix

APPENDIX 3

Collection and process of experimental seawater samples for alkalinity analysis (TA).

Collection of experimental seawater samples for alkalinity analysis

1.   From each experimental flask 300 ml of water were filtered using a 300 μm mesh to retain the larvae and were poured smoothly into a ground glass-stoppered 250 ml borosilicate glass bottle. Using a disposable plastic Pasteur pipette the level was adjusted to leave only a small air space beneath the bottom of the stopper. A volume of 0.75 ml was then removed using a P1000 pipette.

2.   All borosilicate glass bottles were transported to the laboratory and treated in a tray in a fume hood, whilst wearing protective equipment (see below; apart from the mask). To each sample bottle, a 0.75 ml of a 3.5% (w/v = 0.13 M) stock solution of $HgCl_2$ was added. To prevent microbial growth after collection, $HgCl_2$ was added to a final concentration of approximately 0.4 mM to each sample. The bottle was then securely stoppered and the samples placed out of the way in a box for storage until they were analyzed.

Preparation of $HgCl_2$ stock:

The stock solution was prepared by dissolving solid $HgCl_2$ to 3.5% (w/v) in milliQ water. All operations apart from weighing were done within a tray in a fume hood. A lab coat, 2 pairs of nitrile gloves, safety glasses and a disposable anti-dust mask were worn. Using a spatula, $HgCl_2$ was added to a clean screw-capped bottle that has been weighed. The bottle was then re-weigh to determine the mass of $HgCl_2$, and the required volume of milliQ water was added to give a 3.5% (w/v) solution. In order to dissolve the white crystals, the capped bottle was swirled. The bottle was marked with "toxic" tape and placed in a cupboard with other harmful chemicals. The spatula was rinsed with water and the excess water collected in a low-level $HgCl_2$ waste bottle. Contaminated gloves and pipette tips used to aliquot the stock solution were collected as solid $HgCl_2$ contaminated waste (John Gittins and Dave Hydes, *pers. comms.*).

APPENDIX 4

Methodology for medium preparation for phytoplankton culture and growth of algae used as food source for the experimental organisms.

The phytoplankton species *Isochrysis galbana* and *Rhodomonas* sp. were subcultured in the f/2 medium.

1. Seawater was filtered through 0.22 μm (Millipore® Steriup™, Sigma-Aldrich) and sterilized at 100 °C for 20 minutes. Working by Bunsen burner flame, the following was added to the sterilized seawater to prepare 1 l of the f/2 medium:

Component	Stock Solution	Quantity	Molar Concentration in Final Medium
NaNO$_3$	75 g/l dH$_2$O	1 ml	8.82 x 10^{-4} M
NaH$_2$PO$_4$ H$_2$O	5 g/l dH$_2$O	1 ml	3.62 x 10^{-5} M
trace metal solution	(see recipe below)	1 ml	---
vitamin solution	(see recipe below)	0.5 ml	---

2. To prepare the f/2 trace metal solution the following components were added to a final volume of 1 l of distilled water and autoclave (Guillard 1975).

Component	Primary Stock Solution	Quantity	Molar Concentration in Final Medium
FeCl$_3$ 6H$_2$O	---	3.15 g	1.17 x 10^{-5} M
Na$_2$EDTA 2H$_2$O	---	4.36 g	1.17 x 10^{-5} M

$CuSO_4$ $5H_2O$	9.8 g/l dH_2O	1 ml	3.93 x 10^{-8} M
Na_2MoO_4 $2H_2O$	6.3 g/l dH_2O	1 ml	2.60 x 10^{-8} M
ZnSO4 $7H_2O$	22.0 g/l dH_2O	1 ml	7.65 x 10^{-8} M
$CoCl_2$ $6H_2O$	10.0 g/l dH_2O	1 ml	4.20 x 10^{-8} M
$MnCl_2$ $4H_2O$	180.0 g/l dH_2O	1 ml	9.10 x 10^{-7} M

3. For the f/2 vitamin solution, first the thiamine was dissolved and then the amounts of stocks added to a final volume of 1 l of distilled water that was filter sterilized:

Component	Primary Stock Solution	Quantity	Molar Concentration in Final Medium
thiamine HCl (vit. B_1)	---	200 mg	2.96 x 10^{-7} M
biotin (vit. H)	0.1 g/l dH_2O	10 ml	2.05 x 10^{-9} M
cyanocobalamin (vit. B_{12})	1.0 g/l dH_2O	1 ml	3.69 x 10^{-10} M

NOTE: To avoid contamination the barrel of a P1000 pipette was wiped with a tissue soaked with 80% methylated spirit to clean and sterilize. The f/2 medium and stock solution were stored at 4 °C.

4. Every 2 weeks the phytoplankton was subcultured by transferring 1ml of the culture into fresh f/2 medium.

5. The cultures were grown at 18.5 $\pm$ 1 ^{o}C with a 12 hour light: 12 hour dark cycle. Cultures were swirled every other day to suspend the cells in the growth medium.

Methodology for sample collection, material preparation and particulate carbon analyses.

Preparation method for particulate carbon samples

1.   Silver capsules (Elemental Microanalysis, UK) were prepared by combusting them at 450°C for 4-6 hours to remove contaminants.
NOTE: a set of silver capsules for blanks were required for each set of samples.

2.   Larvae were collected manually (50 larvae in triplicate) using a P1000 pipette. The tips were cut in an angle to avoid any damage or loss of larval body parts. Samples were washed three times with PBS (Phosphate buffered saline) to rinse off seawater and avoid contamination.
NOTE: Silver capsules samples were place on a 96-well plate and kept on ice until transported to the laboratory to avoid sample degradation and then stored at -20 °C until they were analyzed.

3.   For the acidification step, a Nalgene dessicator (which can be evacuated) was used. Ideally a plastic dessicator is best as those made of glass have a metal tray which will corrode. To fumigate the samples, a concentrated HCl solution (Fisher, UK) of 50ml was poured into the dessicator below the plastic plate into a beaker. The unlidded 96-well plate with the samples was place in the dessicator. The acid evaporates and then combines with water in the atmosphere to form Hydrochloric acid which degrades inorganic carbon (Verardo *et al*., 1990). The valve in the dessicator was opened and the dessicator evacuated using the vacuum pump until the pressure remained contant at ~20 in. Hg. The valve was closed and the dessicator left undisturbed in the fume hood.
NOTE: Concentrated sulphuric acid will work in the same way, but tends to be less strong.

4.   After 96 hours, the dessicator was open and the vacuum released very slowly (fast vacuum release would cause capsules to jump out of the 96-well plate).

5.   The samples were then dried in an oven at 60°C for 48 hours.
NOTE: It is recommended to use an oven where fumes are taken away in a venting system in order to avoid corrosive acid vapour in the laboratory.

6. The samples were pelleted in aluminium foil, which was precombusted at 450°C for 6 hours. Alternatively, they may be precombusted at 550°C for 3 hours to remove contaminants (Hilton *et al.*, 1986). The folding and wrapping was performed on a folding tile (special ceramic tile). Flat tweezers (pre-cleaned with acetone) were used to fold and handle the capsules. Folding too tightly may cause capsules to break, and loss of samples.

7. The folded samples were placed in 96-well microplates. The sample names and location in the 96-well plate were recorded according to position (e.g. A4, B12 etc). The plates were wrapped in aluminium foil and poly bags to prevent moisture from disturbing samples.

8. The samples were immediately sent by post in padded envelopes to Dr. Bob Head of the Plymouth Marine Laboratory (PML). The samples were then analyzed using a Thermo Finnigan flash EA1112 elemental analyser using acetanilide as the calibration standard.

NOTE: For the analysis of total particulate carbon (TPC) the acidification step should be avoided and the methodology should be followed from the drying process (Step 5).

9. Particulate inorganic carbon (PIC) was calculated by subtracting the POC from the TPC values (Riebesell et al., 2000).

Appendix

APPENDIX 6

Psammechinus miliaris experimental conditions and water carbon chemistry data.

Psammechinus miliaris experimental conditions and water carbon chemistry data. Initial culture conditions at day zero (i) and at the end of the experiment day 21st (f). SD indicates the standard deviation of triplicate measurements.

	Data set derived from the experiments			
	Treatment 1 (control)	Treatment 2	Treatment 3	Treatment 4
A) Experimental conditions [a]				
Temperature (ºC)	14.64 ± 0.22	14.64 ± 0.22	14.64 ± 0.22	14.64 ± 0.22
Salinity	36 ± 0.0	36 ± 0.0	36 ± 0.0	36 ± 0.0
Nitrate (μmol l^{-1}) (i)	0.94 ± 0.61	1.61 ± 0.61	2.60 ± 0.65	1.75 ± 0.21
Nitrate (μmol l^{-1}) (f)	12.70 ± 1.96	10.98 ± 3.94	13.58 ± 1.96	13.25 ± 0.39
Phosphate (μmol l^{-1}) (i)	0.25 ± 0.33	0.06 ± 0.01	0.08 ± 0.02	0.06 ± 0.02
Phosphate (μmol l^{-1}) (f)	0.38 ± 0.18	0.36 ± 0.17	0.38 ± 0.11	0.46 ± 0.07
Silicate (μmol l^{-1}) (i)	4.45 ± 0.19	4.92 ± 0.31	5.48 ± 0.35	4.88 ± 0.63
Silicate (μmol l^{-1}) (f)	5.14 ± 0.37	5.70 ± 0.58	5.94 ± 0.80	5.27 ± 0.56

B) Water carbon chemistry [b]

TA (μmol kg^{-1}) $_{(i)}$	2348.34± 2.13	2396.19 ± 41.31	2388.56 ± 23.60	2356.50 ± 9.30
TA (μmol kg^{-1}) $_{(f)}$	2394.48±25.24	2404.38 ± 14.41	2403.13 ± 8.12	2451.27 ± 11.38
DIC (μmol kg^{-1}) $_{(i)}$	1984.08 ± 3.95	2086.05 ± 21.15	2185.86 ± 11.02	2367.17 ± 22.27
DIC (μmol kg^{-1}) $_{(f)}$	2165.32 ± 8.02	2254.65 ± 12.55	2305.12 ± 16.86	2359.14 ± 122.79
pH$_{total}$ $_{(i)}$	8.29 ± 0.00	8.19 ± 0.04	8.00 ± 0.05	7.42 ± 0.09
pH$_{total}$ $_{(f)}$	8.05 ± 0.03	7.87 ± 0.05	7.74 ± 0.02	7.46 ± 0.05
pCO$_2$ (ppm) $_{(i)}$	207.91 ± 5.11	279.69 ± 34.97	481.17 ± 65.96	2036.39 ± 64.59
pCO$_2$ (ppm) $_{(f)}$	416.96 ± 37.60	665.76 ± 93.59	926.41 ± 61.91	1895.63 ± 199.92
CO$_2$ (μmol kg^{-1}) $_{(i)}$	7.81 ± 0.19	10.51 ± 1.31	18.08 ± 2.47	76.60 ± 17.45
CO$_2$ (μmol kg^{-1}) $_{(f)}$	15.66 ± 1.44	25.01 ± 3.51	34.80 ± 2.32	71.22 ± 7.51
HCO$_3^-$ (μmol kg^{-1}) $_{(i)}$	1725.71 ± 7.69	1857.91 ± 25.56	2018.13 ± 23.12	2246.24 ± 14.39
HCO$_3^-$ (μmol kg^{-1}) $_{(f)}$	1983.80 ± 10.44	2111.16 ± 23.34	2180.38 ± 18.89	2301.01 ± 35.52
CO$_3^{2-}$ (μmol kg^{-1}) $_{(i)}$	250.56 ± 3.95	217.63 ± 21.62	149.65 ± 17.77	44.42 ± 9.57
CO$_3^{2-}$ (μmol kg^{-1}) $_{(f)}$	165.86 ± 13.41	118.48 ± 14.89	89.94 ± 4.39	49.20 ± 6.69
Ω-Cal$_{(i)}$	5.93 ± 0.09	5.15 ± 0.51	3.54 ± 0.42	1.05 ± 0.22
Ω-Cal$_{(f)}$	3.93 ± 0.31	2.80 ± 0.35	2.13 ± 0.10	1.16 ± 0.15

Ω-Arg$_{(i)}$	3.81 ± 0.06	3.31 ± 0.32	2.28 ± 0.27	0.68 ± 0.14
Ω-Arg $_{(f)}$	2.52 ± 0.20	1.80 ± 0.22	1.37 ± 0.06	0.75 ± 0.10

[a] The temperature and Salinity were constant trough the entire experiment.

[b] Water carbon chemistry calculated from TA and DIC values and nutrients in CO2SYST, corrected for density in Matlab

Psammechinus miliaris biological measurements for fertilization, morphological traits, and particulate carbon chemistry.

Appendix

	Depth (water sample)					
	250 m	2000 m	4000 m	4600 m	4710 m	Statistics
	Mean ± SD / n	Mean ± SD / n	Mean ± SD / n	Mean ± SD / n	Mean ± SD / n	One-way ANOVA
A) Fertilization						
Fert. Success (%)	85.5 ± 7.83 / 12 *	72.73 ± 5.58 / 12 **	68.15 ± 7.34 / 11 **	68.88 ± 8.18 / 12 **	66.86 ± 5.4 / 12 **	$F_{4, 53} = 16.14$ $P < 0.001$
B) Morphology [a]						
Postoral arm (mm) [b]	0.366 ± 0.061 / 10**	0.321 ± 0.066 / 10**	0.318 ± 0.054 / 11**	0.346 ± 0.073 / 9**	0.291 ± 0.085 / 9**	$F_{4, 45} = 1.75$ $P = 0.157$
Body length (mm) [b]	0.304 ± 0.064 / 10**	0.280 ± 0.033 / 10**	0.283 ± 0.037 / 11**	0.282 ± 0.066 / 9**	0.250 ± 0.073 / 9**	$F_{4, 45} = 1.15$ $P = 0.347$
C) Particulate carbon[c]						
TPC	0.2248 ± 0.0168 / 3*	0.0791 ± 0.0114 / 3**	0.1080 ± 0.0111 / 3**	0.0886 ± 0.0163 / 3**	0.0733 ± 0.0135 / 3**	$F_{4, 14} = 59.9$ $P < 0.001$
POC	0.0533 ± 0.0154 / 3**	0.0545 ± 0.0089 / 3**	0.0446 ± 0.0051 / 3**	0.0401 ± 0.0102 / 3**	0.0455 ± 0.0076 / 3**	$F_{4, 10} = 1.51$ $P = 0.273$
PIC	0.1714 ± 0.0116 / 3	0.0245 ± 0.0028 / 3	0.0633 ± 0.0065 / 3	0.0485 ± 0.0063 / 3	0.0344 ± 0.0022 / 3	$F_{4, 10} = 177.41$ $P < 0.001$

Appendix

						250-2000, P < 0.001
Treatment pairs for PIC that are significantly different* (numbers represent p-values):						250-4000, P <0.001
						250-4600, P < 0.001
						250-4710, P < 0.001
						2000-4000, P < 0.001
						2000-4710, P = 0.02
						4000-4710, P = 0.004
PIC:POC	3.3989 ± 1.0117 / 3*	0.4528 ± 0.0471 / 3**	1.4226 ± 0.0952 / 3**	1.2386 ± 0.1789 / 3**	0.7625 ± 0.0802 / 3**	$F_{4, 10}$ = 18.27 P < 0.001

[a] 12 to 15 larvae were analyzed for each parameter

[b] Measurements taken during the fifth day of development 4-armed pluteus larvae.

[c] 50 larvae in triplicates were analysed, the particulate carbon values are per larva.

SD indicates the standard deviation of triplicate measurements. Tukey test * stands for a significant difference and ** for a non-significant difference.

Appendix

Carbonate chemistry and oceanographic data derived from the experimental conditions with *Psammechinus miliaris* larvae. The CO_2 scenarios correspond to the different depths for the Porcupine Abyssal Plain (PAP) in the North Atlantic (49 °N, 16 °W). *In situ* oceanographic and water carbon chemistry data corrected for pressure effect (*C*) and in the surface at experimental conditions (*S*). For each parameter the first row represent day zero (D0 at the beginning of the experiment), second row is day one (D1) and the third row corresponds to day fifth (D5). SD indicates the standard deviation of triplicate measurements.

Appendix

	Depth (water sample)				
	250 m	2000 m	4000 m	4600 m	4710 m
A) Oceanographic parameters [a]					
Temperature (°C)	11.67	3.44	2.53	2.54	2.55
Salinity	35.60 ± 0.0	34.91± 0.0	34.91± 0.0	34.91± 0.0	34.92 ± 0.0
Oxygen (ml l^{-1})	6.07	7.37	7.54	7.54	7.54
Nitrate (μmol l^{-1})	9.36 ± 0.37	17.94 ± 0.24	22.61 ± 0.30	22.95 ± 0.27	22.425 ± 0.37
Phosphate (μmol l^{-1})	0.54 ± 0.01	1.15 ± 0.01	1.49 ± 0.00	1.50 ± 0.02	1.48 ± 0.04
Silicate (μmol l^{-1})	3.62 ± 0.14	13.59 ± 0.25	43.11 ± 1.71	43.28 ± 1.36	43.11 ± 1.53
B) Water carbon chemistry [b]					
TA (μmol kg^{-1}) (S)					
D0	2344.55 ± 4.56	2307.63 ± 3.64	2351.76 ± 4.77	2356.22 ± 1.01	2356.34 ± 4.56
D1	2338.92 ± 2.21	2312.29 ± 0.76	2354.77 ± 4.41	2356.19 ± 4.05	2355.64 ± 3.23
D5	2337.29 ± 3.17	2302.87 ± 0.56	2349.14 ± 2.51	2358.34 ± 1.00	2353.64 ± 1.02
DIC (μmol kg^{-1}) (S)					
D0	2116.13 ± 3.06	2130.66 ± 5.09	2175.37 ± 3.77	2176.41 ± 3.83	2175.83 ± 0.94
D1	2138.51 ± 4.19	2152.21 ± 2.92	2175.58 ± 1.89	2182.14 ± 5.22	2174.19 ± 3.89
D5	2143.27 ± 4.46	2148.57 ± 5.33	2184.56 ± 1.11	2188.00 ± 2.03	2188.61 ± 1.00
pCO$_2$ (μatm) (S)					
D0	314.49 ± 6.35	404.55 ± 1.47	407.27 ± 7.12	414.58 ± 6.29	412.91 ± 9.50
D1	365.71 ± 8.50	450.80 ± 10.21	415.69 ± 4.34	429.36 ± 5.51	414.58 ± 7.27
D5	378.91 ± 7.28	464.26 ± 7.30	451.54 ± 6.60	439.62 ± 5.51	452.22 ± 1.83
pCO$_2$ (μatm) (C)	313.03 ± 6.35	307.29 ± 6.60	301.85 ± 2.42	290.56 ± 8.12	289.08 ± 6.86

CO_2 (μmol kg^{-1}) $_{(S)}$						
	D0	14.16 ± 0.52	18.29 ± 0.07	19.31 ± 0.71	18.74 ± 0.51	18.67 ± 0.43
	D1	16.47 ± 0.38	20.38 ± 0.46	18.80 ± 0.65	19.75 ± 0.66	18.56 ± 0.78
	D5	17.06 ± 0.33	20.99 ± 0.78	20.41 ± 0.42	19.88 ± 0.52	20.44 ± 0.08
CO_2 (μmol kg^{-1}) $_{(C)}$		14.10 ± 0.73	16.89 ± 0.00	17.17 ± 0.71	16.52 ± 0.46	16.43 ± 0.39
HCO_3^- (μmol kg^{-1}) $_{(S)}$						
	D0	1940.03 ± 6.51	1982.96 ± 1.36	2028.54 ± 6.71	2025.83 ± 6.06	2024.90 ± 2.46
	D1	1977.47 ± 6.12	2012.22 ± 3.26	2025.36 ± 5.11	2034.32 ± 4.83	2025.8 ± 3.00
	D5	1985.54 ± 5.70	2011.46 ± 3.89	2010.08 ± 2.06	2041.87 ± 3.52	2045.02 ± 1.12
HCO_3^- (μmol kg^{-1}) $_{(C)}$		1940.71 ± 6.50	1990.96 ± 0.28	2041.54 ± 6.55	2040.59 ± 5.95	2039.93 ± 2.35
CO_3^{2-} (μmol kg^{-1}) $_{(S)}$						
	D0	161.95 ± 4.87	129.70 ± 1.25	128.42 ± 4.40	131.83 ± 2.76	132.27 ± 2.76
	D1	144.57 ± 2.55	119.61 ± 1.53	131.43 ± 3.87	126.69 ± 3.61	132.81 ± 3.88
	D5	140.66 ± 2.02	116.12 ± 3.35	122.79 ± 1.55	126.25 ± 2.61	123.14 ± 0.41
CO_3^{2-} (μmol kg^{-1}) $_{(C)}$		161.32 ± 4.85	123.05 ± 0.11	117.34 ± 4.18	119.29 ± 2.60	119.47 ± 2.60
Ω-Cal $_{(S)}$						
	D0	3.84 ± 0.06	3.08 ± 0.01	3.09 ± 0.06	3.14 ± 0.03	3.15 ± 0.03
	D1	3.43 ± 0.06	2.85 ± 0.04	3.13 ± 0.04	3.06 ± 0.09	3.17 ± 0.04
	D5	3.34 ± 0.05	2.77 ± 0.08	2.93 ± 0.05	3.01 ± 0.00	2.94 ± 0.01
Ω-Cal $_{(C)}$		3.65 ± 0.06	1.97 ± 0.01	1.27 ± 0.05	1.16 ± 0.03	1.14 ± 0.02
Ω-Arg $_{(S)}$						
	D0	2.44 ± 0.07	1.96 ± 0.00	1.94 ± 0.04	2.00 ± 0.04	2.00 ± 0.04
	D1	2.18 ± 0.04	1.81 ± 0.02	1.99 ± 0.06	1.94 ± 0.06	2.00 ± 0.05
	D5	2.12 ± 0.03	1.76 ± 0.05	1.86 ± 0.02	1.91 ± 0.00	1.86 ± 0.01
Ω-Arg $_{(C)}$		2.33 ± 0.06	1.27 ± 0.00	0.84 ± 0.03	0.77 ± 0.02	0.76 ± 0.02

pH$_{total\ (S)}$

	D0	8.14 ± 0.01	8.04 ± 0.00	8.03 ± 0.02	8.04 ± 0.01	8.04 ± 0.01
	D1	8.09 ± 0.01	8.00 ± 0.01	8.04 ± 0.01	8.03 ± 0.02	8.04 ± 0.01
	D5	8.07 ± 0.01	7.99 ± 0.02	8.01 ± 0.01	8.02 ± 0.00	8.01 ± 0.00

pH$_{total\ (C)}$ 8.13 ± 0.01   8.05 ± 0.00   7.97 ± 0.02   7.96 ± 0.01   7.96 ± 0.01

a Water sampled obtained with a CTD and Niskin bottles deployed from a vessel

b Water carbon chemistry calculated from TA and DIC values and nutrients in CO2SYST, corrected for density in Matlab.

213

Percentage of fertilization, mortality, and morphometrics of *P. miliaris*. Total particulate carbon (TPC), particulate organic carbon (POC), particulate inorganic carbon (PIC) and the PIC/POC ratio in *P. miliaris* under two pH (8.2 and 7.7) and three temperature (15, 18 and 20 $^{\circ}$C) conditions, exposed during 38 days. Values are per larvae.

	Treatment 1 15 °C / pH 8.2	Treatment 2 15 °C / pH 7.7	Treatment 3 18 °C / pH 8.2	Treatment 4 18 °C / pH 7.7	Treatment 5 20 °C / pH 8.2	Treatment 6 20 °C / pH 7.7
	Mean ± SE / n	Mean ± SE / n	Mean ± SE / n	Mean ± SE / n	Mean ± SE / n	Mean ± SE / n
A) Percentage of						
Fertilization	93.50±1.31 / 16	73.73±1.91 / 16	84.53±1.75 / 16	71.52±3.24 / 16	89.38±2.22 / 16	89.82±2.13 / 16
Mortality	37.60±7.02 / 4	43.77±3.76 / 4	80.81±5.35 / 4	51.87±4.04 / 4	58.62±4.93 / 4	63.35±5.4 / 4
B) Morphology						
Postoral arm (mm) [i]	0.443±0.015 / 11	0.470±0.016 / 13	0.497±0.018 / 12	0.478±0.025 / 10	0.599±0.017 / 12	0.545±0.010 / 9
Postoral arm (mm) [f]	0.722±0.027 / 17	0.673±0.020 / 12	0.746±0.040 / 10	0.704±0.030 / 9	0.754±0.028 / 11	0.772±0.028 / 12
Body length (mm) [i]	0.350±0.007 / 11	0.345±0.011 / 13	0.369±0.013 / 12	0.344±0.018 / 10	0.395±0.014 / 12	0.377±0.006 / 9
Body length (mm) [f]	0.539±0.013 / 17	0.524±0.012 / 12	0.561±0.015 / 10	0.556±0.017 / 9	0.536±0.009 / 11	0.542±0.020 / 12
Stomach area (mm^2) [i]	0.011±0.001 / 11	0.013±0.001 / 13	0.010±0.000 / 12	0.008±0.000 / 10	0.009±0.001 / 12	0.010±0.000 / 9
Stomach area (mm^2) [f]	0.015±0.001 / 17	0.013±0.000 / 12	0.020±0.001 / 10	0.019±0.005 / 9	0.011±0.001 / 11	0.017±0.001 / 12
C) Particulate carbon						
TPC (µg C)	0.410±0.060 / 3	0.346±0.014 / 3	0.303±0.005 / 2	0.306±0.057 / 3	0.323±0.015 / 3	0.414±0.063 / 3
POC (µg C)	0.387±0.053 / 3	0.307±0.002 / 3	0.309±0.022 / 2	0.333±0.028 / 3	0.275±0.022 / 3	0.394±0.043 / 3
PIC (µg C)	0.031±0.006 / 3	0.004±0.001 / 3	0.013±0.007 / 2	0.007±0.000 / 3	0.023±0.002 / 3	0.015±0.001 / 3

Appendix

PIC:POC	0.081±0.005 / 3	0.014±0.006 / 3	0.049±0.030 / 2	0.022±0.002 / 3	0.086±0.015 / 3	0.039±0.003 / 3
D) Carbonate ratios						
$CO_3^{2-} : HCO_3^{-\ i}$	0.158±0.009 / 3	0.039±0.003 / 3	0.160±0.007 / 3	0.048±0.001 / 3	0.166±0.016 / 3	0.042±0.000 / 3
$CO_3^{2-} : HCO_3^{-\ f}$	0.059±0.000 / 3	0.028±0.002 / 3	0.052±0.005 / 3	0.028±0.001 / 3	0.069±0.001 / 3	0.027±0.000 / 3

[i] Values for day 0.

[f] Values for day 38. SE indicates the standard error of measurements.

215

Appendix

217

Protocol for fixation for indirect immunofluorescence.

1E11 antibody (The antibody is a mouse monoclonal antibody. It is an ascites fluid)

1. The embryos/larvae (approximately 20) were collected and washed once with FSW (0.22 Millipore) and fresh 4% Paraformaldehyde (PFA) was prepared (2 ml of stock PFA 20% + 8 ml of FSW).

2. The larvae were fixed by adding drop by drop (1-3) of 4% PFA, until movement stopped. The larvae were suspended for a maximum of 15 minutes in PFA.

3. The samples were then washed three times with phosphate-buffered saline (PBS) for 5 minutes. Supernantant was removed and then post fixed with ice cold MeOH for no longer than 5 minutes.

4. Subsequently the larvae were blocked with 5% normal Goat serum (kept on ice) in PBS containing 0.05% Triton X-100 (PBST) for 30 minutes (which can be left over night).

5. After 30 minutes in block solution the larvae were re-suspended in the diluted (1° antibody was diluted in PBS) primary antibody solution (better results were achieved by leaving it overnight at 4^0 C). The primary antibody can also been left for 3 hours at room temperature (although this is not highly recommended). Dilution factors were:

    a) 1E11 at 1:200 = 1.0 ul of 1E11 AB' (donated by Professor Burke, University of Victoria,   Canada).

    b) 5-HT at 1:50 =4 ul of 5-HT AB' (from Immunostar company (Cat # 20080). Made in Rabbit antiseratone).

6. The primary antibody was rinsed 3 times for 5 minutes in PBST (PBST worked better, because it has a detergent that helped handle the larvae and avoid them sticking to the glass, to the petri dishes or to the pipette. PBST helped to reduce larval lost.

7. For the incubation in the secondary antibody the larvae were left for 1 hour at room temperature. The antibodies dilution factor for the 1E11 AB" was 1:500 (Invitrogen red fluorohphore) and for 5-HT AB" the dilution factor was 1:500 (green fluorophore).

8. Finally the secondary antibody was rinsed off three times for 5 miuntes in PBS and mounted with Glycerol: PBS (1:1) on a slide sealed with a coverslip and clear nail polish.

Notes:

- The simplest fixation that frequently preserves morphology and provides antigen access is treatment in -20^0 C MeOH for 20 minutes. MeOH fixes and permeabilizes simultaneously, whereas fixation with aldehydes requires inclusion of non-ionic detergents such as Triton X-100 (0.1-0.5%) or Tween 20 (0.1-0.5%) during fixation, or requires subsequent steps to permeabilize cells.

- Permeabilization is essential if intracellular antigens are to be detected, or if antigens are localized deep within the embryo. If a surface antigen is to be detected, permeabilization should be avoided.

Methanol fixation:

- Post fixation in ice cold acetone or MeOH (combined with an initial aldehyde fixation) allows for permeabilization of the membrane. MeOH fixation acts by simultaneous denaturation and precipitation of proteins.

- MeOH is an effective fixative for most immunofluorescence applications, however, it is necessary to remove as much seawater as possible from the embryos before adding the MeOH since a precipitate will form. This precipitate may obscure embryos but will disappear after several washes with PBS.

Fixation PFA:

- Formaldehyde fixes cellular structures by cross-linking proteins. Because formaldehyde has a low molecular weight, it can penetrate cells and tissues rapidly. If left standing for long periods, formaldehyde readily oxidizes to form formic acid and polymerizes to form paraformaldehyde. If these solutions have been opened for some time they are not as effective as freshly prepared formaldehyde.

Buffers:

- Ideally, it should be isotonic with the cell so that any perturbation of cellular structure is avoided, and the cell should be maintained as close to its physiological

state as possible. The buffer most frequently used is phosphate buffered saline (PBS) which can be utilized for most applications.

- All buffers should be filtered before use (using 45uM syringe filter or by microcentrifugation) since particulates and debris will readily stick to the surfaces of embryos.

- The most commonly used detergents for permeabilization are Triton X-100 and Tween-20. These detergents extract membrane lipids without interfering with protein interactions.

- PBST (PBS with 0.1% Triton X-100 or Tween-20 added).

Washes:

- Washes are required post-fixation, and also for post-incubation with antibodies. The most common wash used is PBS, although addition of non-ionic detergents such as Triton X-100 and Tween-20 is recommended to reduce background staining, aid permeabilization, and also helps to minimize embryos sticking to the walls of tubes or dishes.

Blocking:

- Block is required to prevent antibody binding to non-specific sites. The blocking agent should be a non-specific protein that is not recognized by either the primary or secondary antibodies. A 3 to 5% solution of normal serum from the same species as the secondary antibody is the best choice. For example, commercially available secondary antibodies are frequently raised in goats, so normal goat serum would be the best choice as a blocking agent. Bovine serum albumen (BSA, 3%) or non-fat dry milk (3%) can be used as alternatives.

Primary Antibody:

- The appropriate dilution of the primary antibody may be based on published protocols or determined empirically.

- Dilutions should be made in filtered PBS or PBST and a brief centrifugation in a microcentrifuge is recommended to remove protein aggregation.

- To remove the excess primary antibody, embryos should be washed several times (three times for five minutes) in sufficient PBS or PBST. If not washed out, unbound primary antibody can bind to free secondary antibody, reducing its effective concentration and causing excessive background staining. Antibodies are sensitive to changes in the composition of the washing solution; therefore, it is recommended that the buffer used to dilute them and the washing buffer are the same.

Secondary Antibody:

- The most common choice for detection methods is: indirect immunofluorescence by epifluorescence microscopy or confocal microscopy. Indirect immunofluorescence requires a second antibody which is conjugated to a fluorochrome and directed against the species used to produce the primary antibody.
- For localization of a single antigen by conventional epifluorescence microscopy, either fluorescein isothiocyanate (FITC) or tetramethylrhodamine isothiocyanate (TRITC) conjugated to the secondary antibody is usually sufficient. However, if performing double or triple labelling to detect multiple antigens simultaneously or combining antigen localization with nuclear or cytoskleletal staining, one must take into consideration the excitation and emission spectra of the combined fluorochromes.

Mounting Specimens:

- A simple mounting medium suitable for immunofluorescence is glycerol:PBS (1:1) followed by sealing of the coverslip with clear nail polish.
- Photobleaching can be avoided by including anti-fade reagents in the final mounting media.

Appendix

APPENDIX 11

223

Area and volume measurements of bisected larvae of seastar *Pisaster ochraceus* and *Orthasterias koehleri* made over two weeks during their regeneration.

Area and volumen estimations during regeneration of *Pisaster ochraceus* larvae

	Control				Age			
	Before bisection	Day 1	Day 3	Day 5	Day 7	Day 9	Day 11	Day 13
	Mean ± SE / n	Mean ± SE / n	Mean ± SE / n	Mean ±SE / n	Mean ± SE / n	Mean ± SE / n	Mean ± SE / n	Mean ± SE / n
Area $(mm^2)_a$	1.550 ± 0.079 / 3	0.246 ± 0.042 / 3	0.172 ± 0.012 / 4	N/A	0.114 ± 0.023 / 3	0.148 ± 0.008 / 2	0.185 ± 0.027 / 3	0.481 ± 0.073 / 7
Area $(mm^2)_b$	1.550 ± 0.079 / 3	0.374 ± 0.030 / 9	0.339 ± 0.042 / 2	N/A	0.117 ± 0.040 / 2	0.316 ± 0.000 / 1	0.239 ± 0.002 / 3	0.591 ± 0.097 / 7
Volume $(mm^3)_a$	0.311 ± 0.016 / 3	0.034 ± 0.009 / 3	0.030 ± 0.004 / 4	N/A	N/A	0.027 ± 0.006 / 2	0.039 ± 0.007 / 3	0.030 ± 0.000 / 1
Volume $(mm^3)_b$	0.311 ± 0.016 / 3	0.049 ± 0.003 / 9	0.073 ± 0.000 / 2	N/A	N/A	0.049 ± 0.000 / 1	0.044 ± 0.004 / 3	0.096 ± 0.012 / 2

Regeneration of *Orthasterias koehleri* larvae								
	Control				**Age**			
	Before bisection	Day 1	Day 3	Day 5	Day 7	Day 9	Day 11	Day 13
	Mean ± SE / n	Mean ± SE / n	Mean ± SE / n	Mean ± SE / n	Mean ± SE / n	Mean ± SE / n	Mean ± SE / n	Mean ± SE / n
Area (mm^2) [a]	2.136 ± 0.414 / 4	0.377 ± 0.012 / 3	N/A	0.250 ± 0.032 / 4	0.249 ± 0.037 / 2	N/A	0.169 ± 0.039 / 3	0.259 ± 0.013 / 6
Area (mm^2) [b]	2.136 ± 0.414 / 4	0.342 ± 0.046 / 4	N/A	0.216 ± 0.007 / 3	0.272 ± 0.032 /2	N/A	0.210 ± 0.000 / 1	0.390 ± 0.032 / 6
Volume (mm^3) [a]	0.514 ± 0.000 / 1	0.100 ± 0.009 / 3	N/A	0.054 ± 0.008 / 4	0.048 ± 0.004 / 2	N/A	0.029 ± 0.004 / 3	N/A
Volume (mm^3) [b]	0.514 ± 0.000 / 1	0.108 ± 0.020 / 4	N/A	0.032 ± 0.003 / 3	0.087 ± 0.009 / 2	N/A	0.035 ± 0.000 / 1	N/A

[a] Area and volume calculated for the anterior lobe.

[b] Area and volume calculated for the posterior lobe. Calculation derived from the use of Stokes' theorem to estimate irregular areas. SE indicates the standard error of measurements.

Appendix

Matlab code for area and volume estimations.

```
% matlab "work". At the end the contour of the image is display with the area values.
% ---------------------------------------------------------------------------
clc
disp('')
disp('Selects the points from the contour of the image')
disp('At the end press Enter to finish the measurements and to calculate the area of the image')
A = imread('Larva.jpg'); % Reads the image to process
ejex = [0, 1];
ejey = [1, 0];
imagesc(ejex,ejey,A); % Scale of axis X y Y.
set(gca,'YDir','normal');
[X,Y] = ginput; % Read the values of the image
nm = length(X);
n = nm+1;
X(n) = X(1); % Last point joins the first one that was measured. This is to avoid open contours
Y(n) = Y(1);

sum = 0;
sumx = 0;
sumy = 0;
format long e; % Precision 10
```

```matlab
for i=1:nm
  dA =   (X(i)*Y(i+1) - X(i+1)*Y(i))/2;
  sum = sum + dA;
  sumy = sumy + (Y(i)+Y(i+1)) * dA / 3;
  sumx = sumx + (X(i)+X(i+1)) * dA / 3;

end
plot(X,Y)
Area = double(sum) % Double precision
```

Appendix